



Liquid crystal properties of triphenylene esters

Saeed Saleh Samman

Submitted in partial fulfilment of the requirement of the degree of PhD in Organic Chemistry

September 2022

© This copy of the thesis has been supplied on condition that anyone who consults it, is understood to recognize that its copyright rests with the author and that no quotation from the thesis, nor any information derived therefrom, may be published without the author's prior written consent

Abstract

Designing discotic liquid crystals often involves ester linkages. Hexaesters of benzene were the first examples of discotic liquid crystals reported by Chandrasekhar.

This thesis presents the synthesis and investigation of monoesters, diads, and diesters of triphenylene.

We present examples of materials that combine linked and twinned design elements to induce the onset of nematogenic behaviour. In the case of pentahexyloxy triphenylenes containing a single aryl ester plus five hexyloxy substituents, the columnar mesophase is retained. Additionally, the stability of the mesophases is not significantly affected by the ester used. In isomeric series (phthalates), linked dyad structures promote nematic phase formation and stability depends on the type of link and the bonding arrangement. Another ester linked dyad system has been prepared from diacid chlorides. For ferrocene links, the geometry can be considered to have intermediate switches between staggered and eclipsed arrangements. The staggered formation of this arrangement makes it unlikely to support liquid crystal behaviour, and this is indeed observed. A further ester-linked dyad system was prepared by new route (biphenyl route). This new dyad structure was characterized and demonstrated columnar liquid crystal behaviour.

Finally, we synthesized and examined a series of triphenylenes bearing two aryl esters and four hexyloxy substituents. The aim was to couple 2,3-dihydroxy triphenylene and 3,6-dihydroxy triphenylene with benzoate by the same method as previously used.

The mesophases formed in all examples are columnar hexagonal; clearing temperatures are higher than for monoesters but again the ester employed does not to affect their stability.

Access Condition and Agreement

Each deposit in UEA Digital Repository is protected by copyright and other intellectual property rights, and duplication or sale of all or part of any of the Data Collections is not permitted, except that material may be duplicated by you for your research use or for educational purposes in electronic or print form. You must obtain permission from the copyright holder, usually the author, for any other use. Exceptions only apply where a deposit may be explicitly provided under a stated licence, such as a Creative Commons licence or Open Government licence.

Electronic or print copies may not be offered, whether for sale or otherwise to anyone, unless explicitly stated under a Creative Commons or Open Government license. Unauthorised reproduction, editing or reformatting for resale purposes is explicitly prohibited (except where approved by the copyright holder themselves) and UEA reserves the right to take immediate 'take down' action on behalf of the copyright and/or rights holder if this Access condition of the UEA Digital Repository is breached. Any material in this database has been supplied on the understanding that it is copyright material and that no quotation from the material may be published without proper acknowledgement.

This thesis is dedicated to my beloved parents

Acknowledgement

First of all, I would like to give thanks to the almighty God for giving me life and the strength to complete this thesis.

I would also like to thank my supervisor, Professor Andy Cammidge, for all his help and support throughout my studies. His encouragement, enthusiasm, and advice have inspired me throughout the past few years.

Thank you also to Dr. Isabelle for her helpful advice and suggestions during work in the lab and help with measurements.

I also want to thank Ahad and Sultanah for their advice, help, and the experiences they have shared over the past few years.

A big thank you to all the people in the lab: Ala, Aziz, Budur, Ibtesam, Faisal, Mamdouh, Muteb, Norah Alsaieri and Shazia for the experiences shared over the past few years, and to the many other students who have made the labs enjoyable places in which to conduct research.

A special thank you to all the staff members of the School of Chemistry at the University of East Anglia, from whom I learnt a lot during meetings, workshops, seminars, and conferences.

I am most grateful to Taibah University for offering me the scholarship to pursue my PhD studies.

I sincerely wish to express my deepest gratitude to my wife, Ola, for her patience and support. My completion of this thesis would not have been possible without her presence with me in the U.K during my studies.

Lastly, my biggest thanks go to my parents, my brother, and my sisters, who have in one way, or another helped me achieve this thesis.

Without all of your support, this couldn't have been done.

Contents:

Abstract.....	II
Acknowledgement	IV
Abbreviation.....	XII
Chapter 1. Introduction	1
1.1 Historical perspective:	1
1.2 Liquid crystals and discotic liquids crystal:	1
1.3 Triphenylene (TP).....	4
1.4 Discotic liquid crystal classification:	4
1.5 Calamitic liquid crystal and their classification.....	7
1.6 Characterization techniques of mesophases:.....	8
1.6.1 Polarized Optical Microscopy (POM)	8
1.6.2 Differential scanning calorimetry (DSC):.....	9
1.7 Properties of triphenylene:.....	9
1.8 Synthesis of Triphenylene:	11
Type 1: oxidative cyclisation of terphenyl	12
Type 2: from biphenyls using palladium-catalysed coupling, a Diels-Alder reaction and oxidative cyclisation	14
Type 3: from naphthyls using Diels-Alder cycloaddition.....	15
Type 4: from phenanthryls using Diels-Alder reactions and photocyclization.....	16
Type 5: from 6-membered rings using cyclotrimerization step:	18
Type 6: Synthesis by adding peripheral rings in one step.....	19
Methods for synthesising unsymmetrical triphenylene cores:.....	20
1.9 Triphenylene applications:.....	22
1.9.1 Liquid crystal displays	22
1.9.2 Organic light-emitting diodes	23

1.9.3 Photovoltaic devices:	24
1.9.4 Organic Field Effect Transistor (OFET):.....	24
1.9.5 Other applications:	25
1.10 Synthesis and mesophase behaviour of Hexaalkoxytriphenylenes:	25
Mechanisms of triphenylene formation:	26
Symmetrical Hexahydroxytriphenylene:	27
1.11 Synthesis and mesophases of Monohydroxypentaalkoxytriphenylene (2-hydroxy-3,6,7,8,9-pentaalkoxytriphenylenes):.....	33
1.12 Synthesis of dimers, triads and their mesophase:	38
Chapter 2: Results & Discussion	41
Aims of the project:	41
Synthesis of MHT strategy:.....	42
Synthesis of triphenylene monoesters:	46
Liquid crystal properties of the first series (95-98):	48
Liquid crystal properties for mono esters (99-102):	55
Synthesis of triphenylene ester dimers 103-104:	57
Liquid crystal properties for dimer with Isophthalate and terephthalate (103-104): .	63
Introduction to ferrocene:	64
Liquid crystal properties of triphenylene dimer 107:	69
An alternative synthesis of diesters:	69
Liquid crystal properties of triphenylene dimer 111:.....	74
Triphenylene diester:.....	75
Synthesis of 2,3-dimethoxytriphenylene 113:	75
Synthesis of 2,3-bis(hydroxy)triphenylene 112:	75
Synthesis of 2,3-Diesters (115-119):.....	76
Liquid crystal properties for 2,3- Diesters (115-119):	79
Synthesis of 3,6-Diester (121):.....	81

3. Experimental section:	84
General information:	84
Synthetic procedures and characterization data:	85
Synthesis of 1,2-Dihexyloxybenzene (DHB) 55	85
Synthesis of 2-hexyloxyphenol 74	86
Synthesis of monohydroxy- penta-hexyloxytriphenylene (MHT) 75 [91]	87
Synthesis of 1-Hexyloxy 2-methoxybenzene 93	88
Synthesis of Methoxy-penta-hexyloxytriphenylene 94	89
Synthesis of (4-Nitrobenzoate) ester 95	90
Synthesis of 4-Methoxybenzoate ester 96	91
Synthesis of 2-Bromobenzoate ester 97	92
Synthesis of 3-Bromobenzoate ester 98	93
Synthesis of (1-Naphthoate) ester 99	94
Synthesis of (2-Naphthoate) ester 100	95
Synthesis of anthracene-2-carbonyl chloride 101a	96
Synthesis of (2-Anthracenoate) ester 101	97
Synthesis of (9-Anthracenoate) ester 102	98
Synthesis of triphenylene dimer 103:	99
Synthesis of triphenylene dimer 104:	100
Synthesis of ferrocene dicarbonyl chloride 105	101
Synthesis of dimer 106	102
Synthesis of triphenylene dimer 107:	103
Synthesis of Tetra(hexyloxy)biphenyl 109	104
Synthesis of bis (2-methoxy phenyl) benzene 1,4 dicarboxylate 110	105
Synthesis of triphenylene dimer 111	106
The synthesis of 2,3-bis(methoxy)triphenylene 113 by using biphenyl :	107
Deprotection of 2,3-bis(methoxy)triphenylene 114:	108

Synthesis 2,3-di benzoate ester 115	109
Synthesis of 2,3-di (1-Naphthoate) esters 116	110
Synthesis of 2,3-di (2-Naphthoate) esters 117	111
Synthesis of 2,3-di (2-Anthracenoate) esters 118	112
Synthesis of anthracene-9-carbonyl chloride 119a	113
Synthesis of 2,3-di (9-Anthracenoate) esters 119	114
Synthesis of 3,6-di (1-Naphthoate) esters 121	115
References:	116
Appendixes	122

List of figures:

Figure 1.1: Structure of benzene hexaesters.....	1
Figure 1.2: Illustration of the molecular structure of a mesogenic material in two dimensions.....	2
Figure 1.3: Liquid crystal classification.....	3
Figure 1.4: Mesophases of cores with DLC.....	3
Figure 1.5: Self-assembling triphenylene as a columnar phase.....	4
Figure 1.6 Schematic representation of the columnar phase showing hexagonal, rectangular, oblique and lamellar columnar.....	5
Figure 1.7 Illustrates typical nematic mesophases	6
Figure 1.8: o-terphenyl crown ether exhibiting smectic phases.....	7
Figure 1.9. Illustration of DSC curve.....	9
Figure 1.10 Structure of triphenylene 2	10
Figure 1.11 Functionalised unsymmetrically substituted riphenylenes.....	20,21
Figure 1.12 Structures of dithiol-functionalised triphenylene ligands and ZnO nanoparticles..	24
Figure 1.13: Triphenylenes mechanism via arene cations or radical cations by the Scholl reaction.....	27
Figure 1.14: Heaxbenzote esters of triphenylene bear additional substituent on the phenyl groups and one methyl groups.....	31
Figure 1.15: Triphenylene hexbenzote esters include two methyl groups.....	32
Figure 2.1: Structure of target compounds.....	41
Figure 2.2: ¹ H NMR spectrum of MHT (75)	44
Figure 2.3: ¹ H -NMR spectrum methoxybenzoate (96)	47
Figure 2.4: ¹ H -NMR of aromatic regions of the first series (95-98)	48
Figure 2.5: The mesophase textures and transition temperatures of triphenylene monoesters with simple benzoates 95 – 98 , showing the similarity of their behaviour.	49

Figure 2.6: ^1H -NMR spectrum of triphenylene-9-anthracenoate (102)	53
Figure 2.7: The aromatic peaks of NMR triphenylene esters 99-102.....	55
Figure 2.8: Columnar mesophase textures and transition temperatures of the second series of triphenylene monoesters, bearing substituents with higher steric demand.....	56
Figure 2.9: The geometry of the connecting group with the dimer.....	57
Figure 2.10: ^1H NMR spectrum of rearrangement compound.....	58
Figure 2.11: Crude MALDI-MS showing presence of monomer and side product.....	60
Figure 2.12: ^1H NMR spectrum of dimer compounds 103 and 104.....	62
Figure 2.13: Liquid crystal properties and transition temperature of 103 and 104.....	63
Figure 2.14: The geometry of the connecting group (ferrocene) within the dimer.....	64
Figure 2.15 The staggered form of Ferrocene (left) and the eclipsed form (right)	64
Figure 2.16: ^1H NMR spectrum of dimer compounds 106.....	67
Figure 2.17: ^1H NMR spectrum of triphenylene dyad using a ferrocene link.....	69
Figure 2.18: ^1H NMR spectrum of benzene dimer 110.....	72
Figure 2.19: ^1H NMR spectrum of triphenylene dimer 111.....	74
Figure 2.20: Texture and transition temperature for dimer 111.....	74
Figure 2.21: The aromatic peaks of NMR triphenylene esters 115-119.....	78,79
Figure 2.22: Columnar mesophase textures and transition temperatures of the triphenylene-2,3-diester 115–119 , bearing different substituents with simple benzoates and higher steric demand.....	80
Figure 2.23: The aromatic peaks of NMR triphenylene esters 121.....	81

List of schemes:

Scheme 1.1 Different routes for preparing triphenylene.....	11
Scheme 1.2: Terphenyl cyclisation is the final step in the synthesis of hexa(hexyloxy) triphenylene 6.....	12
Scheme 1.3: A method for producing 2, 3'-bis(hexyloxy) triphenylene 8.....	12
Scheme 1.4: A synthetic method for 2, 7-bis(hexyloxy) triphenylene 12,13 and 14.	13
Scheme 1.5: Triphenylene 17 synthesis is catalysed by palladium.	14
Scheme 1.6: Synthesis of substituted triphenylene using heterocyclic dienes.....	14
Scheme 1.7: A substituted triphenylene has been synthesised from biaryl 22.	15
Scheme 1.8: Triphenylene 2 was synthesised using the Diels-Alder reaction.....	15
Scheme 1.9: The Friedel-Crafts reaction is used for the synthesis of triphenylene 2.....	16
Scheme 1.10: A synthetic method for 1,4-dimethyl triphenylene.....	16
Scheme 1.11: Benzotriphenylene synthesis 34.....	17
Scheme 1.12: Dimethoxybenzene 35 undergoes an oxidative trimerization to yield 36....	18
Scheme 1.13: Triphenylene 2 is synthesised from cyclohexanone.....	18
Scheme 1.14: Synthesis of substituted hexa-aza-triphenylenes 40.....	19
Scheme 1.15: Cyclisation of 41 to yield 43 by acid catalysis.....	19
Scheme 1.16: Synthesis of triphenylenes 46 from biphenyl.....	20
Scheme 1.17 Asymmetric triphenylene derivatives synthesis.....	21
Scheme 1.18: Oxidative coupling of dialkoxybenzenes.....	26

Scheme 1.19: Triphenylene hexabenzote esters.....	28
Scheme 1.20: Triphenylene hexalkyl esters.....	30
Scheme 1.21: Synthesis of Monohydroxypentaalkoxytriphenylene 75.....	33
Scheme 1.22: Esterification reaction between monohydroxypentaalkoxytriphenylene and anthraquinone.....	34
Scheme 1.23: Esterification reaction of Monohydroxypentaalkoxytriphenylene with acid chloride derivatives.....	35
Scheme 1.24: 2- position bulky group substituted triphenylene esters.....	36
Scheme 1.25: 3,6-position bulky group substituted triphenylene esters.....	37
Scheme 1.26: The synthesis of triphenylene diads esters and their mesophase	38
Scheme 1.27: The synthesis of diads triphenylene esters with 2-vinyl terephthalic acid and the synthesis of that as a polymer and their mesophase.....	39
Scheme 1.28: The synthesis of triad triphenylene.....	40
Scheme 2.1 Synthesis of DHB (55).....	42
Scheme 2.2: Synthesis of monohexyloxyphenol (74) with 1,2-dihexyloxybenzene (55).....	42
Scheme 2.3 Synthesis of monohydroxy-pentahexyloxytriphenylene (MHT) (75).....	43
Scheme 2.4: Alternative synthesis of triphenylene (75).....	45
Scheme 2.5 Synthesis of triphenylene monoester with aryl benzoate (95-98).....	46
Scheme 2.6 Synthesis of triphenylene monoester with bulky, larger aromatic esters (99-102).	51
Scheme 2.7: thionyl chloride mechanism for converting carboxylic acid to acid chloride.....	51
Scheme 2.8: Esterification reaction mechanism with triethylamine.....	52
Scheme 2.9: The mechanism of a Steglich esterification	52
Scheme 2.10: The synthesis of triphenylene diads esters with aryl dicarboxylates units and their mesophase	61
Scheme 2.11: Mechanism of acyl chloride formation using thionyl or oxalyl chlorides....	65
Scheme 2.12: Ferrocene dicarbonyl chloride synthesis.....	65
Scheme 2.13: Mechanism of DMF with oxalyl chloride and then with carboxylic acid.....	66
Scheme 2.14: Synthesis of 2-Naphthol with Ferrocene dicarbonyl chloride.....	67
Scheme 2.15: Triphenylene dimer synthesis 107	68
Scheme 2.16: synthesis of tetrakis(hexyloxy) biphenyl 109	70
Scheme 2.17: Ullmann reaction mechanism by Cu and Ni	71
Scheme 2.18: Diphenyl ester synthesis.....	71
Scheme 2.19: Alternative triphenylene dimer ester synthesis	73
Scheme 2.20: 2,3-bis(methoxy) triphenylene (111) synthesis.....	75
Scheme 2.21: 2,3-dihydroxy triphenylene (114) synthesis.....	76
Scheme 2.22: Synthesis of 2,3-Diesters of triphenylene 115-119	77
Scheme 2.23: Synthesis of 3,6-Diesters (121)	81

Abbreviation

°C	Celsius temperature
DHB	1,2-Dihexyloxybenzene
DLC	Discotic liquid crystals
DMF	N,N-Dimethylformamide
δ	Chemical Shift
EtOAc	Ethyl Acetate
eq	Equivalent
g	gram
HAT6	Hexahexyalkoxy-triphenylene
h	Hour(s)
Hz	Hertz
IR	Infra-Red
J	Coupling constant in NMR spectroscopy (Hz)
MALDI-MS	Matrix Assisted Laser Desorption Ionization-Mass Spectrometry
Me	Methyl
MHT	monohydroxytriphenylene
mmol	Millimole
mol	Mole
Mp	Melting Point
Col _h	Columnar hexagonal
N _C	Nematic Columnar
N _D	Nematic discotic
NMR	Nuclear magnetic Resonance
D	Doublet
Pet.Ether	Petroleum ether
ppm	Parts per million
RT	Room temperature
TLC	Thin layer chromatography

Chapter 1. Introduction

1.1 Historical perspective:

In 1888, Reinitzer discovered that a phase of matter exists between solid and liquid [1]. Natural cholesteryl materials were observed to appear cloudy at specific temperatures. At temperatures below this range, the material was crystalline, and at higher temperatures, it became a clear liquid. The intermediate cloudy phase has been described as a liquid crystal (LC) because it has some of the characteristics of a crystal while being "soft" like a liquid. LC phases can also be described as mesophases, leading to materials showing liquid crystal behaviour being referred to as mesogens. It became clear that these materials had many industrial applications during the 1960s, such as display technology [2]. While liquid crystal molecules were generally expected to be rod-like, several hexaesters of benzene were then discovered in 1977 by Chandrasekhar to possess mesomorphic properties **1** [3].

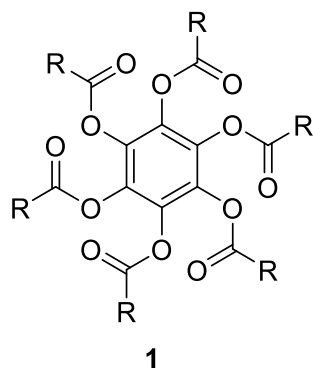


Figure 1.1: Structure of benzene hexaesters

1.2 Liquid crystals and discotic liquid crystal:

As shown in Figure 1.2, LCs exhibit a degree of long-range order (a characteristic of crystallinity). The molecular structure of an LC consists of a rigid core, which is usually aromatic, and a flexible tail.

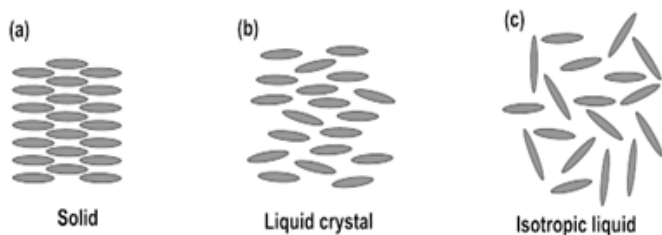


Figure 1.2: Illustration of the molecular arrangement of a rod-like mesogenic material in two dimensions.

In Figure 1.2, examples of structures formed in mesogenic materials in solid, liquid, and LC phases are shown, with increasing degrees of order. It has been observed that various degrees of order have been observed in LC mesophases, and it is possible for one material to exhibit more than one mesophase during its transition between liquid and solid states [4]. A mesophase transition is either lyotropic or thermotropic depending on the factors driving it. Essentially, lyotropic changes are caused by changes in density caused by the influence of solvents [5]. While the composition of the intermediate phases in thermotropic liquid crystals depends on temperature, which can be produced by heating the crystalline solid or cooling isotropic liquid. These are classified as calamitic (rod-like), bent-core (banana-like), and discotic (disc-like). These classes are classified according to the shape of the intermediate particles. However, the nematic, smectic, and columnar liquid crystal phases are classified according to the properties of the molecular arrangement (figure 1.3). This thesis is mainly concerned with units related to triphenylene, which are discotic liquid crystals [6].

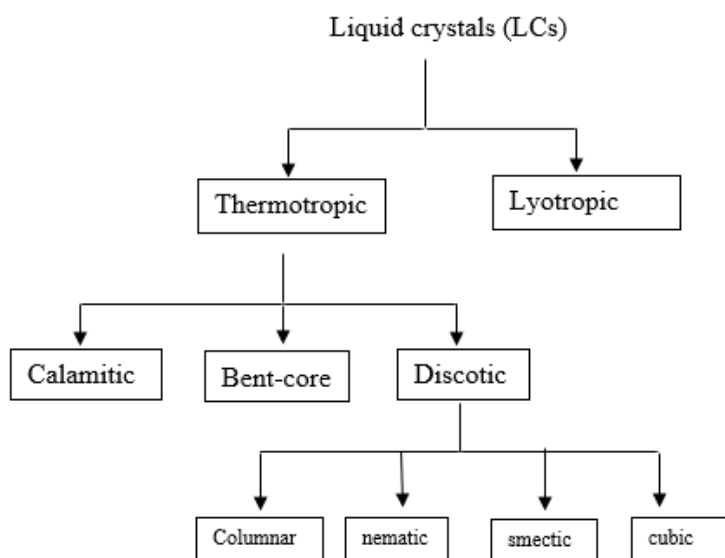


Figure 1.3: Liquid crystal classification.

There are many distinctive properties of thermotropic liquid crystals. They are typically interconnected structures that are fluid, processable, and self-healing. The orientational arrangement of liquid crystals indicates that they are anisotropic and exhibit anisotropic optical properties.

Discotic liquid crystals can be generated from many nuclei, including, phthalocyanine, naphthalene, perylene, anthracene, porphyrin, and triphenylene etc (Figure 1.4). The use of triphenylene cores to produce discotic mesogen molecules has received significant attention recently, and it is where the current work is focused [6].

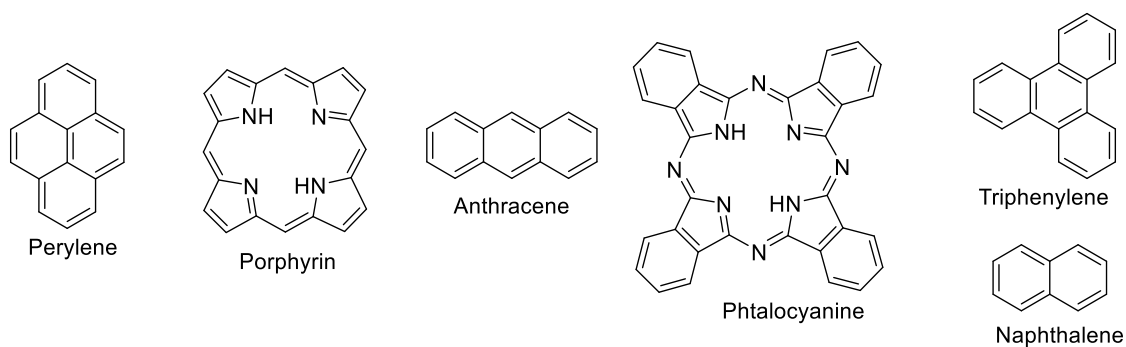


Figure 1.4: Mesophases of cores with DLC.

We are going to focus on the phases of discotic thermotropic liquid crystals, as it is the objectives of this thesis. In thermotropic mesogens, the temperature at which the solid transitions to LC are the melting temperature, T_M , while the temperature at which the LC transitions to liquid is the clearing temperature, T_C [7].

1.3 Triphenylene (TP)

Triphenylene was produced and reported most often from the explored DLCs. Triphenylene (TP) as a DLC nucleus was first presented in 1978 by Billard et al. [6]. Thermal and chemical stability, relative accessibility, a wide range of intermediate phases, and outstanding electrical properties are just some of the advantages accessible by triphenylene derivatives [8]. Thus, these materials are widely used. Consequently, there has been a significant amount of research on the synthesis of DLC-based TPs, with over 500 documented in the literature to date. The columnar intermediate phases are the most common among the triphenylene-derived compounds, while the nematic phases are less common (Figure 1.5).

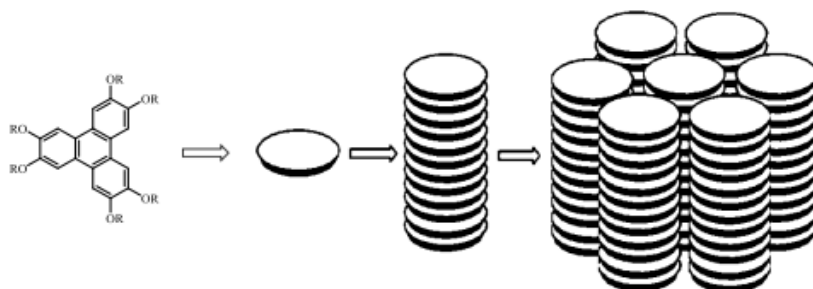


Figure 1.5: Self-assembling triphenylene as a columnar phase.

1.4 Discotic liquid crystal classification:

Columnar, nematic, smectic, and cubic are four different discotic liquid crystal mesophase types. They are based on the shape and symmetry of the molecules. Only one of these mesophases exists in most discotic molecules, with columnar being the most common. Polymorphism is a situation that can have more than one [9].

Upon discovering columnar phases, it was demonstrated that disc-like molecules could give rise to discotic phases or columnar phases, including nematic-discotic phases, nematic-columnar phases, and ordered columnar phases. All of these molecules have molecular cores arranged parallel to each other with a common rotational axis.

It is, however, a nematic-discotic phase when the cores are capable of moving in a wide space. It can be found in nematic-columnar phases when molecules stack to form cylindrical structures in one dimension, but without showing the same direction axis among columnar units.

1. Columnar

The most stable mesophases are columnar structures and are described here. Figure 1.6 illustrates the common arrangements, illustrating how they differ in terms of intercolumn and intracolumn arrangements [10]. The disordered columnar phase is characterized by low positional order and flexibility along the inter-column director. In contrast, when there is a short-range inter-column distance, the columnar units align into different lattices and produce more ordered mesophases in hexagonal, tetragonal, rectangular, oblique, or lamellar arrangements.

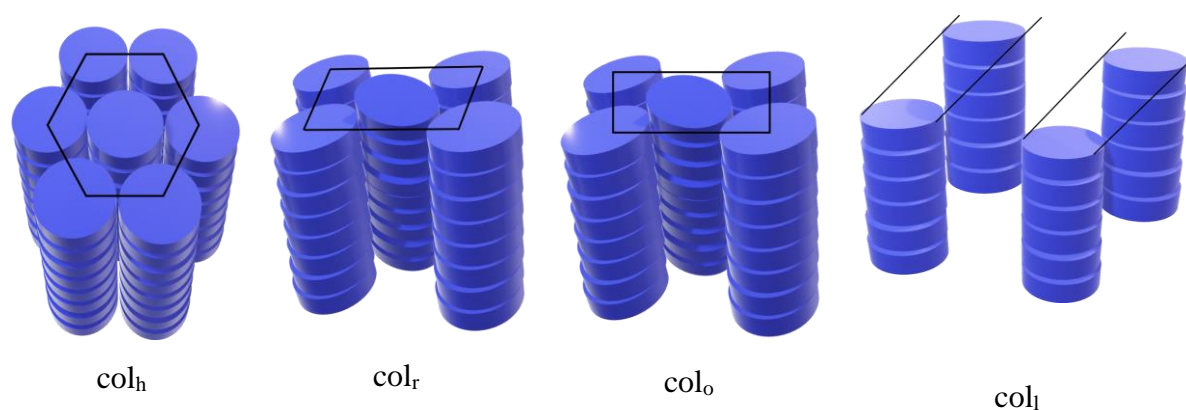


Figure 1.6 Schematic representation of the columnar phase showing hexagonal, rectangular, oblique and lamellar columnar [9].

The hexagonal columnar phase (Col_h) is distinguished by a two-dimensional hexagonal arrangement between the columns and appears when the molecular plane is perpendicular to the columnar axis. Columnar Rectangular (Col_r) phase occurs when the molecular plane looks inclined with respect to the columnar axis and the cross section of the column is elliptical in a two-dimensional rectangular configuration. Columnar oblique (Col_o) mesophase maintains a

perpendicular relationship between columns and plane, but the packing direction for molecules shifts in relation to the long-range orientation of the column. Lastly, a type of lamellar structure called the columnar lamellar structure (Col_h) can be formed. The molecules in this phase are organised in layers similar to calamitic-type molecules in a smectic phase. It has the lowest degree of order: the molecules are stacked in columns (ordered or disordered); nevertheless, these columns do not form two-dimensional structures: they only display order in orientation, of a medium range [11]. A number of new columnar phases have also been reported using new liquid crystalline materials, including supramolecules, polymers, and mixable materials such as metallo-mesogens [10].

The nematic-discotic phase exhibits schlieren textures as well under crossed polarization. In spite of this, since the birefringence differs in anisotropy, it produces different textures, such as ordered fanshape focal-conoid structures or snow-like textures for those columnar hexagonal structures [11].

2. Nematic

Nematic phases can be derived from both calamitic and discotic mesogens (the latter shown in Figure 1.7) and is the most disordered mesomorphic phase. The orientational order characterises this mesophase, but not the positional order. In practice, the molecules are oriented parallel to each other in a preferred direction defined by the director but are free to move in space [12].

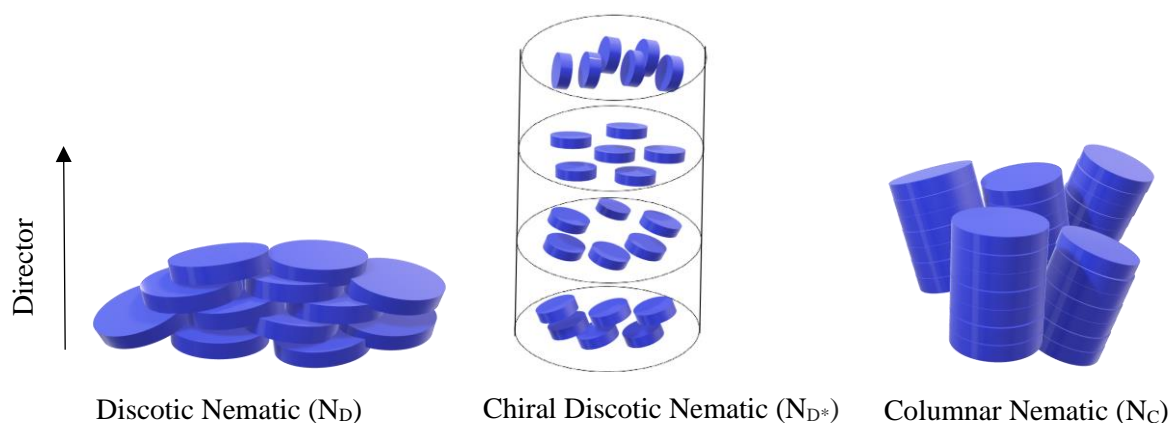


Figure 1.7 Categories of typical nematic mesophases (i) Discotic Nematic, N_D (ii) Chiral Discotic Nematic, N_{D*} (iii) Columnar Nematic, N_C [13].

The discotic nematic phase is a one-dimensional phase that does not have a director of significance [14]. As a result of the large number of defects present in such materials, they are not frequently tested for electrically addressable displays. However, due to their capability of exhibiting negative birefringence or rich colours, they may prove suitable for LCD viewing angles or sensitive thermometers [15].

3. Smectic

Smectic phases occur when there are fewer peripheral chains or when they become unbalanced. The layer of discs is separated by peripheral chains [16]. It is considered a rare phase for discotic liquid crystals since it does not produce columnar aggregates. As seen in Figure 1.8, the smectic discotic phase of o-terphenyl crown ether [17]. This phase is also known as the lamellar phase and is similar to the calamitic mesogens in the smectic phase.

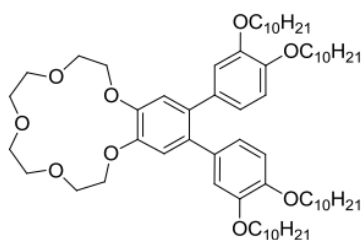


Figure 1.8: o-terphenyl crown ether exhibiting smectic phases.

4. Cubic

Although phthalocyanine derivatives display this phase, cubic liquid crystals are more common in lyotropic systems [18]. A column network is formed in this phase by branching columns [19].

1.5 Calamitic liquid crystal and their classification

There is generally one or more flexible alkyl chains attached to the aromatic rigid core of a calamitic mesogen [20]. A mesogen with short alkyl chains usually forms nematic phases, whereas a mesogen with a long alkyl chain forms smectic phase.

A cyano group at the terminal of a molecule can facilitate polar interactions between molecules in liquid crystalline phases by increasing their length and polarisability. Molecule packing can be affected by lateral substituents. The addition of a fluoro group enhances

polarisability but disrupts molecular packing, shifting the isotropic-nematic transition. There are two main liquid crystalline phases available to calamitic mesogens: nematic and smectic. Nematic liquid crystals can form via either calamitic or discotic mesogens. An important characteristic of this phase is the lack of long-range translational order and long-range orientational order [21].

1.6 Characterization techniques of mesophases:

A variety of techniques are available for determining the types of mesophases, their transition temperatures, and their structures. One of the main methods is polarised optical microscopy, followed by differential scanning calorimetry.

1.6.1 Polarized Optical Microscopy (POM)

In fact, liquid crystals were discovered and characterised during the first few years of research using this technique. This technique facilitates the identification of the various phases due to the different microscopic textures they present, as well as the determination of their transition temperatures. For this technique, a microscope with a heating plate is needed, which allows analysers to heat and cool the sample, as well as two crossed polarizers, between which the slide with the sample is placed. Upon passing through the first polarizer, the light generated by the lighting source remains linearly polarized. In the case of an isotropic sample on the slide, the polarisation of the light will not vary when passing through it and will be terminated in the second polarizer (called the analyser) located at a 90-degree angle to the first. As a result, nothing will be visible under a microscope. It should be noted that if the sample is in the liquid crystal phase, the polarisation of the light will vary so that some of it can pass through the analyser. Thus, the microscopic texture of the mesophase can be observed. The heating plate allows for the temperature of the sample to be varied, allowing the determination of not only the textures of the mesophases present, but also the melting, clearing, and transition temperatures between them. A good characterization requires several cycles of heating and cooling of the sample, paying close attention to the transition temperatures, the textures, and the appearance of monotropic and enantiotropic phases [22].

1.6.2 Differential scanning calorimetry (DSC):

Using this technique, the transition, melting, and clearance temperatures can be determined precisely, as can the values of their corresponding thermal characteristics, such as enthalpy and entropy. The method depends on the different absorption and emission of heat by the sample and the inert reference during the heating and cooling processes. Heat is applied to both materials simultaneously, each in its own oven at the same temperature. It is necessary to apply an additional amount of heat when the sample undergoes a phase change in order to maintain the same temperatures. As a result, the heat flow vs. temperature diagram (Figure 1.9) shows a peak in response to this additional heat input. The area of these peaks is proportional to the enthalpy of the process. The energy released by the sample during a phase transition can also be recorded [23].

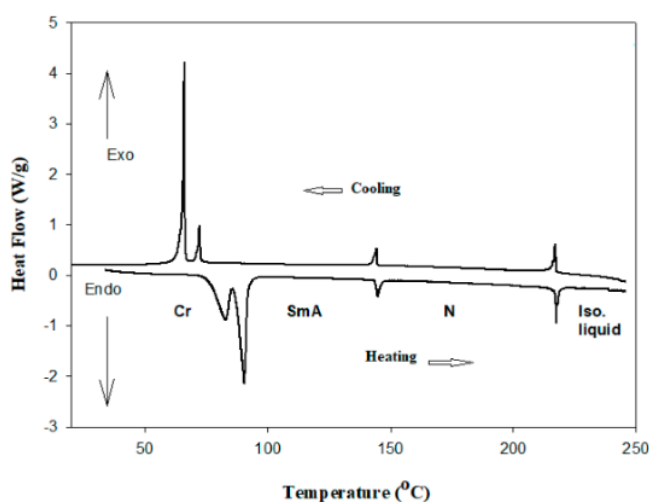


Figure 1.9. Illustration of DSC curve

1.7 Properties of triphenylene:

Triphenylene (TP) was discovered by Schultz from benzene's pyrolytic products [24]. According to the structure of this compound, it is a symmetrical, planar, aromatic hydrocarbon, consisting of four benzene rings fused together and having the molecular formula $C_{18}H_{12}$ (Figure 1.10). It is possible to visualize benzenes as three outer rings connected by single carbon-carbon bonds. It is an aromatic hydrocarbon with a delocalized 18-electronic system. It

is also possible to synthesise and generate many more TP derivatives since it is a trimer of benzene. There has been extensive literature research on the properties of this material for more than a century. Although there are twelve possible substitution positions in the TP structure **2**, the most common are located at peripheral sites 2, 3, 6, 7, and 10.

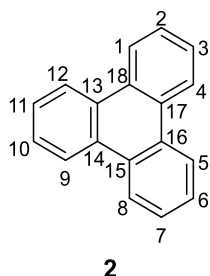
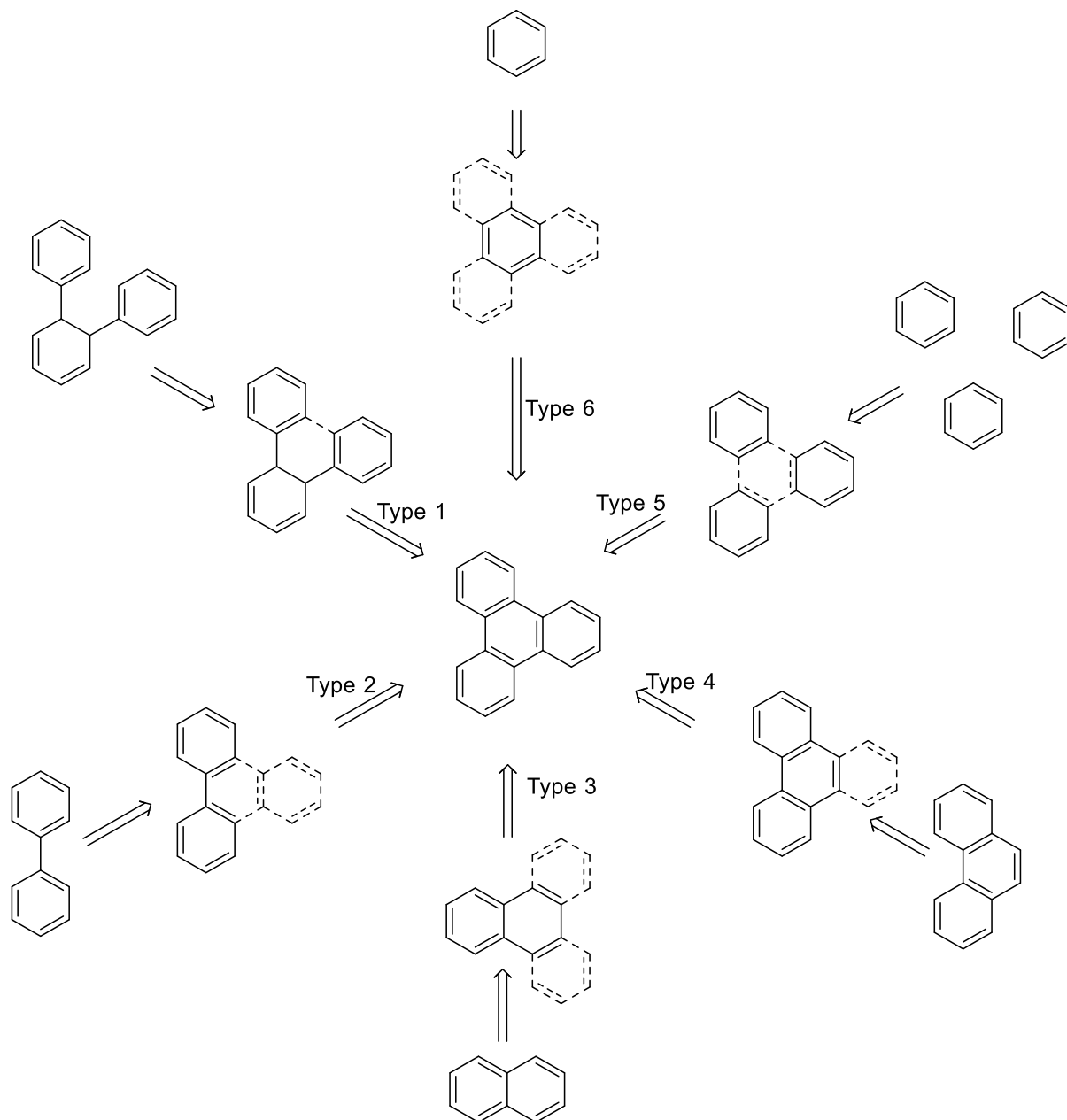


Fig.1.10 Structure of triphenylene **2**

There have been developed several methods to synthesize triphenylene since it was discovered. It was initially the aim to synthesise triphenylene itself. Substituted triphenylene has been the focus of more research attention in recent years. The first types of substituted triphenylene investigated were symmetrical hexaethers [25].

1.8 Synthesis of Triphenylene:

There are six different main routes for preparing triphenylene, as shown in Scheme 1.1 [25].

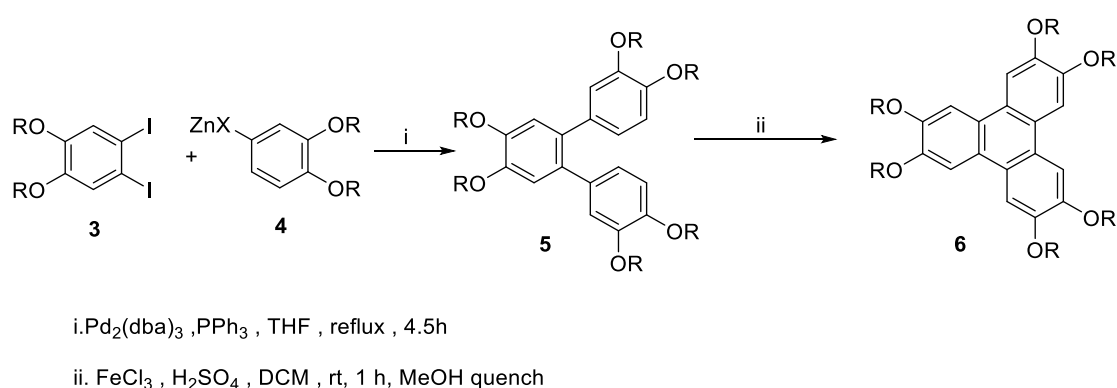


Scheme 1.1 Different routes for preparing triphenylene

Type 1: oxidative cyclisation of terphenyl

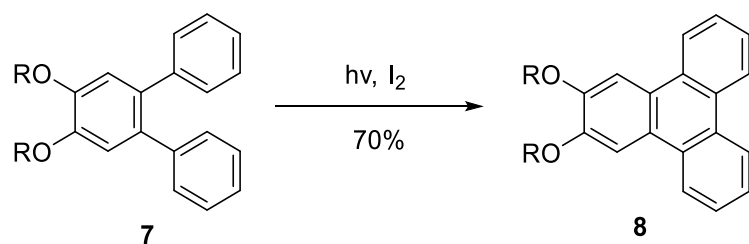
The formation of the terphenyl moiety is produced by either Ullman or, more often, palladium-catalysed cross-coupling.

The conversion to the triphenylene system is then obtained via either oxidative cyclisation or photocyclisation (Scheme 1.2). This strategy is used to prepare both symmetrically and unsymmetrically substituted triphenylenes, hexakisalkoxytriphenylene (HAT) and monohydroxytriphenylene (MHT). The oxidative cyclisation couplings necessitate the use of a number of oxidising agents, including VOCl_3 , MoCl_5 , VOF_3 , $\text{K}_3\text{Fe}(\text{CN})_6$, and FeCl_3 .



Scheme 1.2: Terphenyl cyclisation is the final step in the synthesis of hexa(hexyloxy) triphenylene **6**.

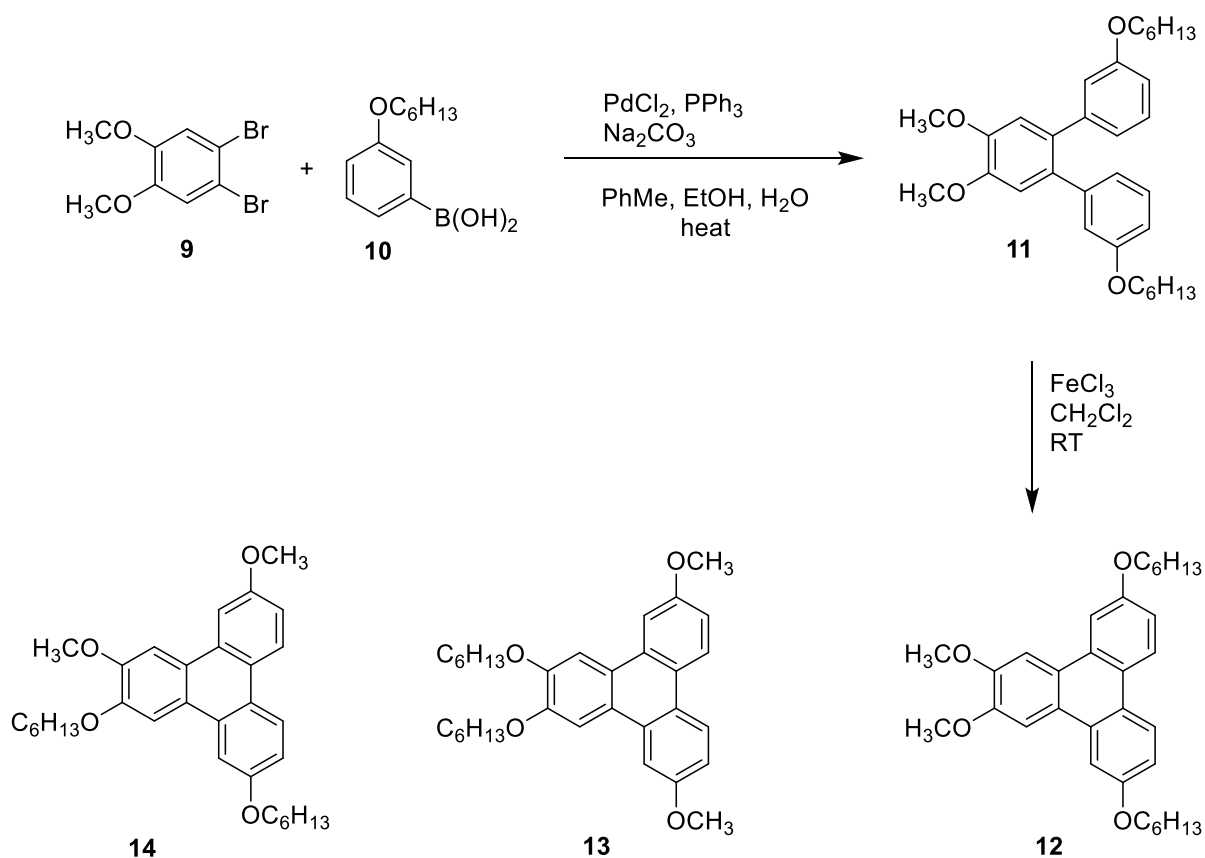
TP can also be produced by a symmetrical or unsymmetrical photocyclization technique. It is also possible to increase yields of triphenylene by using iodine as an oxidant during irradiation of the terphenyl [26].



Scheme 1.3: A method for producing 2, 3'-bis(hexyloxy) triphenylene **8**.

Using palladium-catalyzed couplings in combination with oxidative cyclization is a common way to synthesise terphenyls. The catalysts tris(dibenzylideneacetone) dipalladium [$\text{Pd}_2(\text{dba})_3$] and triphenylphosphine PPh_3 were used to produce the required terphenyls.

For the preparation of triphenylene derivatives, dichloromethane was combined with iron chloride and sulfuric acid [27].

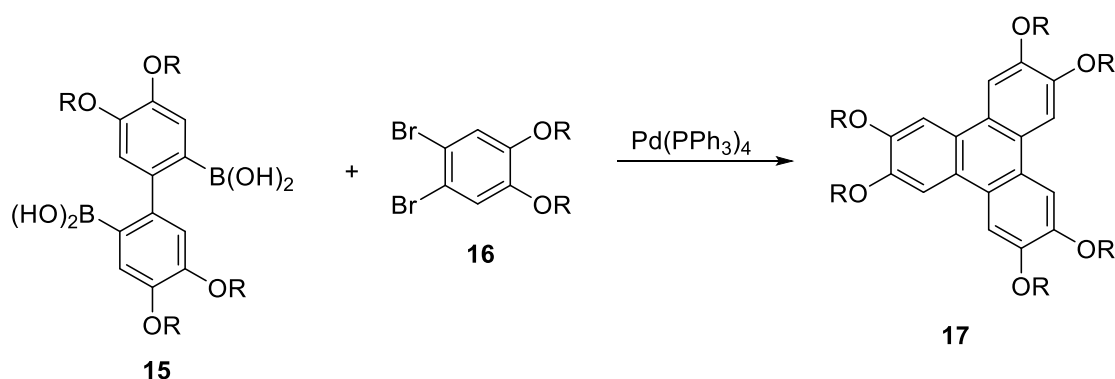


Scheme 1.4: A synthetic method for 2, 7-bis(hexyloxy) triphenylene **12**; variation can yield **13** and **14**.

Additionally, Suzuki coupling (scheme 1.4) has been applied to synthesise triphenylene symmetrically [28] and unsymmetrically by coupling other terphenyls (from boronic acid **10**) with o-dihalobenzenes.

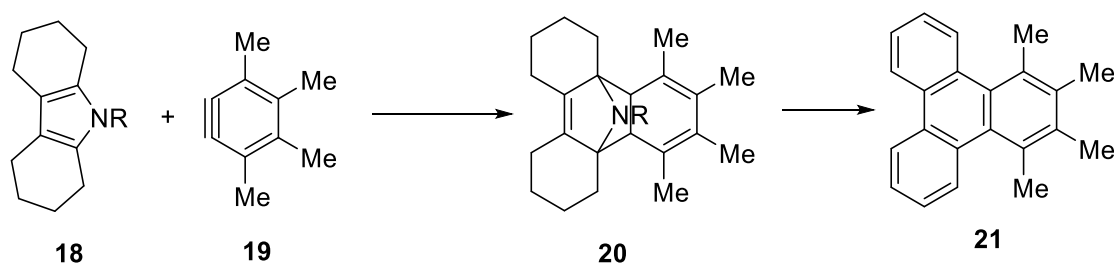
Type 2: from biphenyls using palladium-catalysed coupling, a Diels-Alder reaction and oxidative cyclisation

Biphenyl is an important precursor in this method for synthesising TP. A target compound can be obtained using three methods: palladium-catalyzed coupling, Diels-Alder cycloaddition, or oxidative coupling. Suzuki couplings are reactions in which palladium-catalyzed coupling is employed. In order to synthesise biphenyl, boronic acid is typically used as a coupling agent, which forms a C-C bond with the substituent aryl group. Triphenylene can be synthesised through substitution of both reactants with different R-groups. TP synthesis has been achieved with this interesting approach.[25]



Scheme 1.5: Triphenylene **17** synthesis is catalysed by palladium.

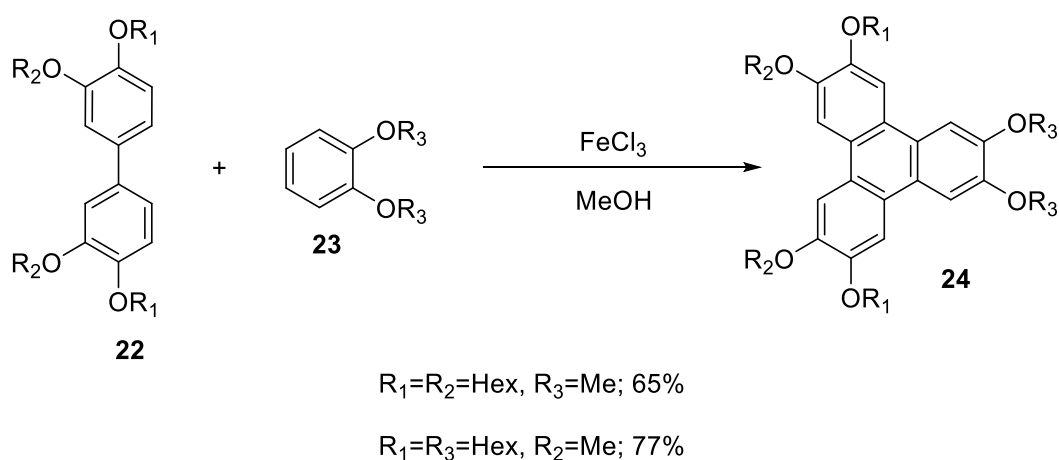
In a second strategy, the target is formed by reacting biphenyl with aryne **19**. This reaction involves a Diels-Alder cycloaddition. It is an efficient method for synthesizing triphenylene. As indicated in scheme 1.6, the reaction of heterocyclic dienes with benzyne leads to the formation of an adduct **20** that is capable of being converted into triphenylene **21** via heating followed by oxidation by 2,3-Dichloro-5,6-dicyano-1,4-benzoquinone DDQ. [29]



Scheme 1.6: Synthesis of substituted triphenylene using heterocyclic dienes.

As in the previous example, oxidative cyclization can be applied to biphenyl depending on which oxidants can be utilized.

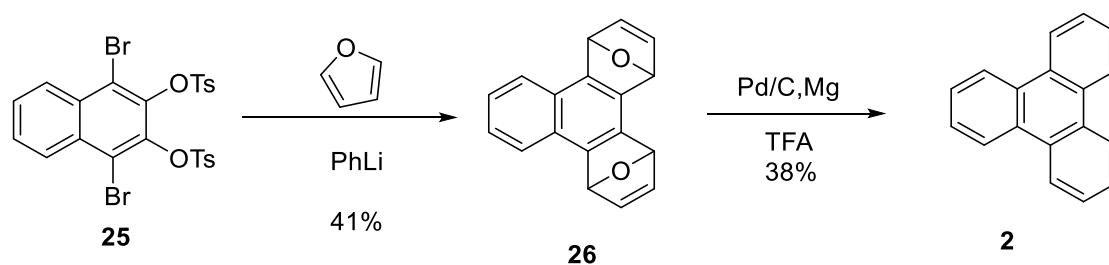
A substituted biaryl **22** was reacted with dialkoxybenzene **23** in the presence of FeCl_3 to produce triphenylene derivatives in a reasonable yield, as illustrated in Scheme 1.7 [30]. The method developed by Boden et al. has demonstrated that substitutions can occur in the α -position, which was previously difficult to attain due to its steric hindrance. [31]



Scheme 1.7: A substituted triphenylene has been synthesised from biaryl **22**.

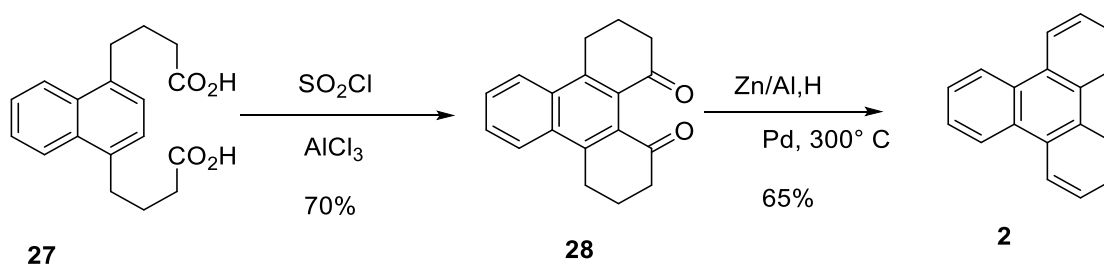
Type 3: from naphthyls using Diels-Alder cycloaddition

Triphenylene is synthesised by using naphthalene as peripheral rings. As a starting material for the production of triphenylene, naphthalene and its derivatives are used in two ways. As illustrated in the following scheme, the common method is the Diels-Alder cycloaddition. In the step following the metal-halogen exchange, naphthalene or its derivatives generate an aryne, which then reacts with furan as a diene. The next step in obtaining triphenylene **2** is treating compound **26** with Pd/C and Mg , followed by the addition of TFA for deoxygenation [32].



Scheme 1.8: Triphenylene **2** was synthesised using the Diels-Alder reaction.

Triphenylene **2** is synthesised using the Diels-Alder reaction. Using a similar method as described above, Friedel-Crafts reactions can also be utilised to produce triphenylene. Substituted naphthalene **27** undergoes cyclization to give diketones **28** [33], [34]. The use of palladium catalysts for the reduction and dehydrogenation can result in triphenylene (scheme 1.9).

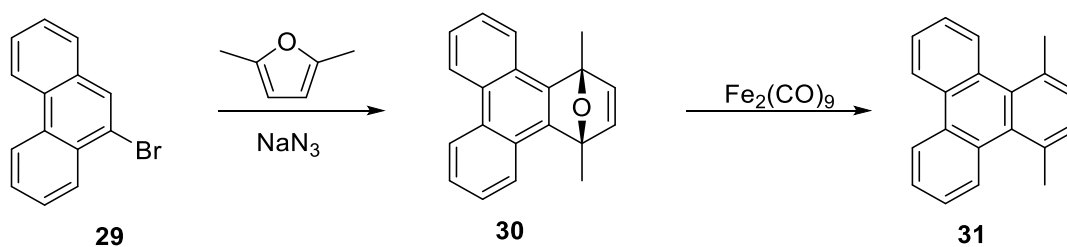


Scheme 1.9: The Friedel-Crafts reaction is used for the synthesis of triphenylene **2**.

Type 4: from phenanthryls using Diels-Alder reactions and photocyclization

A phenanthrene derivative is an important precursor in the production of triphenylene in this method, which involves the Diels-Alder reaction, photocyclization, and palladium catalysis. These types of reactions are usually carried out by Diels-Alder reactions with a deoxygenation step to yield triphenylenes.

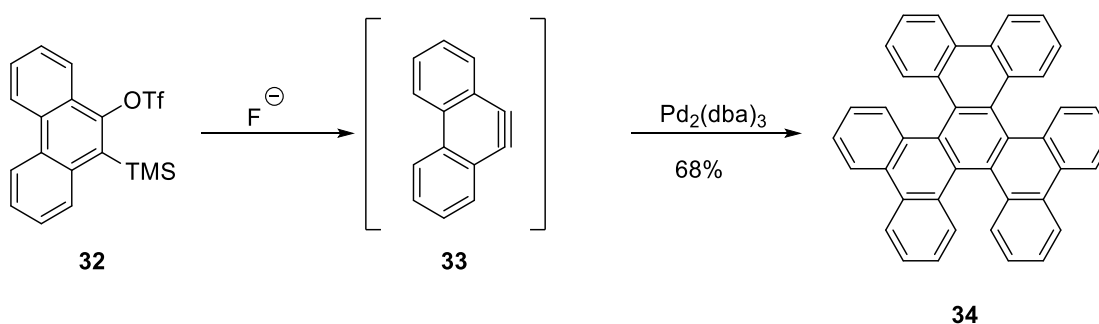
The following scheme illustrates how the phenanthrene derivative **29** reacts with furan in the presence of sodium amide, followed by a step of deoxygenation to give the compound **31**.



Scheme 1.10: A synthetic method for 1,4-dimethyl triphenylene [35]

A photocyclisation method has also been used to form benzotriphenylenes from phenanthrene derivatives.

The palladium-catalyzed trimerization of phenanthrene is another method of obtaining triphenylene derivatives, which should be included in this classification because it is based on phenanthrene as a starting material [25].

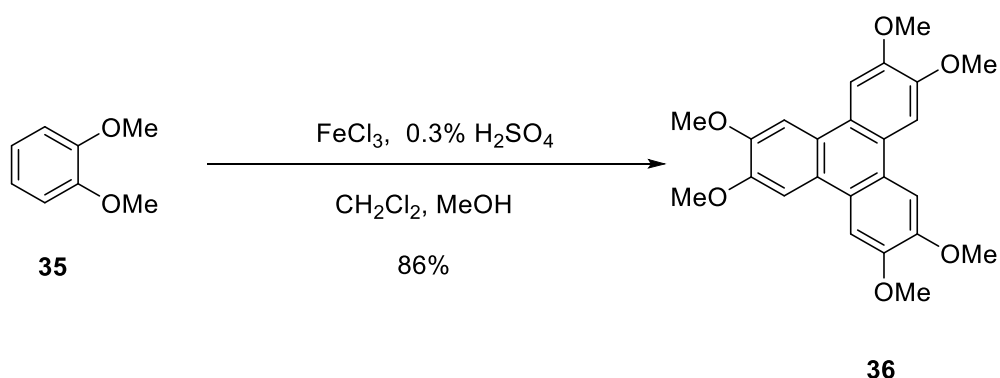


Scheme 1.11: Benzotriphenylene synthesis **34**.

Therefore, TP can be prepared with substituents other than alkoxy in a way that is difficult in other ways, for instance benzoannelated triphenylene [36]. In addition to Friedel-Crafts cyclization, cationic cyclizations, and classical carbanion reactions, the Wittig reaction can also be used to prepare functionalized triphenylenes [25].

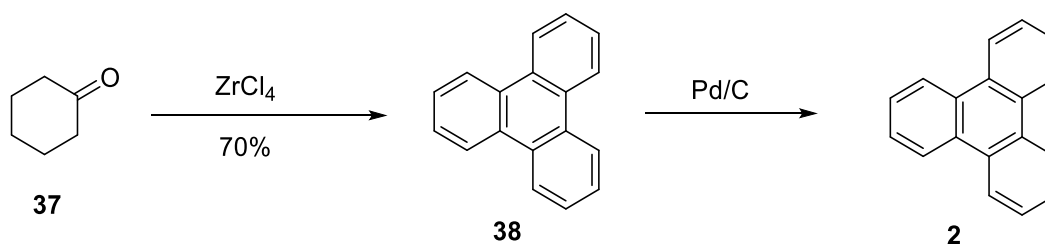
Type 5: from 6-membered rings using cyclotrimerization step:

Triphenylene is synthesised by the formal trimerization of 6-membered rings. One of the classic ways of synthesising triphenylene is by oxidative trimerization, as demonstrated in the figure below, which provides an example of this process. Since the discovery of hexaalkoxytriphenylenes' liquid crystal nature and properties, a significant amount of research has been devoted to their synthesis. In this procedure, symmetrically substituted alkoxytriphenylenes are readily formed. The oxidative trimerization of catechol derivatives **35** was successfully achieved in 1960 by Mannich by using FeCl_3 as an oxidant agent in sulphuric acid. Bushby and co-workers [30] later improved the experiment, and they optimised the conditions in order to achieve a higher yield. In the modified experiment, concentrations of sulfuric acid H_2SO_4 were decreased to 0.3%, and methanol was used as the reducing agent for work-up to stop the reaction [37].



Scheme 1.12: Dimethoxybenzene **35** undergoes an oxidative trimerization to yield **36**.

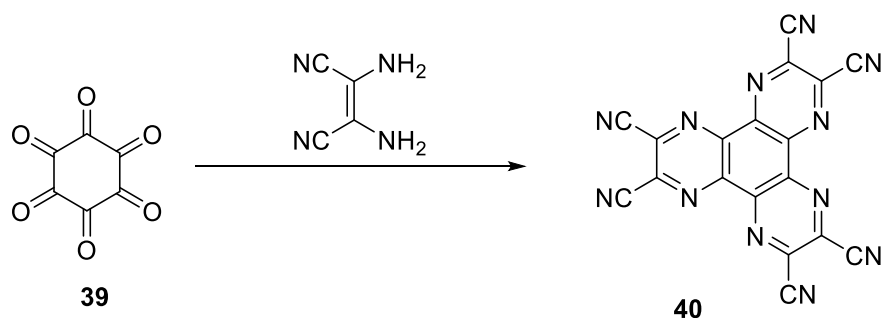
It is possible to use a number of oxidising agents (e.g., MoCl_5 or VOCl_3) in conjunction with these conditions to produce a variety of substituents, including hydroxyls, crown ethers, and chiral groups. It should be noted that Mannich's original procedure for the oxidative cyclization of cyclohexanone, the H_2SO_4 catalysed trimerization, has hardly been used since 1960, but alternative procedures have been developed that utilise catalysts such as HfCl_4 , ZrCl_4 , or Cp_2ZrCl_2 [38]. Aldol/dehydration reactions are used instead of oxidative cyclizations in these cases. The intermediate must then be dehydrogenated in order to yield triphenylene.



Scheme 1.13: Triphenylene **2** is synthesised from cyclohexanone.

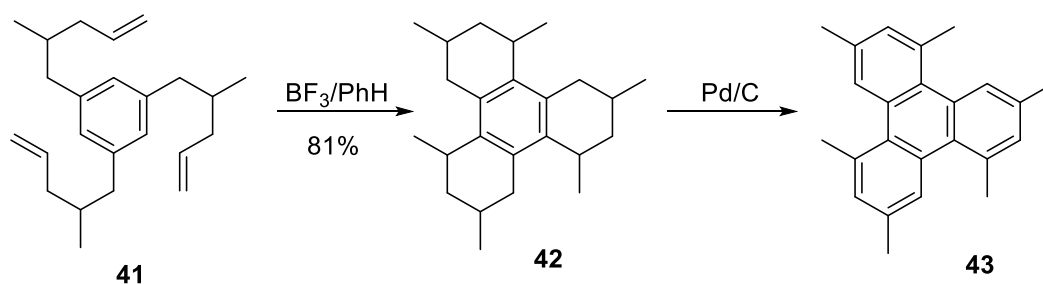
Type 6: Synthesis by adding peripheral rings in one step

Prior methods of synthesising TP and its derivatives relied on varying precursors. Although there have been a few preparations of TP by one-pot synthesis, this method is often used to prepare compounds that are difficult to synthesise using standard techniques. Recently, aza-triphenylenes have attracted increasing attention for their synthesis and properties. Examples of compounds in the literature of this type are shown in Scheme 1.14. [39]. The majority of heterocyclic analogues similar to compound **40** have been prepared by the condensation of hexaketocyclohexane **39** with 1,2-diaminoethylene derivatives.



Scheme 1.14: Synthesis of substituted hexa-aza-triphenylenes **40**.

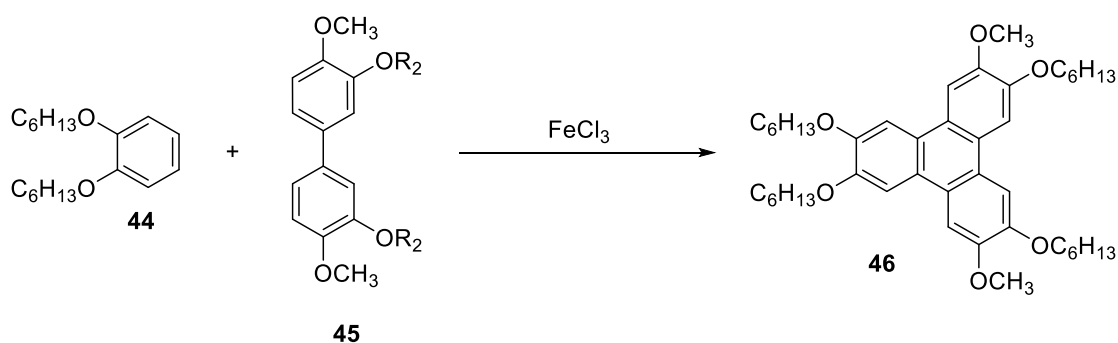
It is also possible to utilise acid cyclisation methods with benzene derivatives to synthesise TP derivatives, as in the example shown in the scheme showing the cyclisation of **41** using an acid catalyst. This produces **42**, which can be further dehydrogenated with palladium on carbon to produce **43** (Scheme 1.15) [40]. It is possible to compare these reactions directly to those previously described (Scheme 1.9), since they are also Friedel-Crafts cyclisations.



Scheme 1.15: Cyclisation of **41** to yield **43** by acid catalysis.

Methods for synthesising unsymmetrical triphenylene cores:

Triphenylene structures containing unsymmetrically substituted triphenylenes have received much research attention because they offer the possibility of introducing functional groups. In order to produce these compounds, oxidative coupling of benzene derivatives and biphenyl derivatives with iron (III) chloride has long been used. A reductive step is required using methanol during this process. An oxidative coupling of 1,2-disubstituted benzene **44** with its biphenyl derivative **45** is illustrated in Scheme 1.16. Ferric chloride is used in the process that yields unsymmetrically substituted triphenylene **46**.



Scheme 1.16: Synthesis of triphenylenes **46** from biphenyl.

In addition to using this successful procedure [41], electron-withdrawing aldehydes and nitrile groups, electron-deficient pyridines, and electron-rich thiophenes and furans were also explored by modifying a functionalised TP core [42].

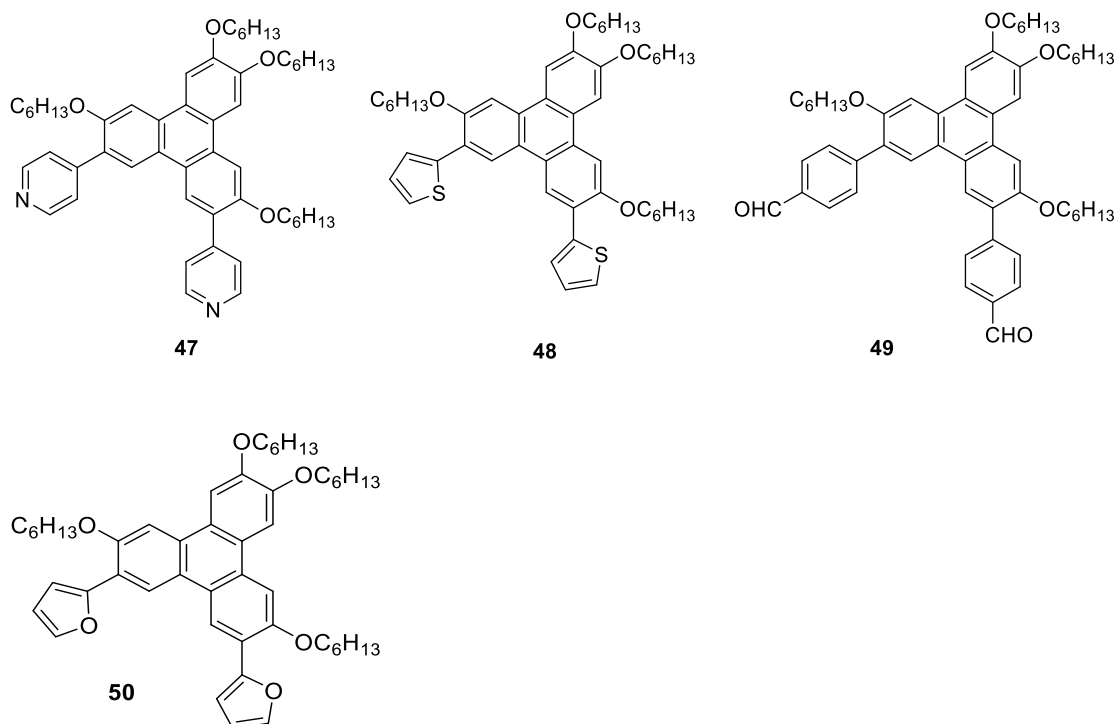
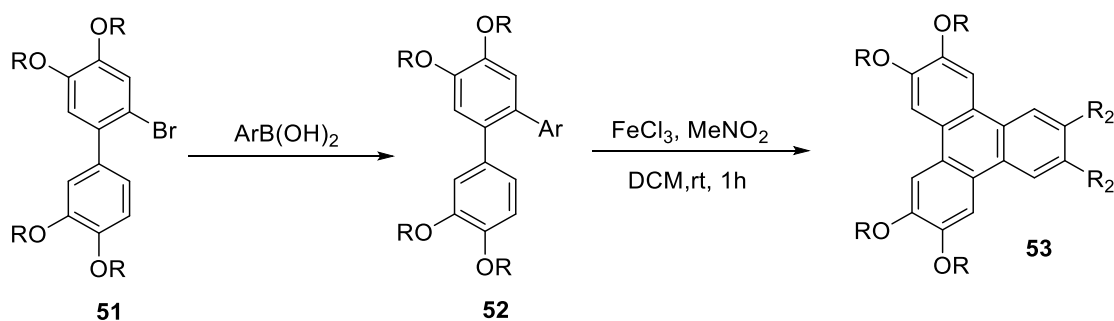


Figure 1.11 Functionalised unsymmetrically substituted triphenylenes.

According to Zhang *et al.* (2017), new triphenylene derivatives were synthesised using the triphenylene core as the starting point. Suzuki cross-coupling reactions between biphenylene derivatives and different boronic acids resulted in the intermediate terphenyl **52**. Through the use of ferric chloride, it is possible to create tetra (alkyloxy) triphenylene **53** [43].



Scheme 1.17 Asymmetric triphenylene derivatives synthesis.

1.9 Triphenylene applications:

1.9.1 Liquid crystal displays

It is necessary for electronic devices, such as computers, to transmit information to an optoelectronic device (display), so that we can interact with them. Therefore, the development of these screens has evolved along with the advancement of technology. A major factor contributing to the success of liquid crystal displays (LCDs) is their application on flat screens and their low power consumption, which allows them to be installed in portable instruments such as calculators, watches, laptops, mobile phones, etc. It operates by controlling the light that passes through it, which is composed of small areas called pixels, to expose the information: certain areas remain dark, whereas others remain bright. These devices can utilise both ambient light, which consumes less energy, as well as electrically generated light. The amount of this light that passes through the device may be controlled in order to create areas of intermediate clarity, resulting in grayscale. The first LCD to be produced was the twisted nematic device (TN-LCD), developed in 1971 by Martin Schadt and Wolfgang Helfrich, as well as independently by James Fergason [44]. It is composed of a nematic liquid crystal, either in pure form or as a mixture of several mesogens. It lies between two alignment layers arranged perpendicularly, allowing the director to make a 90° turn. In order for the generated polarised light to be parallel to the direction of orientation of the layers, two polarizers are placed at the top and bottom of the cell. Once the incident light has passed through the first polarizer, it passes through the cell, rotating the polarisation plane by 90° , passing through a second polarizer to produce a bright pixel (off state). When the liquid crystal molecules position themselves perpendicularly to the cell when an electric field is applied, the cell's polarisation plane is not changed, and it is unable to traverse the second polarizer, resulting in a black pixel (on state) [45].

The main issue with this device is the loss of image quality when the viewer is not centred on the screen. Fuji Photo Film developed discotic liquid crystal film to solve this problem, which increases the viewing angle and improves contrast [46].

A second type of LCD uses chiral smectic liquid crystals in preference to nematic ones. In these structures, the helix can be unwound by introducing the material between two surfaces coated with an aligning agent, thereby causing a spontaneous polarization perpendicular to said surfaces and obtaining surface-stabilized ferroelectric liquid crystals [47]. The generated cell is placed between two crossed polarizers forming an angle of 90° between them. The polarized light is blocked at the second polarizer when the material is not affected by it. In this case, the

cell appears black (off state). As a result of the electric field applied, the molecules are able to change their orientation, which allows them to rotate the plane of polarization of the incident light, allowing it to pass through the second polarizer and appear brighter (on state). The viewing angles of these devices are better and the switches between the two states are faster than those of nematic devices. This type of application is not suitable for discotic liquid crystals. As Chandrasakhar and his collaborators discovered, nematic discotic liquid crystal displays have a slower change time between states than calamitic [48].

1.9.2 Organic light-emitting diodes

OLEDs are light-emitting devices that use an organic sheet as the source of light. There are two types of OLEDs: monolayer and multilayer [49]. In monolayer OLEDs, the organic material is sandwiched between a transparent anode and a metallic cathode. Under the influence of the field, the electrons and holes injected into the organic material are transported.

In multilayer OLEDs, the electrodes are separated from the emitting material by an electron-transporting layer and a hole-transporting layer. As a result, the energy barriers for the injection of charges from the electrodes to the emitting material can be reduced. OLEDs are characterized by their external quantum efficiency, which is defined as the number of photons emitted per number of charge carriers [50].

Luminescent materials for this type of application must satisfy a series of requirements, including energy levels suitable for injecting charges from electrodes, thin layers without gaps, and thermal, photochemical, and electrochemical stability [49].

In recent years, various discotic liquid crystals have been employed as electroluminescent materials for OLEDs because of their conductivity [51].

There are two main advantages of OLEDs over LCDs: They are much thinner and lighter, which means that they do not require a backlight, and a range of angles can be used in viewing. The organic layer is created via thermal evaporation. This process means that the thickness of the layer can be controlled under vacuum settings. Determining the colour of the photon requires knowing the energy difference between the highest occupied molecular orbital (HOMO) and the lowest unoccupied molecular orbital (LUMO) [52].

1.9.3 Photovoltaic devices:

Photovoltaic devices, or photovoltaic cells, convert light energy into electricity. This is the opposite of the process that occurs in OLEDs. It is known that the photovoltaic process consists of four stages: absorption of a photon by the cell in the form of an exciton, diffusion of the exciton to the interface between the electron donor material and the electron acceptor, dissociation of the exciton into electrons and holes, and transport of these charges to the electrodes (cathode and anode) [53].

This type of device requires materials with high mobility of charge carriers. In addition, liquid crystals form large monodomains within which molecules can be oriented in a certain direction, are capable of eliminating structural defects, and have longer exciton diffusion lengths. Schmidt-Mende and his collaborators in 2001 were the first to use discotic liquid crystals in photovoltaic cells. Specifically, they used hexabenzocoronene derivatives as electron donor materials and perylene as a material [54].

As reported by Chen and colleagues, the reason for the enhanced separation of charges and transfer efficiency is the modification of nanoparticles with triphenylene fragments. An example of that modification was the use of zinc oxide nanoparticles to introduce dithiol-functionalised triphenylene ligands (Fig.1.12) [55].

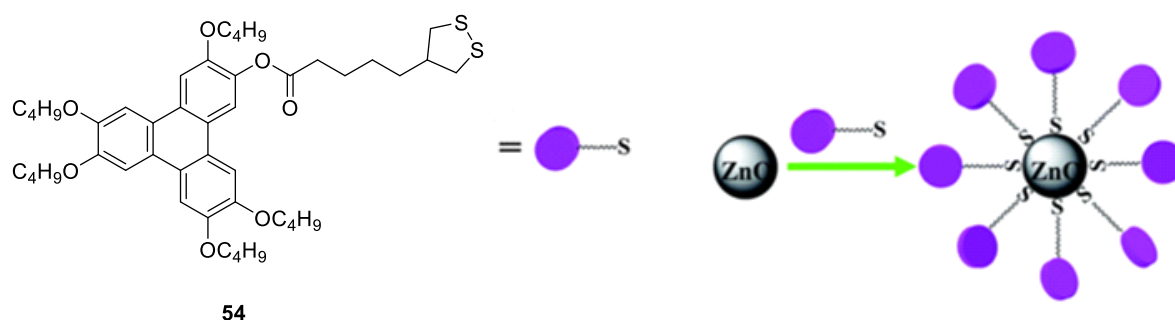


Fig.1.12 Structures of dithiol-functionalised triphenylene ligands and ZnO nanoparticles.

1.9.4 Organic Field Effect Transistor (OFET):

It is a device that operates by applying an external electric field to a third electrode to control the flow of charge between a cathode (source) and an anode (sink).

Thus, the external voltage applied causes current to flow or not flow between a source and sink. In organic field-effect transistors (OFETs), organic semiconductor materials serve as a charge carrier between a source and a sink [49].

As a result of liquid crystals' conductive properties, they have been used as semiconductors in OFETs. Creating load conduction channels between the sink and the source is required for its operation. In discotic liquid crystals, due to their columnar packing, conduction channels are generated along the columnar axes, requiring them to adopt a homogeneous alignment. As a result of their layered structure, smectic calamitic liquid crystals can also be used as semiconductor materials. To promote transport in this situation, the molecules must adopt a homeotropic alignment. There have been promising results obtained with mesogens derived from thiophene [56].

1.9.5 Other applications:

Lasers: It is possible to make lasers using chiral calamitic liquid crystals [57]. Their advantages include the ability to fabricate smaller lasers, ease of manufacture, as well as the possibility of designing modular devices [58].

Thermal sensors: they operate on the principle that chiral nematic liquid crystals can change their pitch, and therefore the wavelength of reflected light, as a result of thermal effects. As a result, different temperatures are indicated by different colours [59].

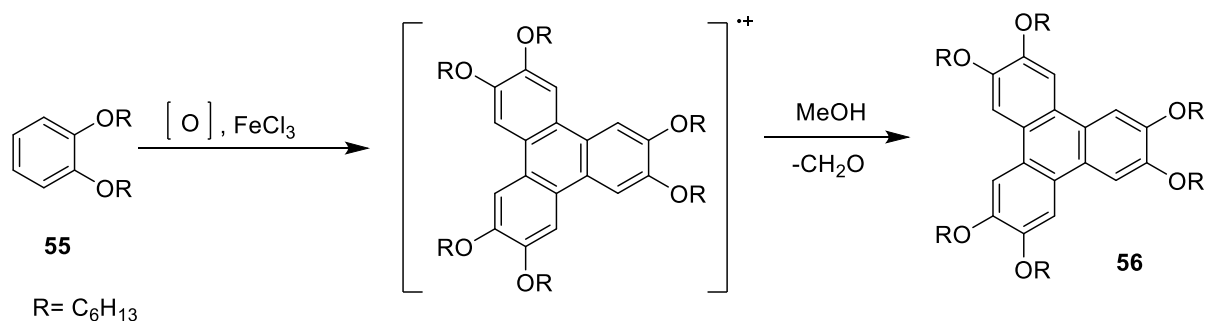
Mesoporous Solids for Catalysis: Lyotropic liquid crystals can be used to create porous inorganic materials. When the micelles are removed, the material has the same size and order of pores as the micelles [60].

The operation of gas sensors is based on the different electrical response's liquid crystals exhibit in the presence and absence of dopants, allowing them to detect vapours of chemical substances [61]. There are also Xerographic processes: they are the basis for the operation of photocopiers and laser scanners. It is possible to generate electrostatic images of the documents to be copied using this photoconductive material [62].

1.10 Synthesis and mesophase behaviour of Hexaalkoxytriphenylenes:

Hexaalkoxytriphenylenes have traditionally been synthesized by oxidative trimerization of 1,2-dialkoxybenzene by using the Scholl reaction (Scheme 1.18). The original method of trimerization used chloranil [63] as an oxidant in 67% sulfuric acid [64]. Using the first method,

1,2-dimethoxybenzene can be trimerized with excellent yields, while the reaction is slow, and cannot be performed at scales greater than 1 gram. To obtain high yields, Bengs et al. introduced the use of FeCl_3 in H_2SO_4 as an alternative oxidizing agent [65], and Boden et al. showed that the acid was used in small quantities or was not necessary, in some cases, to obtain high yields, if FeCl_3 in CH_2Cl_2 was used as an oxidizing medium. Methanol has also been introduced as a powerful reduction agent for radical carbocations, releasing formaldehyde and simplifying the purification of the desired product. Due to its high yield and large scale, this method has been widely used for many types of dialkoxybenzenes [37]. In recent years, other oxidizing agents, such as MoCl_5 [66] and VOCl_3 [67], as well as alternative reaction solvents, such as nitromethane [68], have been used to improve the solubility of oxidizing agents.



Scheme 1.18: Oxidative coupling of dialkoxybenzenes.

One of the most widely studied classes of discotic liquid crystals are triphenylene derivatives. In common with other disk-like compounds, triphenylene exhibits a strong tendency to form columnar mesophases, particularly the symmetrical derivatives **56** [69].

Mechanisms of triphenylene formation:

Despite the fact that Scholl reactions are one of the oldest methods of forming C-C bonds, the mechanism behind triphenylene formation, which is composed of three successive Scholl reactions, has yet to be fully clarified, with the final cyclization step causing the most controversy in the literature. It has been established that there are two possible mechanisms for this reaction: the first utilizes arenic cations while the second utilizes radical cations (Figure

1.13). The first mechanism was suggested by King et al. based on computational results [70], whereas the second mechanism was suggested by Rathore et al., based on experimental evidence, including the confirmation of the existence of the radical cation [71]. There is a possibility that both mechanisms may operate simultaneously due to the coexistence and ease of exchange between the arenic ions and radical cations used in the Scholl reaction (acid and oxidizing conditions).

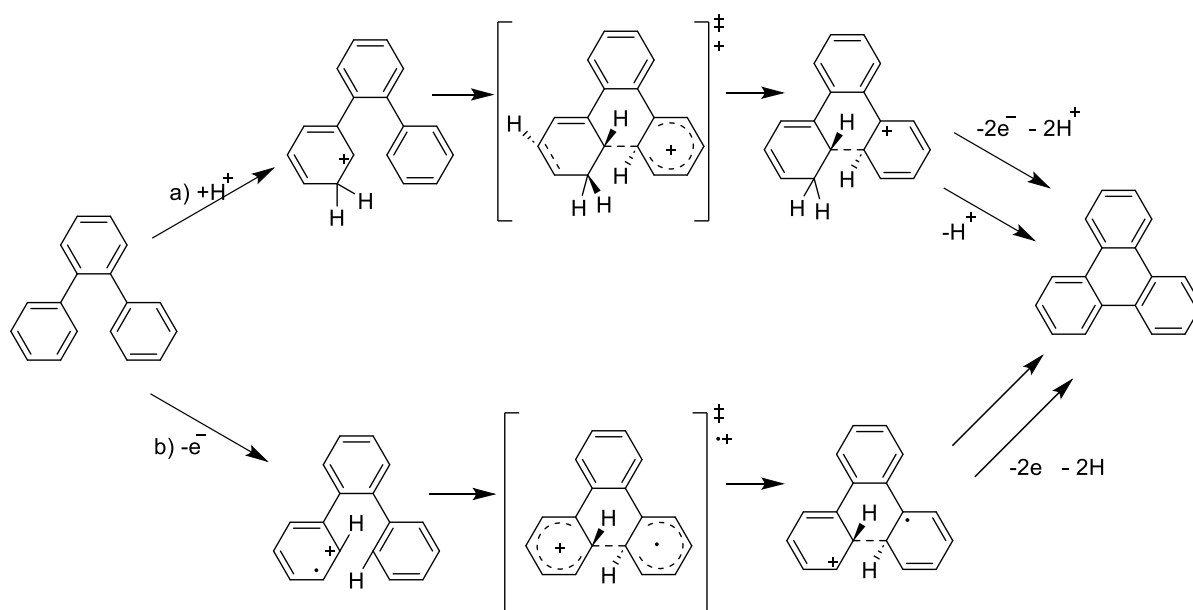
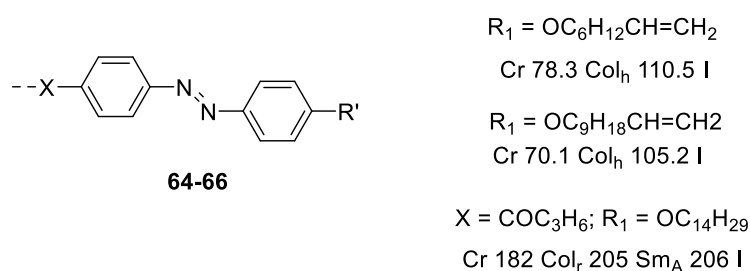
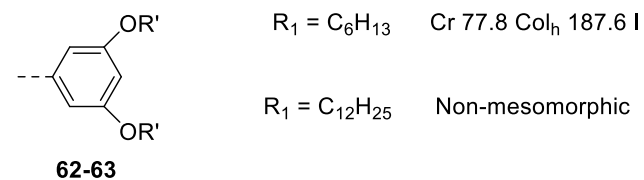
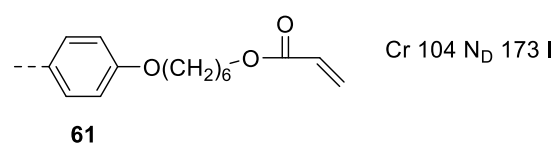
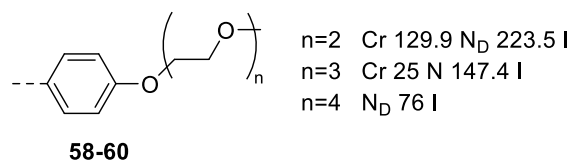
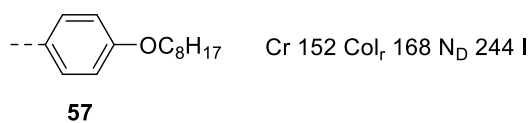
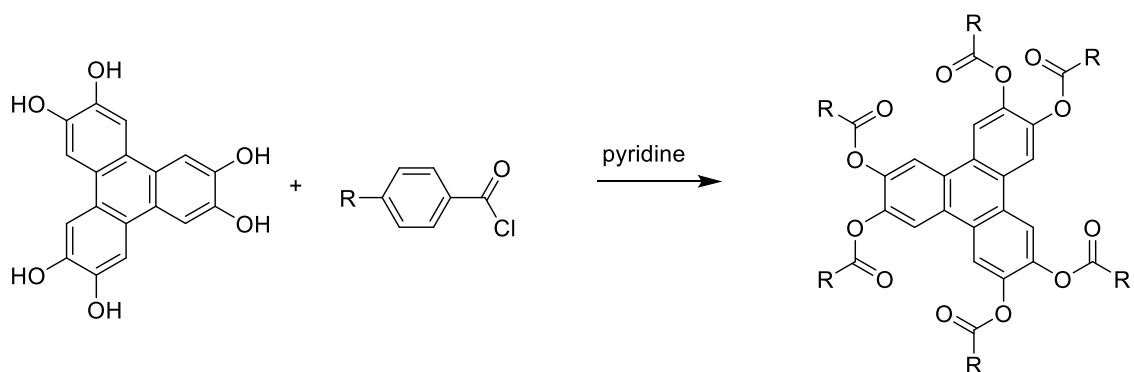


Figure 1.13: Triphenylenes mechanism via arene cations or radical cations by the Scholl reaction [72].

Symmetrical Hexahydroxytriphenylene:

A series of triphenylene compounds **57-63** have been prepared by esterification reaction of hexahydroxytriphenylene with benzoyl chloride derivatives in pyridine to produce different triphenylene hexaester compounds [73]. Their synthesis is shown in Scheme 1.19.



Scheme 1.19: Triphenylene hexabenzate esters.

Numerous groups have investigated the mesomorphic properties of triphenylenes based on these symmetrical benzoate derivatives, mostly because they produce the rarer nematic mesophase in some cases.

Cheng and coworkers [74] studied the structure and phase transitions of **57** in detail and confirmed it.

It has been reported by Kohmoto and co-workers that triphenylene derivatives containing polyethyleneoxide as side chains have been synthesized. Nematic phase was observed at room temperature for these derivatives (**58–60**) [75].

The compounds were transformed from N phase to Col_h phase when alkali metal ions like Li⁺, Na⁺, etc. were added. N phase to Col_h phase transformation was found to be highly dependent on counter ions. Nematics with terminal acrylate functionality are also tolerated, such as **61** [76].

For symmetrical benzoate derivatives **61** with (terminal acrylate unit), nematic phase widths decreased, whereas **57** and **58** with (alkoxy and polyethyleneoxide) showed increased phase widths.

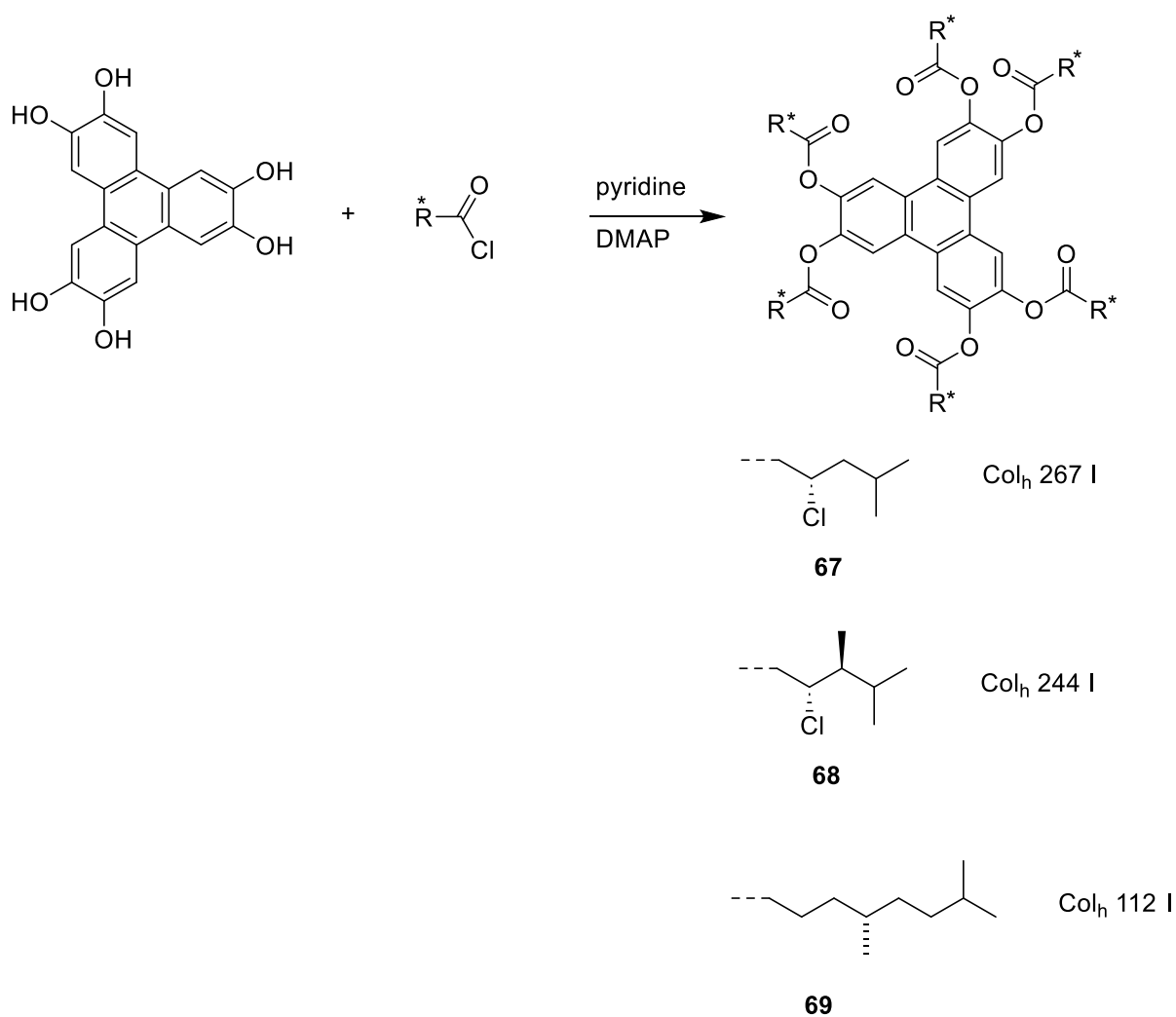
Two triphenylene compounds (**62–63**) substituted with 3,5-dialkoxy benzoates have been synthesized by Picken and colleagues [77]. Among the compounds examined, only compound **62** was found to possess distorted hexagonal mesophases with strong lateral order, which is somewhat unusual.

The hexagonal Columnar phase (Col_h) of triphenylene-based discotic liquid crystalline monomers containing an azobenzene moiety has also been reported by Rahman *et al.* [78]. The phase behaviour changed from discs-like (Col_r) to rod-like (SmA) by changing the linkage with longer alkyl terminal chains from C10 to C14 (**66**) [79].

In addition, it has been shown that it is possible to produce chiral triphenylene esters **67–69** by esterifying with chiral carboxylic acids, which display hexagonal columnar mesophases (Scheme 1.20).

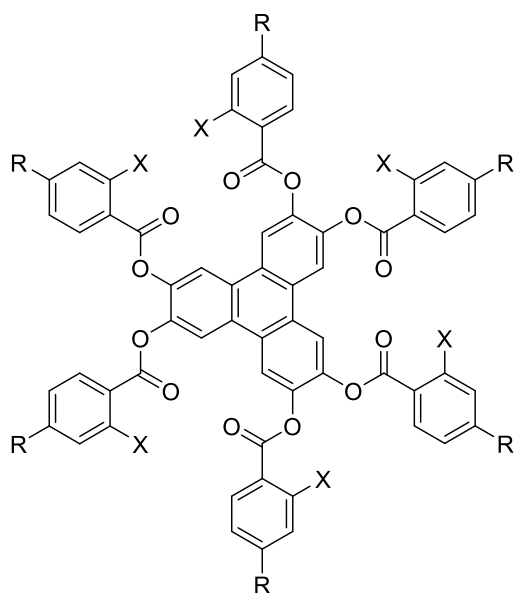
The process of synthesis for these derivatives is the same as that for the prior derivatives with the extra step of the addition of DMAP [80].

As a result of the mesomorphic properties of the series, chiral Col_h phases have been discovered.

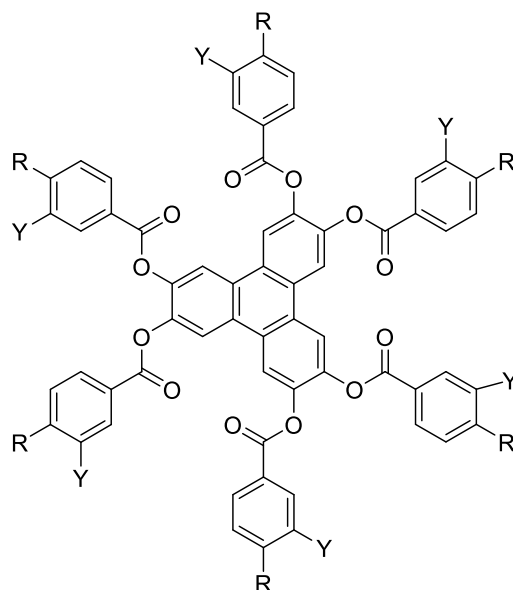


Scheme 1.20: Triphenylene hexalkyl esters.

In addition to the derivatives shown in Scheme 1.19, substituted derivatives containing additional substituents on the phenyl groups have also been prepared. The method of synthesis for these derivatives follows the same approach as that used with the previous derivatives.



- 70a** R= OC₁₀H₂₁, X= Me Cr 107 N_D 162 I
70b R= OC₁₀H₂₁, X= Et Cr 117 N_D 131 I
70c R= OC₁₀H₂₁, X= i-Pr mp 93 (monotropic N_D below 70)
70d R= OC₁₀H₂₁, X= F Cr 150 N_D 213 I

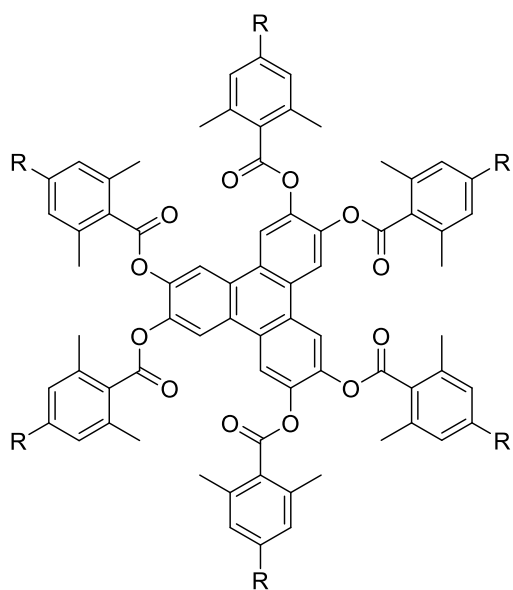


- 71a** R= OC₁₀H₂₁, X= Me Cr 102 N_D 192 I
71b R= OC₁₀H₂₁, X= Et Cr 129 N_D 206 I
71c R= OC₁₀H₂₁, X= i-Pr Cr 161 N_D 202 I
71d R= OC₁₀H₂₁, X= t-Bu Cr 194 N_D 225 I

Figure 1.14: Hexabenzotriphenylene esters bear additional substituent on the phenyl groups and one methyl group.

Although the mesophase ranges tend to be wider when the additional group is introduced meta to the ester link, there is considerable tolerance for introducing a single alkyl substituent on the benzoate (Figure 1.14) [81, 82]. Derivatives **71d** exhibited broad nematic phases. Significantly, it was possible to switch between Col_h and N_D phases by increasing temperature for an additional group, which introduced meta to the ester link.

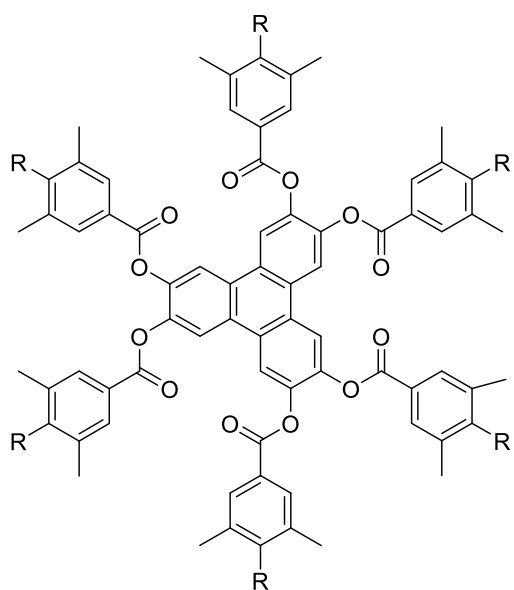
The behaviour of nematic mesophases in derivatives that contain two methyl groups on each benzoate is similar (Figure 1.15). The transition temperatures are significantly lowered when methyl groups are aligned ortho to the ester link [83], and no columnar phase is observed. Derivatives **73a** had a wide range of nematic phases.



72a R= OC₆H₁₃, Cr 170 N_D 196 I

72b R= OC₈H₁₇, Cr 155 N_D 170 I

72c R= OC₁₀H₂₁, Cr 108 N_D 134 I



73a R= OC₆H₁₃, Cr 150 Col_h 210 N_D 243 I

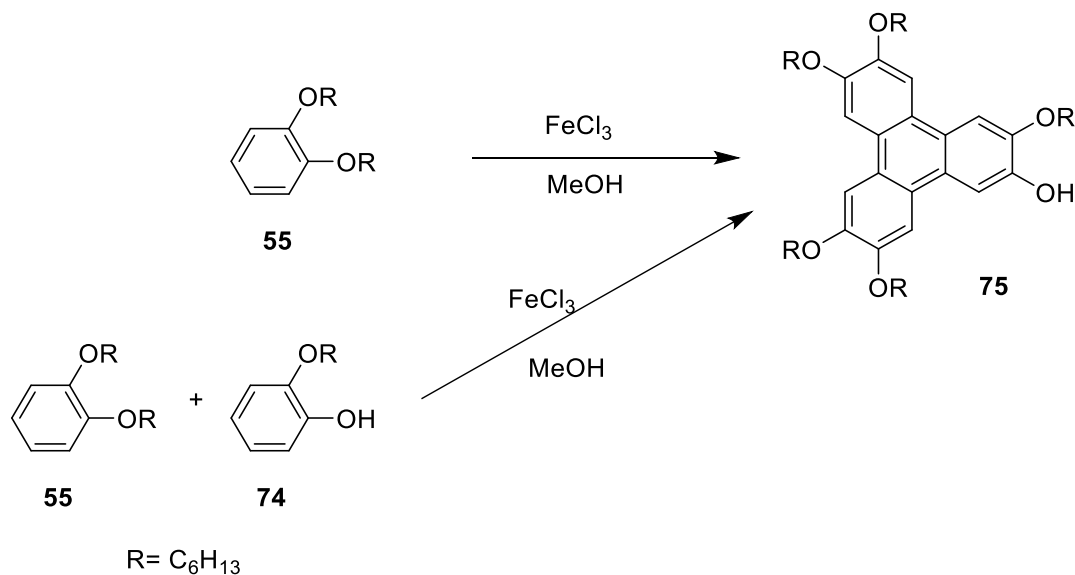
73b R= OC₈H₁₇, Cr 170 Col_h 195 N_D 215 I

73c R= OC₁₀H₂₁, Cr 157 Col_h 167 N_D 182 I

Figure 1.15: Triphenylene hexabenzote esters including two methyl groups.

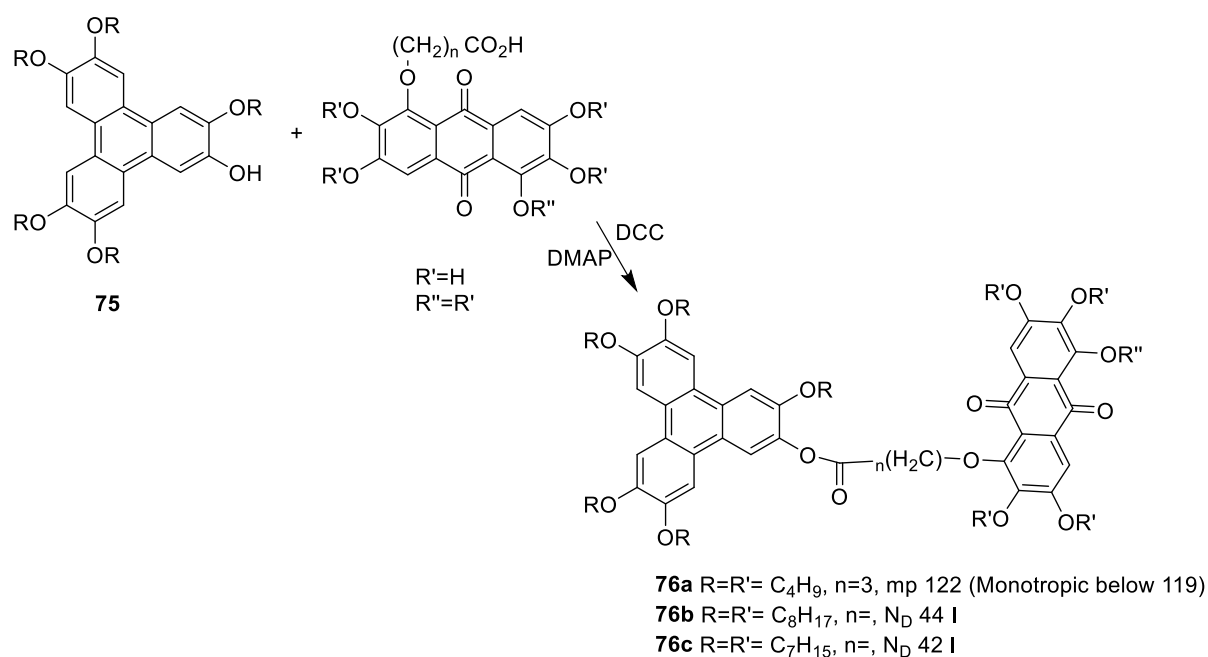
1.11 Synthesis and mesophases of Monohydroxypentaalkoxytriphenylene (2-hydroxy-3,6,7,8,9-pentaalkoxytriphenylenes):

Monohydroxy functionalised triphenylene is a key precursor in the synthesis of different LCs. This may be made via by two known routes. it can be synthesized directly from dihexyloxybenzene **55** (oxidative trimerization followed by hydrolysis) [84] or from dihexyloxybenzene **55** and hexyloxyphenol **74** via oxidative trimerization [85].



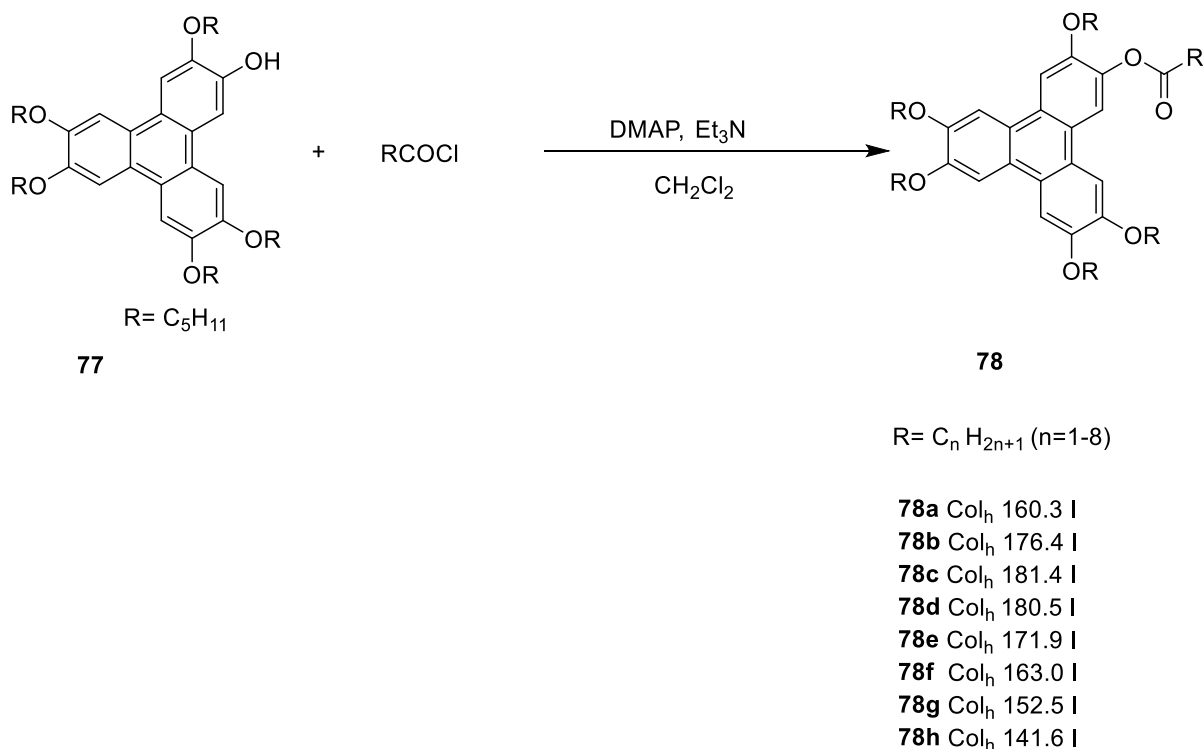
Scheme 1.21: Synthesis of Monohydroxypentaalkoxytriphenylene **75**.

Compounds **76a-c** were prepared by Prasad and coworkers linking triphenylene (donor) and anthraquinone (acceptor) units. They have been prepared by esterification reaction of monohydroxypentaalkoxytriphenylene with anthraquinone intermediate in DCC/DMAP to produce different monohydroxypentaalkoxytriphenylene esters compounds. These compounds exhibited mesomorphism as shown in scheme 1.22 [86]. Thermal studies showed that both substituents **76b** and **76c** display discotic mesophases, namely N_D phases.



Scheme 1.22: Esterification reaction between monohydroxypentaalkoxytriphenylene and anthraquinone.

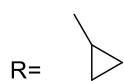
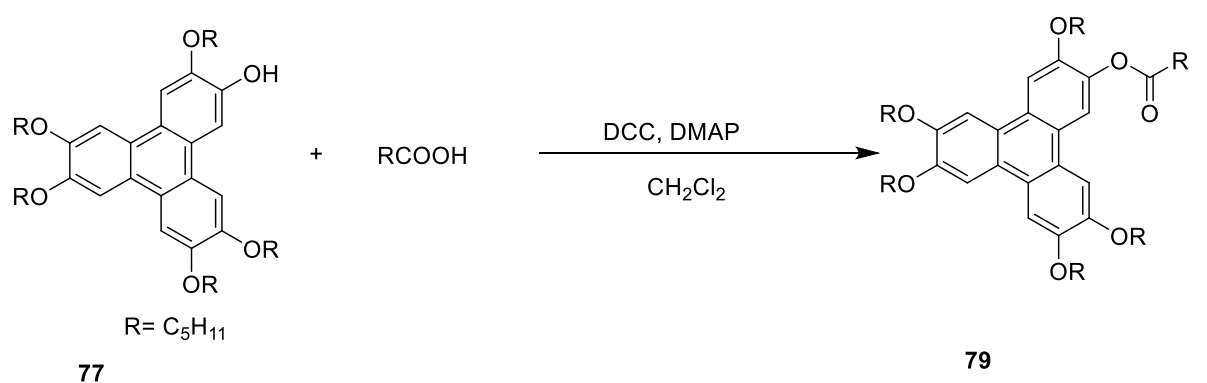
Another example of the esterification reaction of Monohydroxypentaalkoxytriphenylene, $\text{R}=\text{C}_5\text{H}_{11}$ with acid chloride derivatives in triethylamine and DMAP produced a sequence of triphenylene compounds **77a-h**. The mesophase was hexagonal-columnar (Col_h) for all compounds as shown in scheme 1.23 [87]. Increasing the n -alkyl chain resulted in higher transition temperatures for Col_h mesophases for $n = 1-4$ while decreasing for $n = 5-8$.



Scheme 1.23: Esterification reaction of Monohydroxypentaalkoxytriphenylene with acid chloride derivatives.

It was reported by Wei and co-workers that two series of 2- (**79a-f**) and 3,6-position bulky group substituted triphenylene esters (**81a-f**) were synthesised by adjusting the steric hindrance of bulky substituents by using cycloalkylane, adamantane, and furan molecules. They exhibited stable hexagonal columnar mesophases over a wide temperature range. Increases in steric hindrance caused by different cycloalkyl substituent conformations significantly influenced both intermolecular and intramolecular ordering of columnar phases. Larger dipole-dipole interactions and steric hindrances resulted in smaller column spacing and intramolecular distance, favouring long-range ordered and perfectly aligned monodomains.

A columnar phase would become unstable if the substituents were too rigid, such as adamantane and aromatic substituents. An illustration of the synthetic routes for these triphenylene derivatives can be found in Scheme 1.24 and scheme 1.25 [88]. In particular, for 3,6-position group nonsymmetrical derivatives, mesophases with very broad temperature ranges were observed, and higher than substitution at position 2.



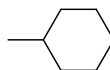
79a Col_h 171.34 I



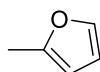
79b Col_h 181.38 I



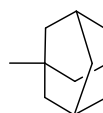
79c Col_h 184.39 I



79d Col_h 192.28 I

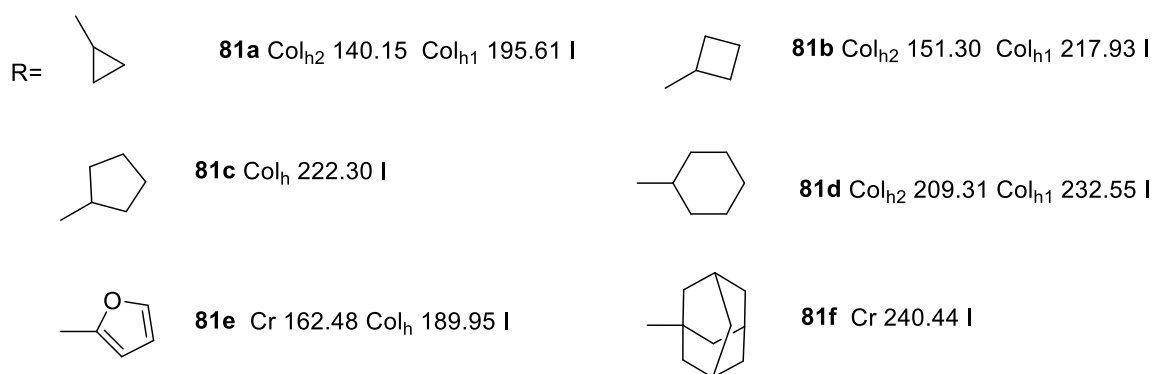
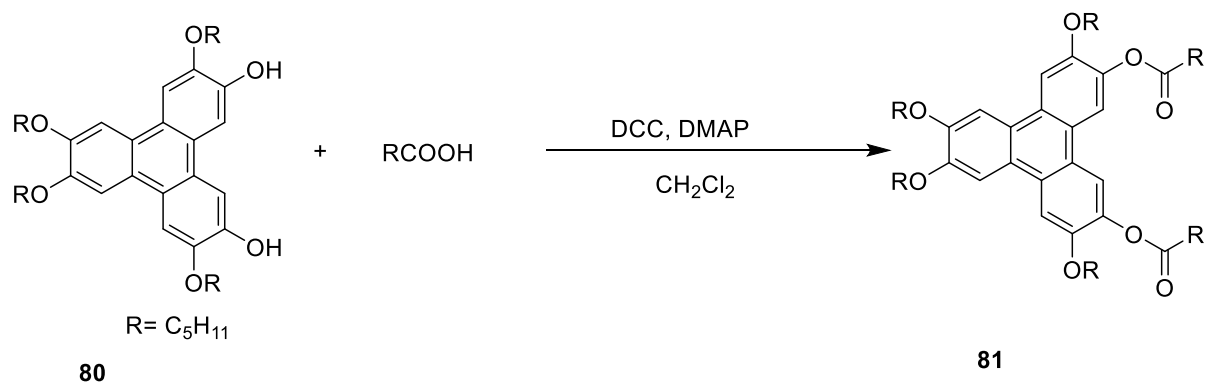


79e Cr 6.73 Col_h 174.10 I



79f Col_{hp} 133.72 Col_h 184.64 I

Scheme 1.24: 2- position bulky group substituted triphenylene esters.



Scheme 1.25: 3,6-position bulky group substituted triphenylene esters.

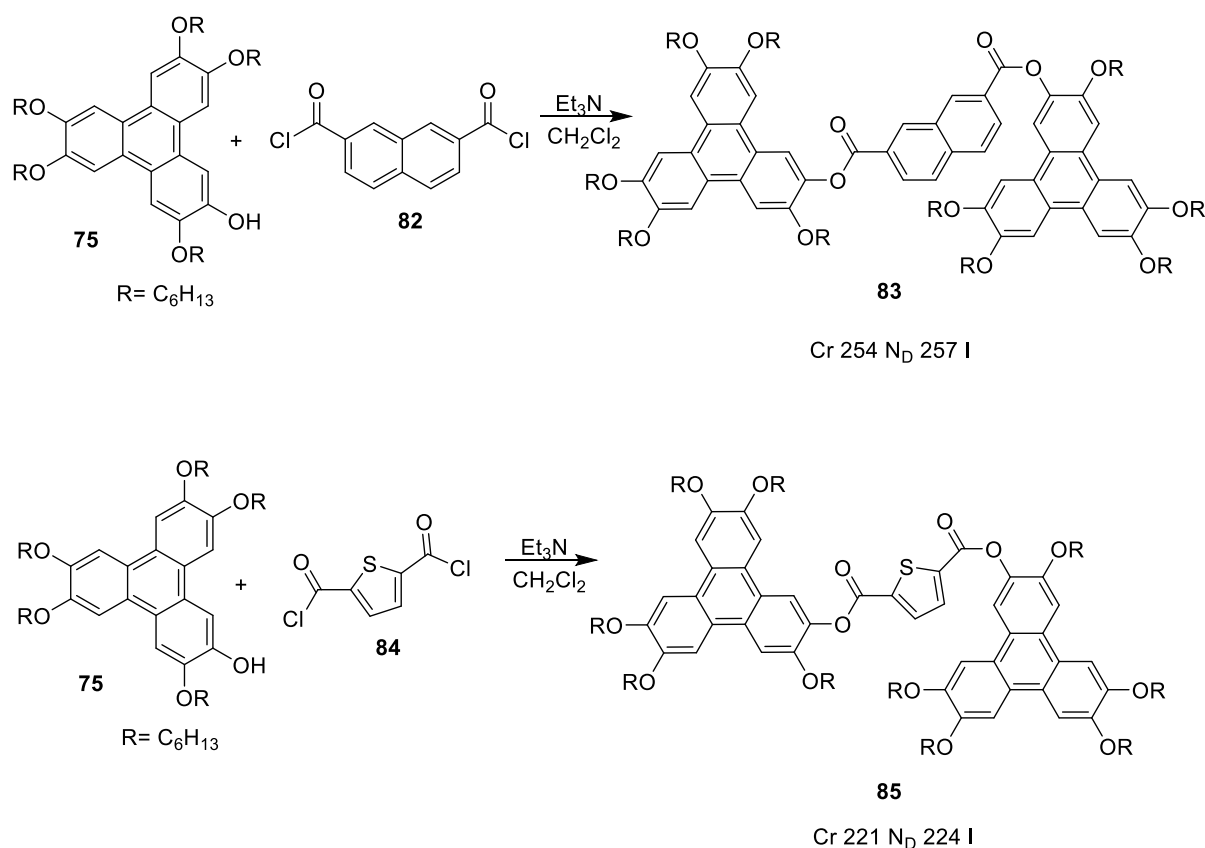
1.12 Synthesis of dimers, triads and their mesophase:

The work of our group involves twinning triphenylenes through ester and other linkages that break the symmetry of the compound, and investigating the effects of this modification on the behaviour of liquid crystals.

A number of connectors were synthesized with MHT and investigated in order to generate diads with various mesophase behaviours. The process involves converting carboxylic acid linkers into acid chlorides using oxalyl chloride. MHT has been connected to the 1,4-naphthalene dicarbonyl dichloride or with the 2,5-dicarbonyl dichloride thiophene spacer by adding triethylamine in dry DCM. This work is part of the current project, but these compounds were synthesised by other members of the group and therefore not included in the description of results and discussion.

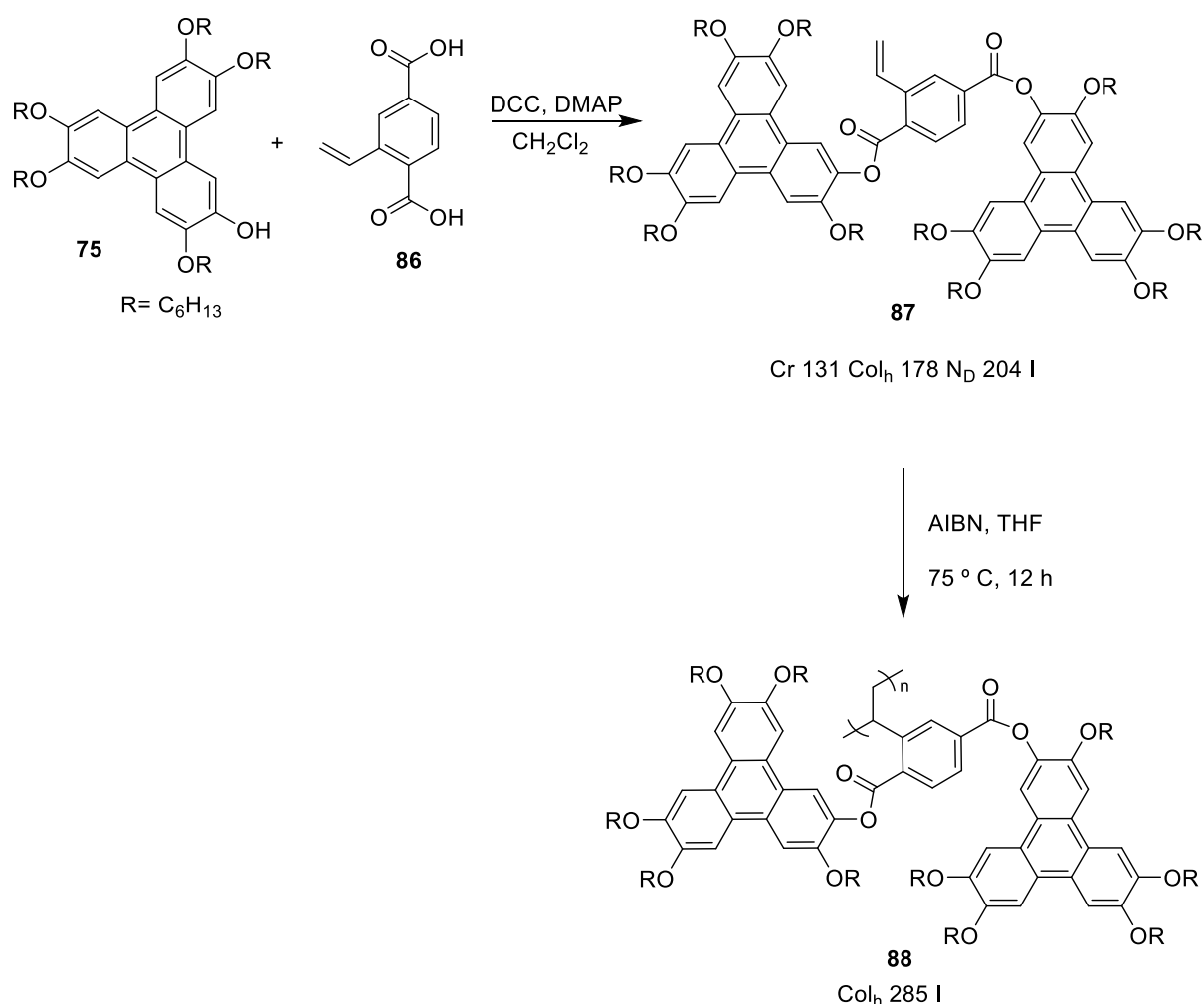
Nematic phases can form in the discotic system not only as a result of the spacer but also the angle of the linkage and the distance/flexibility of the linker (disorder).

In thermal studies, both substitutions **83** and **85** were found to exhibit N_D phases (Scheme 1.26). [89]



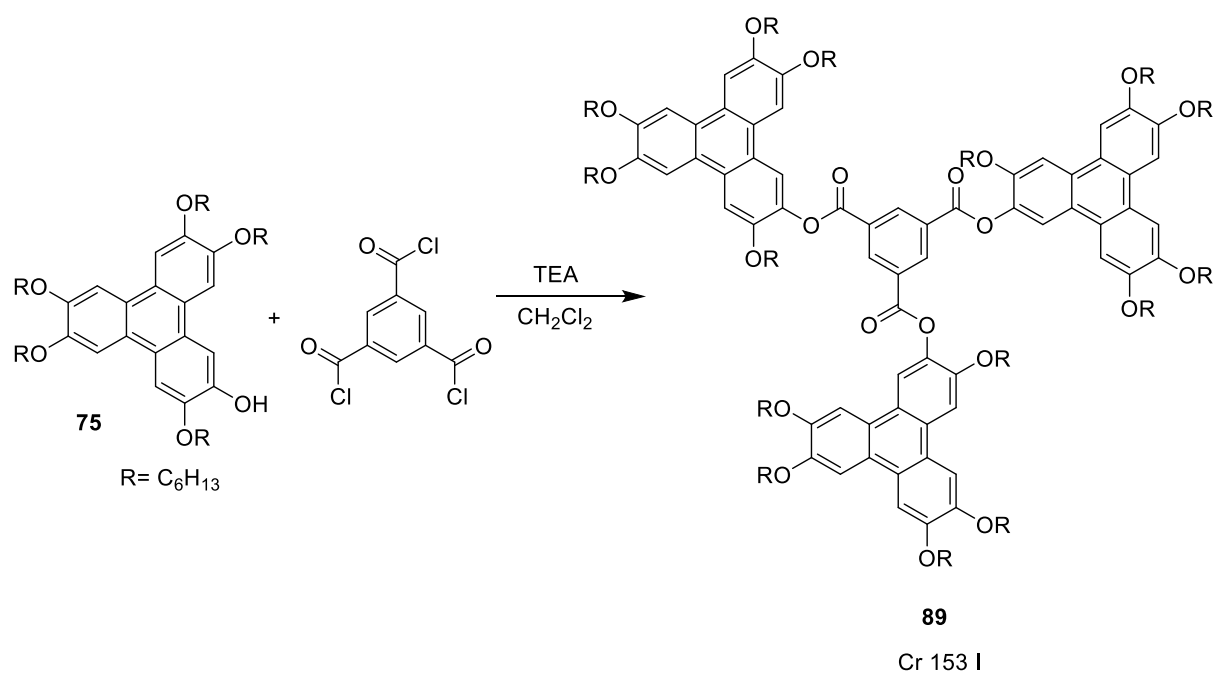
Scheme 1.26: The synthesis of triphenylene diads esters and their mesophase.

A dimer can also be formed by the reaction of 2-hydroxyl-3,6,7,10,11-pentakis(hexyloxy)triphenylene with 2-vinyl terephthalic acid via DCC condensation in DMAP and DCM. It can be transformed to a polymer with two triphenylene (Tp) units in the side chains **88** by using a conventional free radical polymerization (scheme 1.28). In the mesophase of dimer **87**, there is a hexagonal columnar structure and nematic arrangement. While poly[bis(3,6,7,10,11-pentakis(hexyloxy)triphenylen-2-yl)2-vinyl terephthalate **88** exhibits a hexagonal columnar mesophase with a relatively high glass transition temperature due to the strong coupling effect between the Tp moieties and the main chain [90].



Scheme 1.27: The synthesis of diads triphenylene esters with 2-vinyl terephthalic acid and the synthesis of that as a polymer and their mesophase.

A triad triphenylene with ester linkages (1,3,5-Benzene tricarbonyl trichloride) **89** is synthesized using dry DCM and TEA.



Scheme 1.28: The synthesis of triad triphenylene.

Despite promising characteristics, the product failed to exhibit liquid crystal behaviour and exhibited a single melting point of 153 °C. It is possible that π - π stacking interactions are enhanced due to the high degree of symmetry and aromaticity of this molecule [89].

Chapter 2: Results & Discussion

Aims of the project:

The purpose of the work described in this thesis is to synthesise a series of unsymmetrical triphenylene compounds that have one or two diverse aryl ester groups and to describe the mesomorphic behaviour of these compounds. Twins linked through different geometries were also to be targeted. The purpose of this project is also therefore to prepare dimeric systems linked by aromatic esters and specifically to demonstrate the impact of linking groups (geometry) on the behaviour of mesophases.

In several studies of liquid crystalline triphenylene, one or two ester functionalities have been demonstrated and described previously. The purpose of the present study is to complement these investigations in order to gain further insight into the relationship between structure and mesophase, and in particular to observe any onset of nematic behaviour.

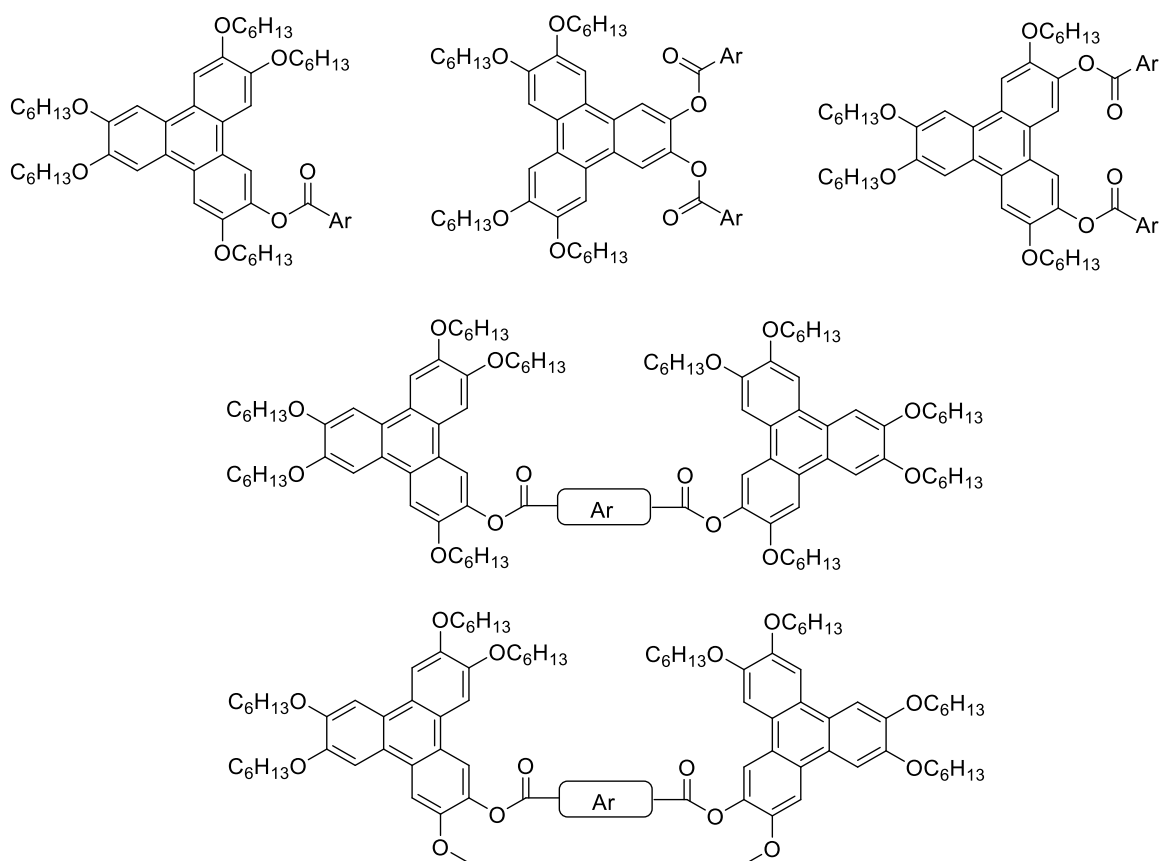
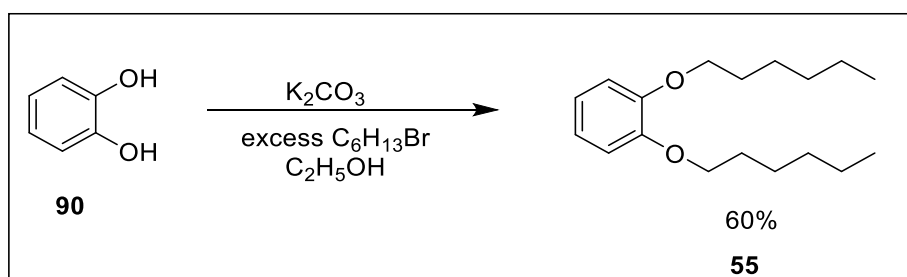


Figure 2.1: Structure of target compounds

Synthesis of MHT strategy:

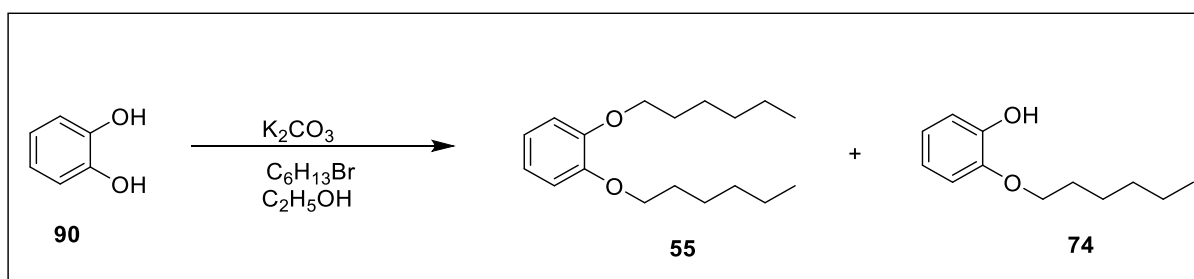
The key starting material for our series of monoesters is monohydroxy-pentahexyloxytriphenylene (MHT) and its synthesis starts from 1,2-dihexyloxybenzene (DHB). 1,2-Dihexyloxybenzene DHB is synthesised using catechol as a starting reagent, followed by Williamson ether synthesis (alkylation) with excess of hexyl bromide in a basic medium. The crude product was purified by distillation to give 1,2-dihexyloxybenzene DHB (**55**) in a yield of 60 % as a colourless oil. (Scheme 2.1).



Scheme 2.1 Synthesis of DHB (**55**)

Then, synthesis of 2-hexyloxyphenol was achieved from reacting catechol with 1 equivalent of bromohexane and potassium carbonate in ethanol. It was stopped after the proton peak of CH_2Br at 3.4 ppm of bromohexane disappeared.

After working up, the ethanol and DCM were evaporated from the mixture. The crude product was dissolved in petroleum ether and passed through silica gel. After evaporation of the solvent, a colourless oil was collected, resulting in a mixture of mono- and disubstituted catechols (2-hexyloxyphenol (69.8 %) (**74**) and 1,2-dihexyloxybenzene (27.8 %) (**55**)). (Scheme 2.2).



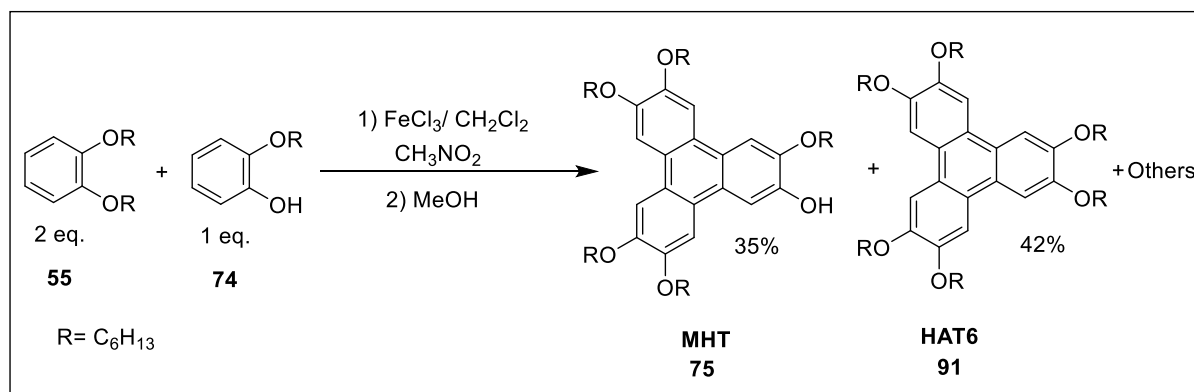
Scheme 2.2: Synthesis of monohexyloxyphenol (**74**) with 1,2-dihexyloxybenzene (**55**)

We adopted a novel approach published by our group in 2015 with a very high yield of up to 35 % of MHT **75**,[91] which prepared the path for us to conduct the research.

A mixture of 2:1 equivalent of DHB and mono-hexyloxyphenol is required for MHT production. This is accomplished by utilising NMR to calculate the ratio of isolated DHB to mono-hexyloxy-phenol and changing it to 2:1 by adding a specified amount of DHB.

Then these mixtures were reacted in an ice bath in DCM with 5 equivalents of FeCl₃. Adding nitromethane (MeNO₂) to the reaction mixture improved the yield since it increases FeCl₃'s solubility.

A TLC analysis was performed to monitor complete consumption of starting materials and the reaction was quenched by methanol. The crude was easier to separate using column chromatography since it displayed coloured bands corresponding to the various components. MHT 35% (**75**) and HAT6 42% (**91**) are both colourless compounds, but the presence of coloured bands allowed us to identify the band that corresponded to the target, MHT. Other side products (hydrolysed products) have formed, but they were not separated. It was found that using isopropanol with DCM is better than using MeOH with DCM for crystallisation after purification by column chromatography. It was determined that the correct compound (MHT) had been produced and the ¹H NMR spectrum matched the reported data (Scheme 2.3).



Scheme 2.3 Synthesis of monohydroxy-pentahexyloxytriphenylene (MHT) (**75**)

The NMR spectrum can be divided into three characteristic zones based on the regions that are common to all alkoxytriphenylenes (figure 2.2). Aromatic hydrogen signals are typically found in the region above 7 ppm. Six protons in the aromatic region of the NMR spectrum are shown in figure 2.2. Singlets appear at 7.96 ppm, possibly for the proton closest to the unprotected hydroxyl group, followed by overlapping peaks between 7.83 ppm and 7.7 ppm and another Singlets appear at 7.77 ppm. The phenolic OH, exhibits a singlet for 1H at 5.90 ppm. Overlapping multiplets of 10H are detected at around 4 ppm, attributed to methylenes bound to oxygen, which is typical of aryl ethers.

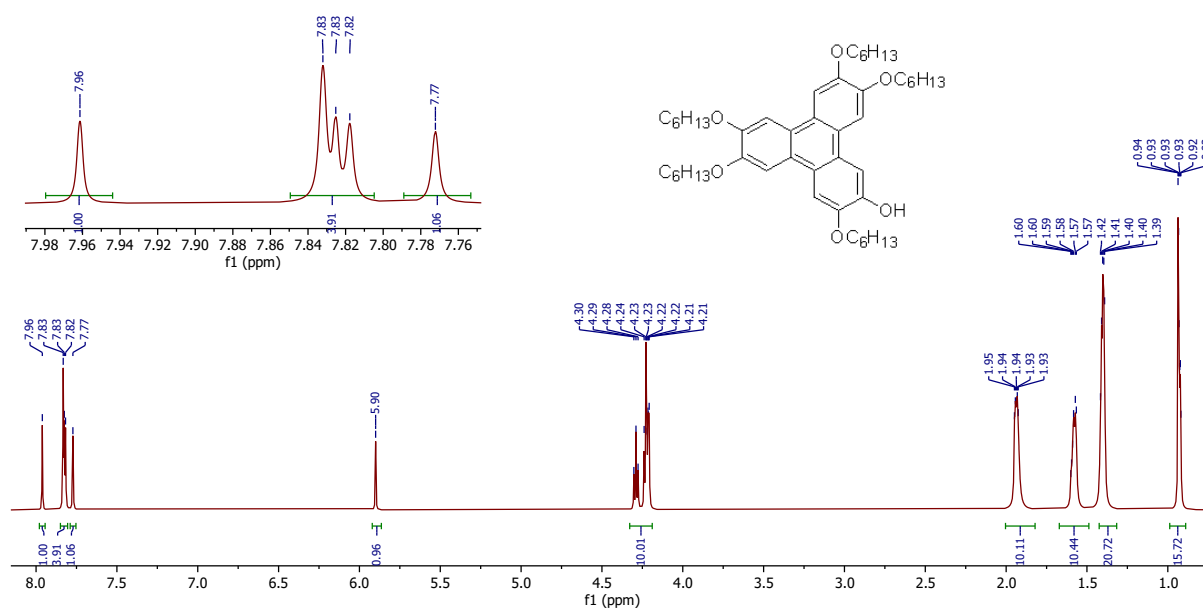


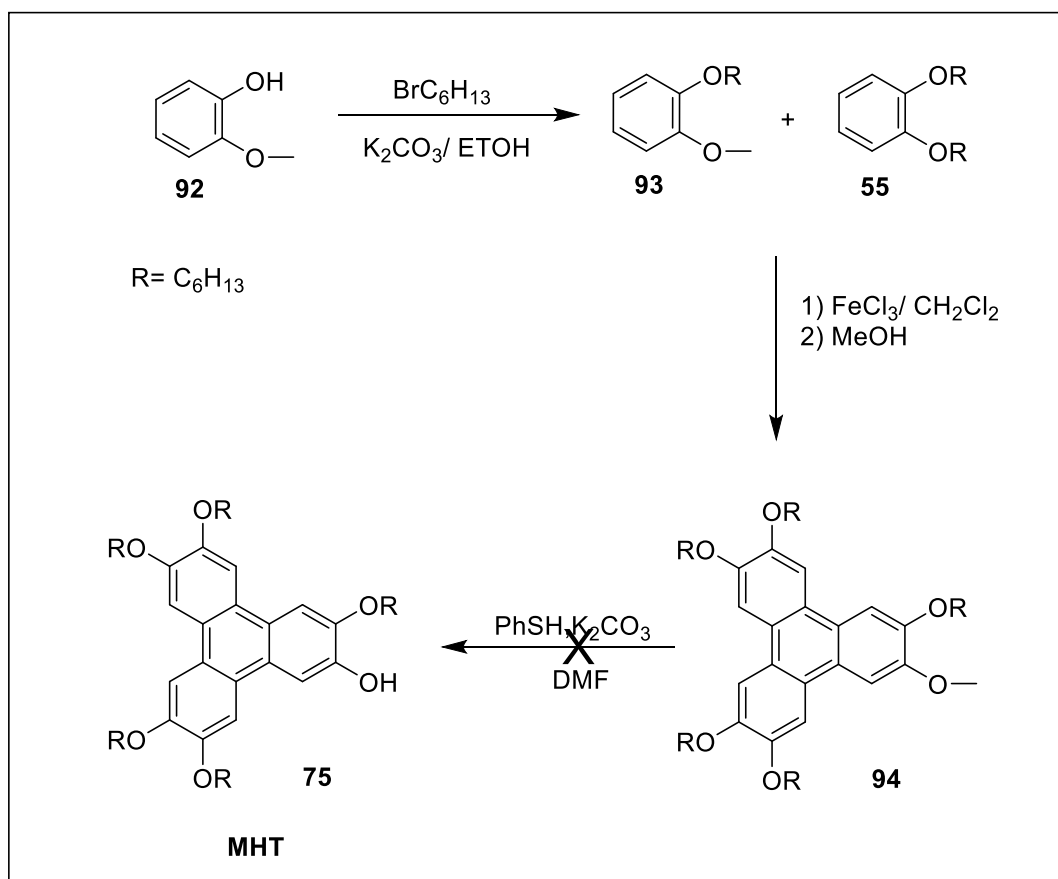
Figure 2.2: ¹H NMR spectrum of MHT (75)

Due to the difficulties encountered in previous syntheses, due to MHT purification, it is worth noting that we looked at alternative methods for this synthesis.

One alternative synthesis of monohydroxytriphenylene is the deprotection methoxytriphenylene (**94**) and it involves the cleavage of the methoxy groups to phenolic groups. Methoxytriphenylene (**94**) was achieved in the same way as for triphenylene (**75**) described earlier. However, it used DHB (**55**) (1 equivalent) and 1-hexyloxy-2-methoxy benzene (**93**) (1 equivalent) and reaction with FeCl₃. The crude product was purified by column chromatography to produce methoxytriphenylene core. Thiophenol has been applied to triphenylene ether hydrolysis. A mixture of methoxytriphenylene (**94**) (1 equivalent), thiophenol (1.5 equivalent), and potassium carbonate (2.5 equivalent) in dry DMF (4 ml) was heated at reflux for 2 h and cooled to room temperature (Scheme 2.4).

This reaction resulted in a number of problems. The first issue was that the TLC, used to monitor the reaction, showed many spots and the colour of the mixture was black instead of colourless, indicating decomposition. Also, it was not possible to identify anything from the crude NMR spectrum. The MALDI-MS spectra did not confirm that the target compound had formed.

Therefore, although later improved, we did not make MHT by this method and instead returned to the synthesis of MHT by using a mixture of 2:1 equivalent of DHB and mono-hexyloxyphenol with FeCl_3 on a large scale.

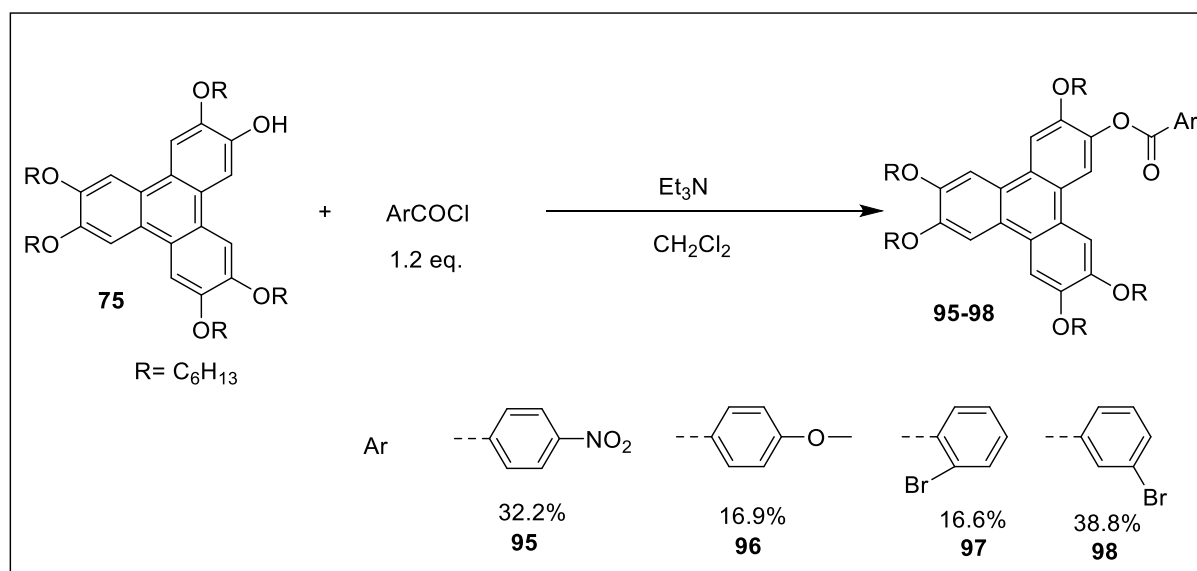


Scheme 2. 4: Alternative synthesis of triphenylene (**75**)

Synthesis of triphenylene monoesters:

For first series, we chose to prepare monoester-pentahexyloxytriphenylenes with simple aryl benzoates (bearing donating or withdrawing groups) and check the influence of these substituents on the possible mesophases. We selected 4-Nitrobenzoyl chloride, 4-Methoxybenzoyl chloride and isomers for bromobenzoyl chloride as reactants. They are commercial compounds that can be reacted with MHT directly. In typical procedures, MHT was mixed with an excess of the appropriate acid chloride (1.2 equivalent) in dry DCM at room temperature under N₂. Then dry triethylamine was added slowly at 0°C because it is an exothermic reaction (Scheme 2.5). TLC analysis was performed, and NMR spectroscopy of an aliquot confirmed the product was formed.

Purification of the ester products proved difficult but was achieved using careful chromatography and recrystallisation. It was found that it was very important to use highly pure MHT in the reaction because the side products from its formation and decomposition were hard to separate from desired products. This itself was not a trivial process because MHT has a strong tendency to decompose in the presence of oxygen, accelerated by light and perhaps acid/base.



Scheme 2.5 Synthesis of triphenylene monoesters with aryl benzoates (**95-98**).

The ¹H -NMR spectra were run in CDCl₃ and proves the formation of the monoester compounds (**95-98**). The aliphatic regions for all substituents are almost the same as for MHT

and the singlet proton of the hydroxyl group has vanished. However, for the structure with methoxy benzoate (**96**), there is a singlet peak of methoxy at 3.93 ppm integrating for three hydrogens and a multiplet of O-CH₂ peaks integrating for 10 hydrogens.

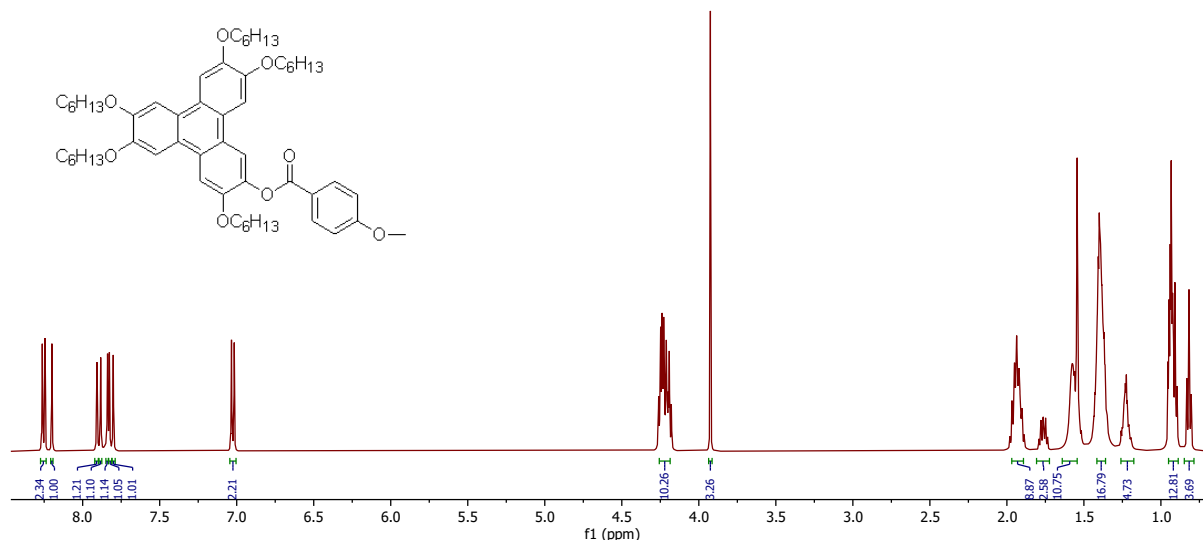


Figure 2.3: ¹H -NMR spectrum methoxybenzoate (**96**)

The aromatic regions of the 4 desired structures (**95-98**) are compared in figure 2.4. Nitrobenzoate (**95**) has 6 singlet protons for the triphenylene units between 8.22 and 7.79 ppm., and the other for the benzene protons which appear as doublet at 8.48 ppm with $J = 8.8$ Hz which integrates for two hydrogens and another doublet at 8.40 ppm with $J = 8.8$ Hz, which integrates for two hydrogens as well. The 2 protons of benzene next to the nitro group were downfield because of the nitro group, which is a withdrawing group. Furthermore, in the aromatic regions of methoxy benzoate (**96**), six singlet protons between 8.20 and 7.80 ppm are present for each triphenylene unit. It also shows the benzene protons that appear as doublets at 8.26 ppm with $J = 8.9$ Hz that integrate for two hydrogens, and another doublet at 7.02 ppm with $J = 8.9$ Hz, which integrates for two hydrogens as well. Because the methoxy group is a donor group, the protons next to it are shielded. In addition, As can be seen in the ¹H -NMR spectrum, the aromatic regions of the desired structure with 2-bromo benzoate (**97**) have six singlet protons for the triphenylene units and the other for the benzene protons. The protons of the benzene ring appear as a doublet of doublet at 8.24 ppm with $J = 8.0$ and 2.0 Hz, integrating for one hydrogen; another doublet of doublet at 8.24 ppm with $J = 8.0$ and 2.0 Hz, integrating for one hydrogen; and a multiplet between 7.51 and 7.41 integrating for two hydrogens. Also, the aromatic regions of 3-bromo benzoate (**98**) contain six singlet protons, which correspond

to triphenylene units, and the others to benzene units. A proton between bromine and carbonyl appears as a triplet at 8.45ppm with $J = 2.0$ Hz, which integrates for one hydrogen, and it is more deshielded than the other triplet at 7.43ppm. This is due to the electronegativity of bromine.

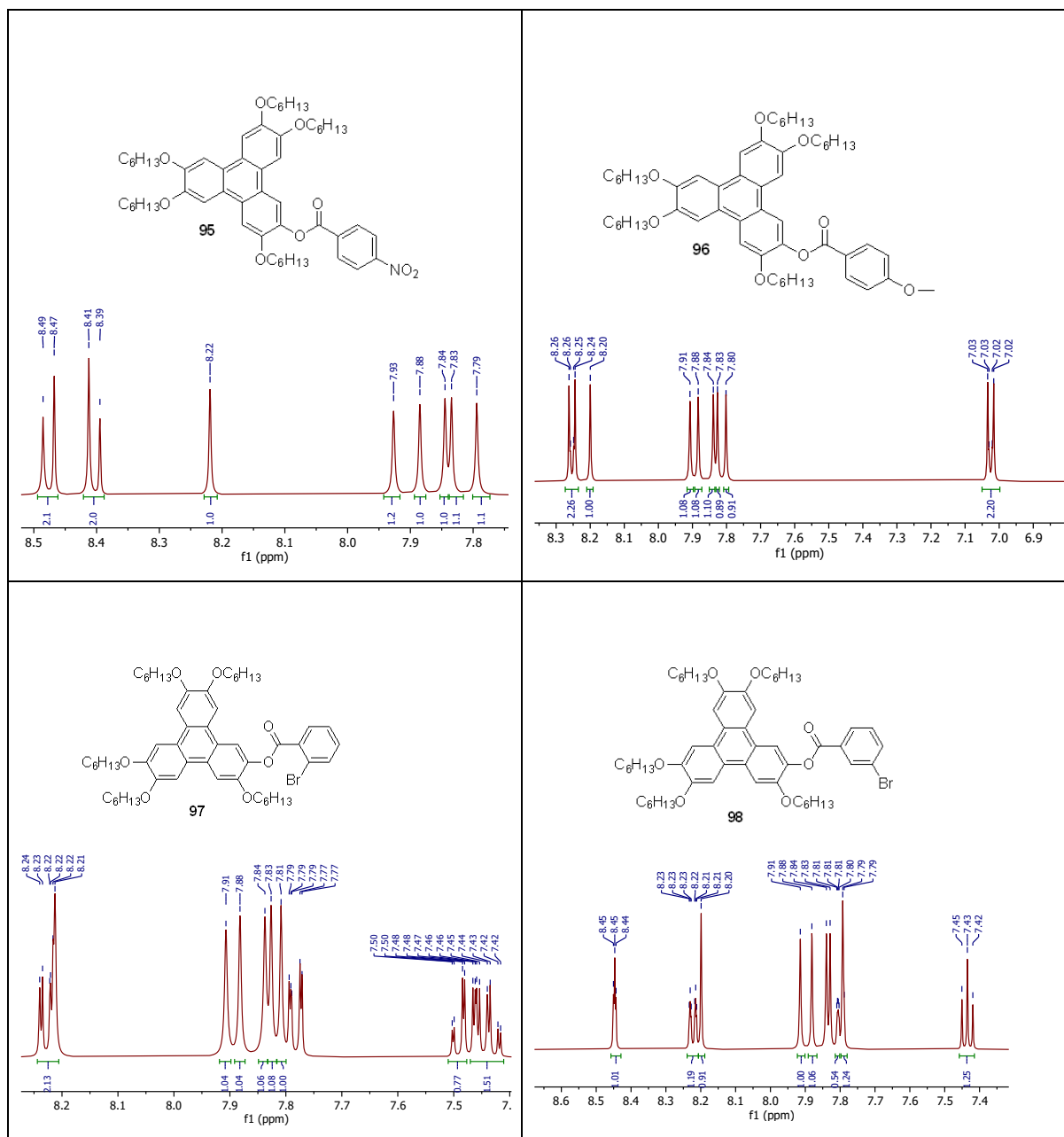


Figure 2.4: ^1H -NMR of aromatic regions of the first series (95-98)

Liquid crystal properties of the first series (95-98):

It has been demonstrated that adding polar ester groups can increase clearing temperatures, broaden the mesophase range, suppress crystallization, and stabilize columnar phases [92]. The

thermal properties of compounds **95-98** were investigated by POM and, in all cases, the textures observed for these compounds corresponded to a hexagonal columnar mesophases. Figure 2.5 shows the transition temperatures and mesogen textures for the materials. Furthermore, it is found that the columnar mesophase can be maintained at room temperature in a glassy state. There is a little difference in the transition temperatures from columnar to isotropic states for this series, but it can be noted that the mesophase is stabilised by an electron withdrawing group (-NO₂ vs -OMe).

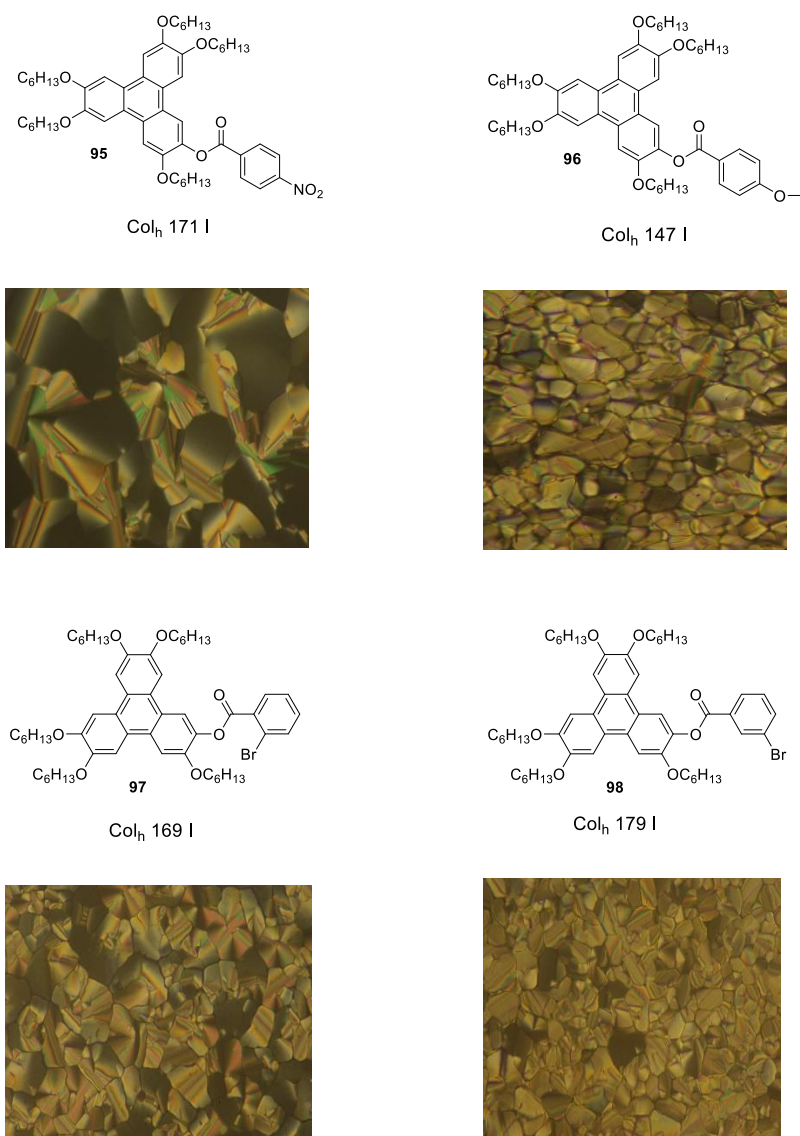


Figure 2.5: The mesophase textures and transition temperatures of triphenylene monoesters with simple benzoates **95** – **98**, showing the similarity of their behaviour.

In the next part of the investigation, we aimed to increase perturbation in the triphenylene system by increasing the size of the aromatic ester.

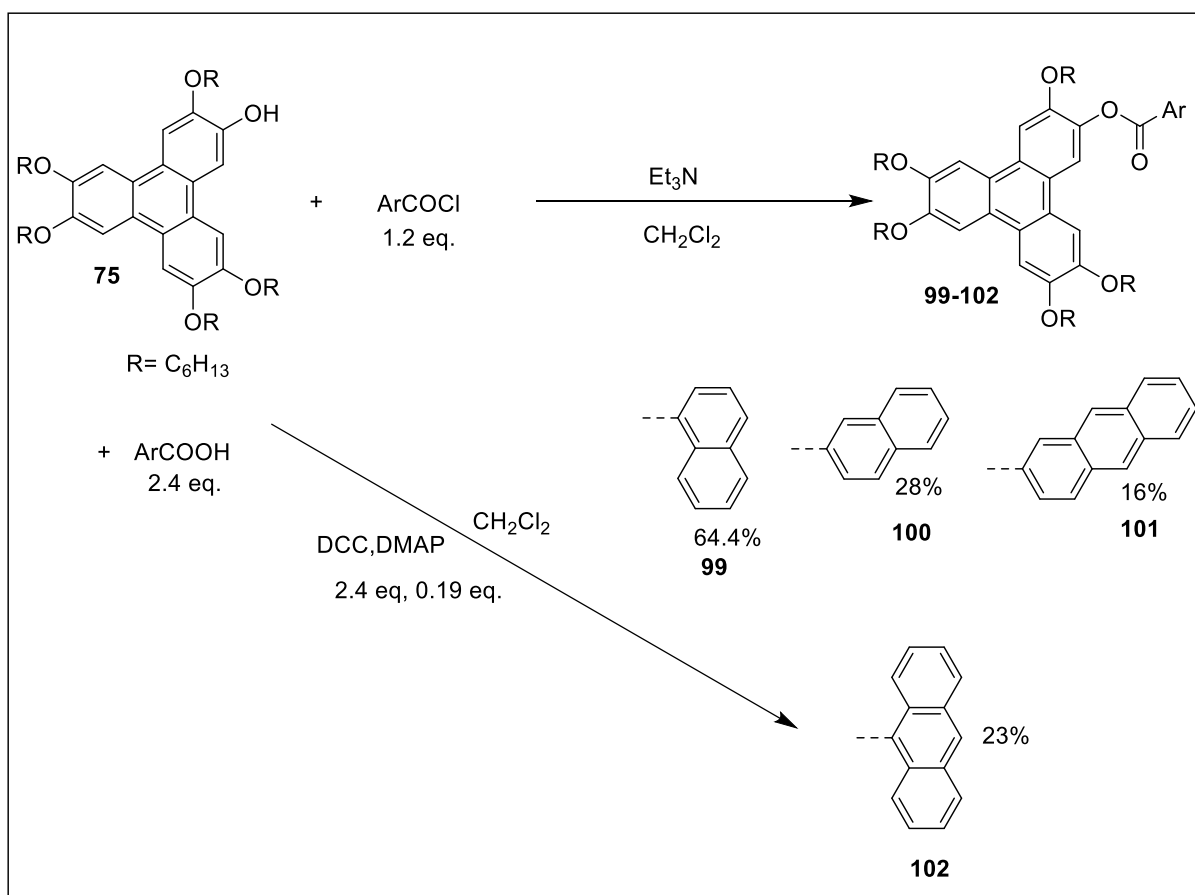
We selected 1-naphthoyl, 2-naphthoyl, 2-anthracenoyl and 9-anthracenoyl derivatives to explore. Some acid chlorides are commercial chemicals, and they can react directly with MHT. We chose to convert 2-anthracene carboxylic acid to acid chloride by using SOCl_2 before reacting it with MHT. When comparing the NMR spectrum of 2-anthracene carboxylic acid with its acid chloride, peaks were shifted and the peak of OH disappeared. Therefore, these compounds (acid chloride) (**99-102**) react with MHT by following the same process as for simple triphenylene monoesters (Scheme 2.6).

However, 9-anthracene ester (**102**) was synthesised directly from 9-anthracene carboxylic acid using a different procedure employing DCC and DMAP. We chose it since it is a one-step method (Scheme 2.6).

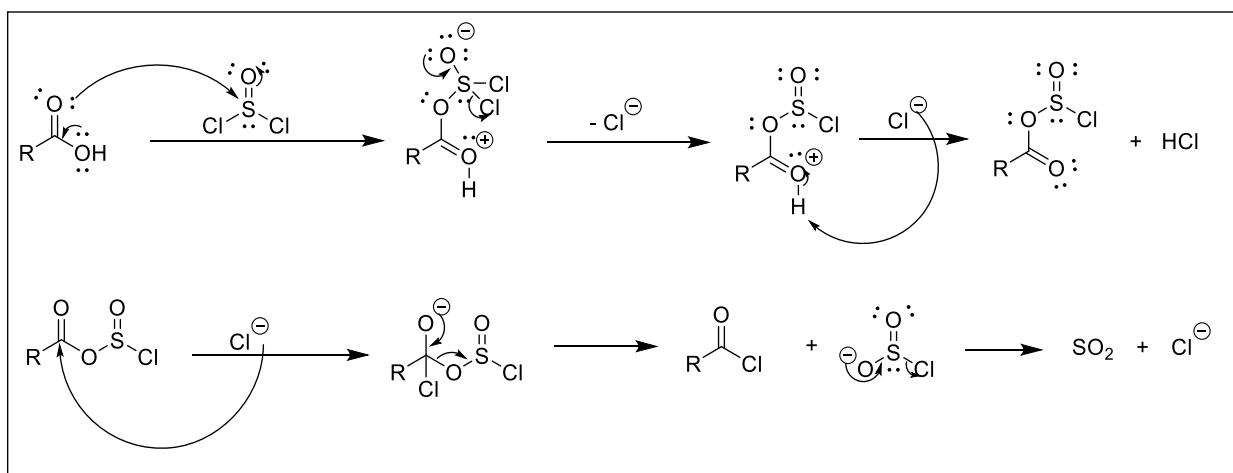
In the first attempt, the reactants MHT, anthracene-9-carboxylic acid (2.4 eq.), DMAP (0.19 eq.), and DCC (2.4 eq.), were stirred in dry DCM at RT for 2 days, but there was no new spot of the product in TLC.

Secondly, the ester was synthesised successfully by mixing MHT, anthracene-9-carboxylic acid (2.4 eq.), and DMAP (0.19 eq.), then vacuum was applied, and the vessel filled with nitrogen. This process was repeated three times, followed by dissolving it with dry DCM at RT, cooling it to 0°C , and adding DCC (2.4 eq.) with dry DCM slowly in the last step. A TLC was used to monitor the entire reaction. It was evident that there was a new spot, which was the product, and other spots of remaining starting materials.

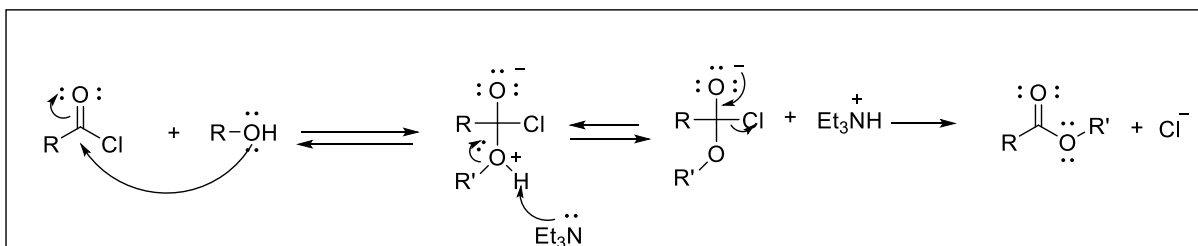
The reaction was left for more than 2 days until the starting material did not remain in TLC. This is a slow reaction process. Then it was purified by column chromatography and recrystallized.



Scheme 2.6 Synthesis of triphenylene monoester with bulky, larger aromatic esters (**99-102**).

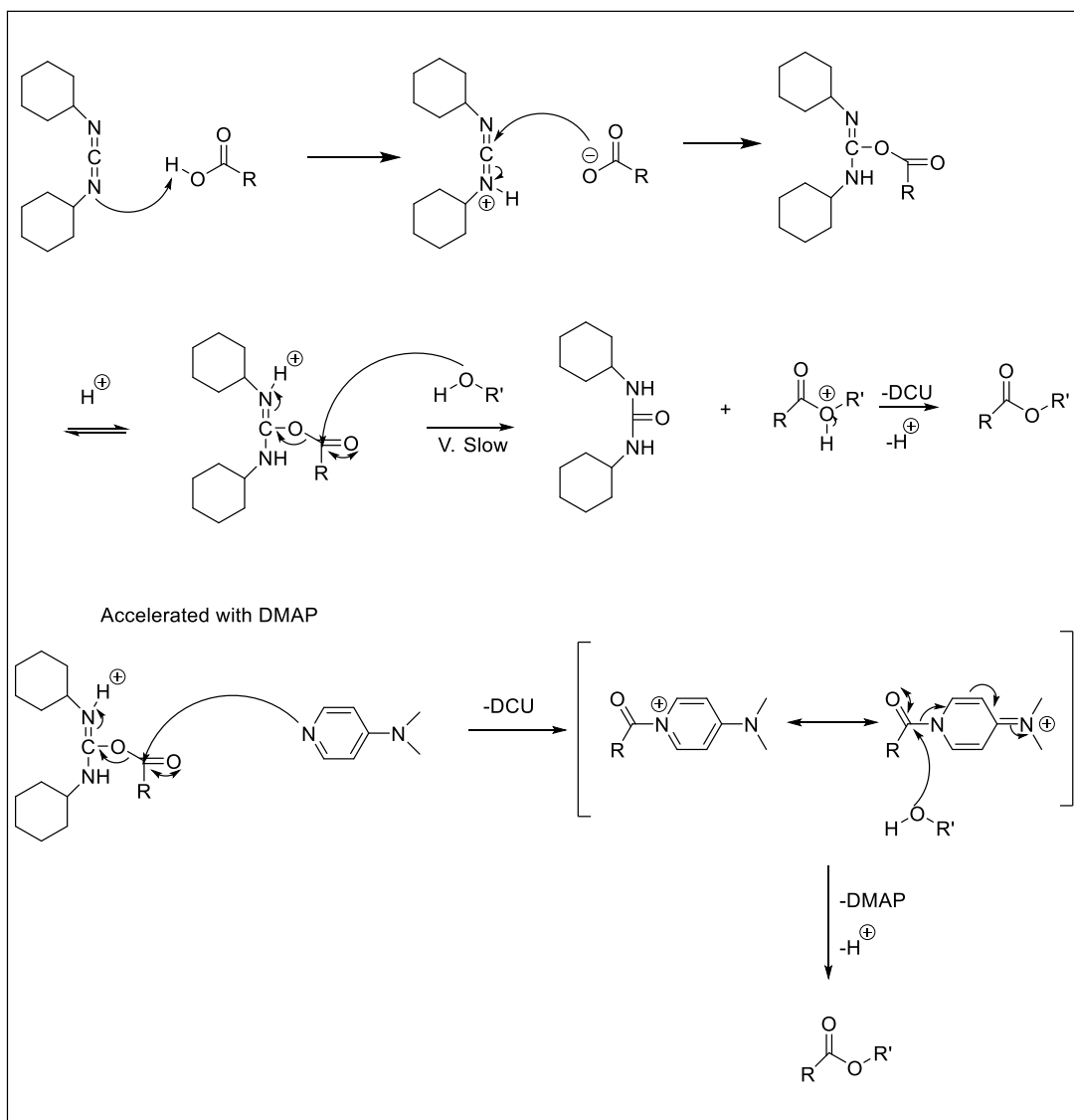


Scheme 2.7: Thionyl chloride mechanism for converting carboxylic acid to acid chloride [93].



Scheme 2.8: Esterification reaction mechanism with triethylamine [94].

The reaction with DCC/DMAP is called the Steglich reaction. The reaction occurs at room temperature, under mildly basic conditions, and its mechanism is shown in Scheme 2.9. It is suitable for esterification of alcohols, thiols, carboxylic acids, including vitamin A [95].



Scheme 2.9: The mechanism of a Steglich esterification.

Steglich esterification uses 4-dimethylaminopyridine (DMAP) as a catalyst and dicyclohexylcarbodiimide (DCC) as the coupling reagent. By coupling DCC with carboxylic acid, an O-acylisourea intermediate is formed, which exhibits a similar reactivity to the deprotonated carboxylic acid. As a result of this reaction, the stable dicyclohexylurea (DCU) and the ester can be liberated from the activated carboxylic acid; however, the pace of this reaction is quite slow in comparison with esterifications using strong nucleophiles such as amines. Since the reaction with alcohol occurs slowly, it is possible to isolate the O-acylisourea as a side product. In order to form the activated amide ("active ester"), DMAP is added to the reaction, which is a stronger nucleophile than an alcohol. DMAP acts as an acyl transfer agent. This intermediate is then rapidly reacted with the alcohol to yield the desired ester [96].

The ^1H -NMR spectra obtained indicated that monoester compounds (**99-102**) were formed. For all substituents, the aliphatic regions are almost identical to those of MHT, and the singlet proton of the hydroxyl group has disappeared. For TP-9-ANTHR (**102**), Figure 2.6, a peak of O-CH₂ appears as a triplet at 4.43 ppm with a coupling constant value of 6.6 Hz which integrates for two hydrogens and as multiplets Between 4.31 and 4.17 which integrates for 8 hydrogens, while for other triphenylene ester substituents, it appears as a multiplet integrating as 10 hydrogens.

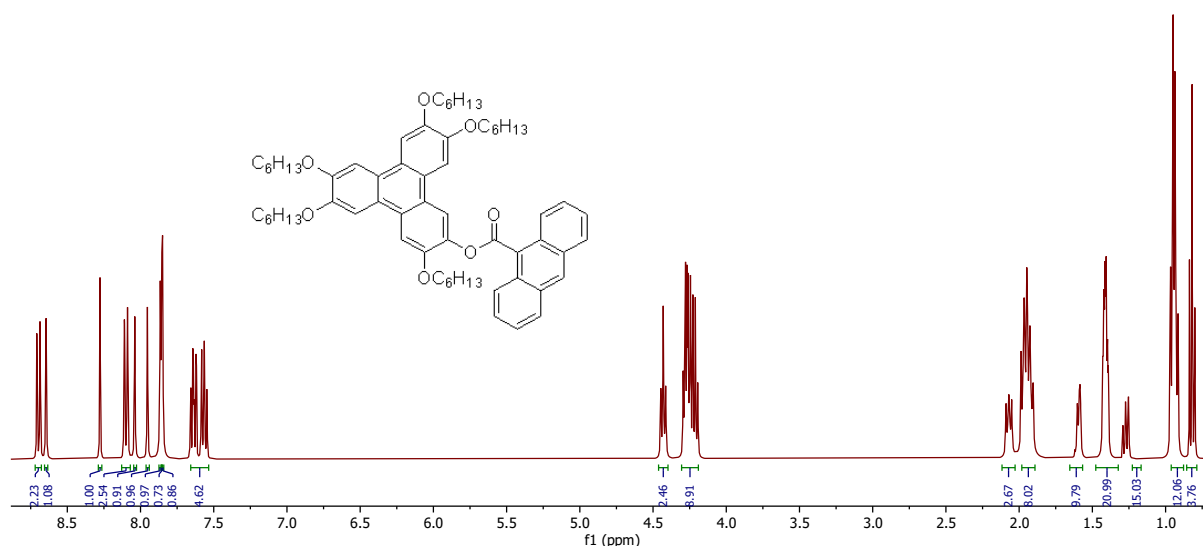


Figure 2.6: ^1H -NMR spectrum of triphenylene-9-anthracenoate (**102**)

The aromatic regions of ^1H -NMR spectrum for (**99-102**) are shown in figure 2.7. Triphenylene-1-naphthoate (**99**) shows six singlet protons for the triphenylene protons at 8.26, 7.94, 7.90, 7.84, 7.83, and 7.82 ppm, and the other for the naphthalene protons, which appear as a doublet at 9.11 ppm with $J = 8.7$ Hz, integrating one hydrogen, doublet of doublet at 8.59 with $J = 8.0$,

1.3 Hz, integrating one hydrogen, doublet at 8.14 ppm with $J = 8.0$ Hz, integrating one hydrogen, a doublet at 7.96 ppm with $J = 8.0$ Hz, integrating one hydrogen, and a multiplet at 7.69-7.57 ppm, integrating three hydrogens.

Triphenylene- 2-naphthalenoate (**100**) has a spectrum composed of six singlets for the triphenylene protons at 8.26, 7.93, 7.90, 7.84, 7.83, 7.82 ppm and others for the naphthalene protons. It appears as a singlet at 8.90 ppm, integrating one hydrogen, doublet of doublet at 8.29 with $J = 8.5, 1.7$ Hz, integrating one hydrogen, doublet at 8.04 ppm with $J = 8.5$ Hz, integrating one hydrogen, doublet at 7.99 ppm with $J = 8.6$ Hz, integrating one hydrogen, doublet at 7.95 ppm with $J = 8.5$ Hz, integrating one hydrogen, doublet of doublet of doublet at 7.66 with $J = 8.2, 6.9, 1.3$ Hz, integrating one hydrogen, and doublet of doublet of doublet at 7.60 with $J = 8.2, 6.9, 1.3$ Hz, integrating one hydrogen. The triphenylene-2-anthracenoate (**101**) shows six singlet protons for the triphenylene protons at 8.31, 7.97, 7.93, 7.88, 7.86, 7.86 ppm and others for the anthracene protons. It appears as three singlets at 9.14, 8.67, and 8.52 ppm, integrating one hydrogen each; a doublet of a doublet at 8.22 with $J = 8.5, 1.7$ Hz, integrating one hydrogen; a doublet at 8.13 ppm with $J = 8.0$ Hz, integrating one hydrogen; a triplet at 8.07 ppm with $J = 7.7$ Hz, integrating two hydrogens; and a multiplet between 7.60 and 7.51, integrating two hydrogens.

There is a plane of symmetry surrounding triphenylene-9- anthracenoate (**102**), which implies that those nuclei which are symmetrically arranged on one side and on the other side of the plane will produce the same signal by NMR.

The ^1H NMR spectrum of triphenylene-9- anthracenoate (**102**) shows six singlets at 8.28, 8.04, 7.95, 7.86, 7.85, and 7.85 for triphenylene protons. Others for anthracene rings appear as a doublet at 8.70 ppm with $J = 8.7$ Hz, integrating two hydrogens; one singlet at 8.64 ppm, integrating one hydrogen; a doublet at 8.10 ppm with $J = 8.7$ Hz, integrating two hydrogens, integrating one hydrogen each; and multiplets between 7.68 and 7.53, integrating four hydrogens (Figure 2.7).

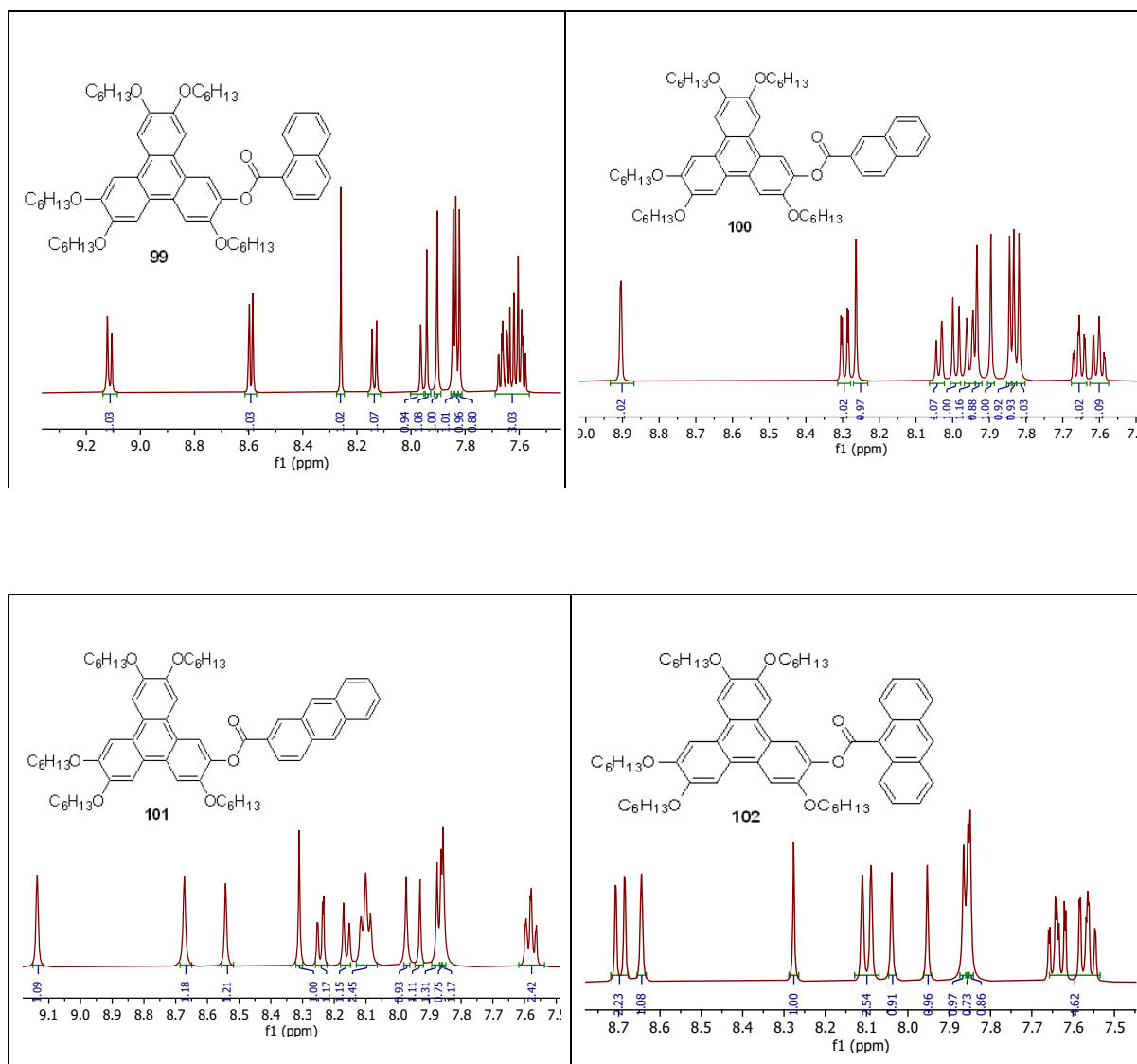


Figure 2.7: The aromatic peaks of NMR triphenylene esters **99-102**

Liquid crystal properties for mono esters (99-102):

The second series of substituted triphenylene mono esters was successfully synthesised at 2-positions by altering the steric hindrance of the bulky substituents using a variety of aromatic rings, including naphthalene and anthracene. Figure 2.8 shows the transition temperatures for the materials and also their mesophase textures, which show all form hexagonal columnar mesophases. The mesophases remained stable over a broad temperature range. Moreover, the columnar mesophase can be kept in a glassy state at room temperature. (Figure 2.8).

Again, it can be concluded that these substituents have only a small effect on the stability of the mesophase, with large anthracene esters showing lower clearing temperatures. However, it is surprising to note that a change from 2- to 9-substitution results in almost no change.

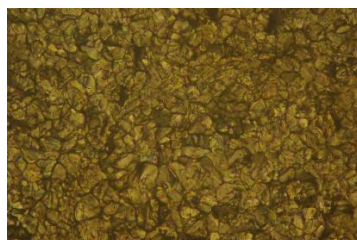
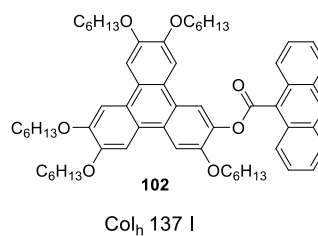
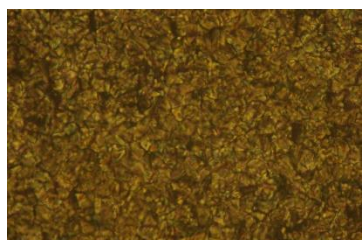
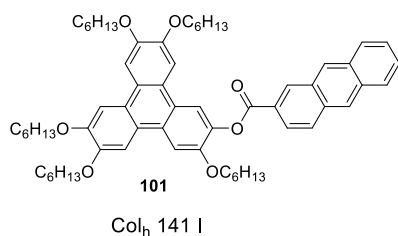
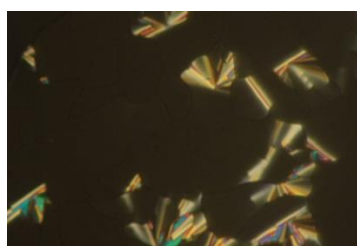
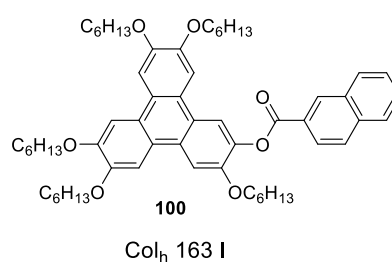
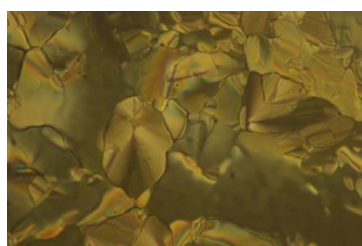
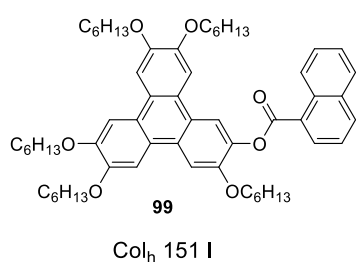


Figure 2.8: Columnar mesophase textures and transition temperatures of the second series of triphenylene monoesters, bearing substituents with higher steric demand.

In conclusion, mesophase stability and type is only marginally affected by the structure of its single aryl-ester. In most cases, the unsymmetrical materials were isolated as pure precipitates that clear at $\sim 150\text{ }^{\circ}\text{C}$, which is significantly higher than the symmetrical hexa(hexyloxy)triphenylene HAT6 ($\sim 100^{\circ}\text{C}$). The mesophases are columnar hexagonal in all cases, characterized by characteristic textures upon cooling. A single ester group introduced in the examples examined in this study did not directly lead to nematic behaviour, however it prevented crystallization, resulting in a columnar phase that persists at room temperature as a glass [89].

Synthesis of triphenylene ester dimers 103-104:

Connecting groups in triphenylene liquid crystals are generally capable of conjugating with the aromatic core (so often we see an oxygen link for ethers or esters). In addition, mesomorphic properties can be expected to be affected by the geometry of the connecting group with a core, which affects mesophase stability.

Our group synthesised dimers linked by 2,5-thiophene and 2,7-naphthalene as mentioned previously. The geometry of the connecting group with the dimer is bent and flexible (Figure 2.9). As a result of the spacer, nematic phases are formed in the discotic system, probably due to the geometry and its influence on the ease with which columnar arrangement can be achieved.

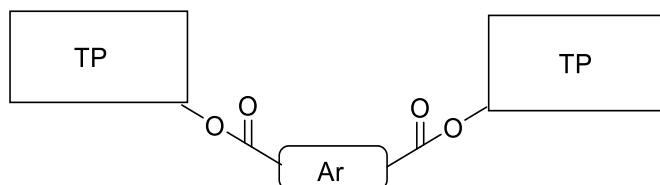


Figure 2.9: The non-linear geometry of the connecting group with side-to-side dimers.

The next aim of the project was to extend the series and to synthesise additional dimers with aryl dicarboxylate linkers. There are two types of joining units to be discussed, benzene dicarboxylates linked through 1,3- (bent) and 1,4- (linear) arrangements. These spacers have been chosen as a result of their rigidity and geometric constraints (configuration). This type of bridge can be contrasted and compared to fully flexible alkyloxy spacers (columnar) and the linear, rigid di-alkyne bridges (nematic).

Previous attempts to synthesise these compounds (mostly using MHT with dicarboxylic acid by using DCC/DMAP in DCM) had met with significant difficulty and they could not previously be obtained in pure form.

The main parameters taken into consideration are temperature, quantity of DCM solvent and the DCC reagent. The main problem with the reactions is found to be formation of side products from the DCC. ^1H NMR indicates that the rearrangement product from DCC intermediates is formed at 0 °C. As shown in figure 2.10, the peak at 7.6 ppm is the aromatic protons for benzenes. Carboxylic acid reacts with DCC when heated, resulting in this intramolecular reaction.

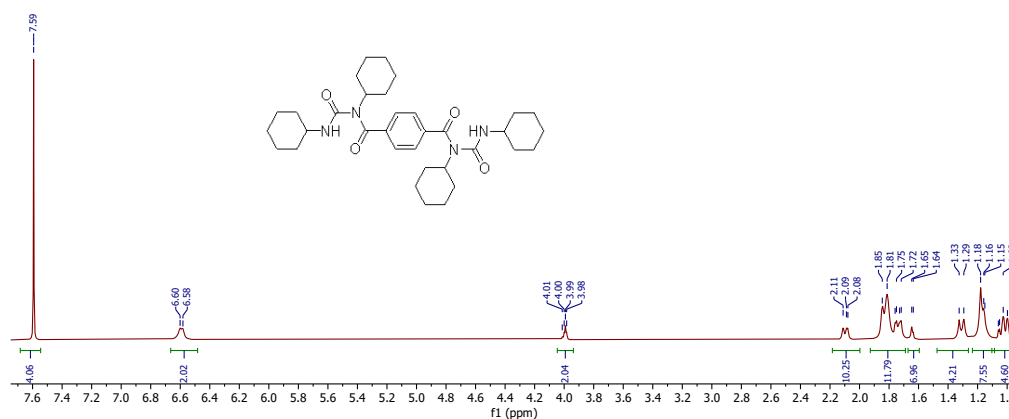


Figure 2.10: ^1H NMR spectrum of one side product from direct reaction of DCC with terephthalic acid.

In many normal DCC coupling reaction, the formation of such side products is an inconvenience, often overcome by addition of excess reagent and acid. The situation is much more of a problem for diacids which can't be used in excess, and also lead to formation of singly substituted products (so mixed ester-ureas) even at -10°C (table).

entry	Temperature	DCM solvent	eq. DCC	Product
1	0 °C for 4 h then reflux	30 ml	2.5 + 2.5	Rearrangement (intramolecular process) unimolecular

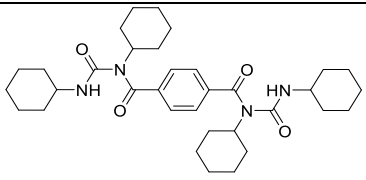
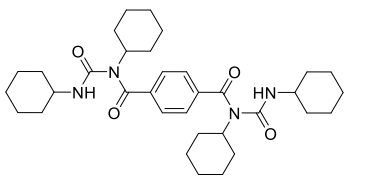
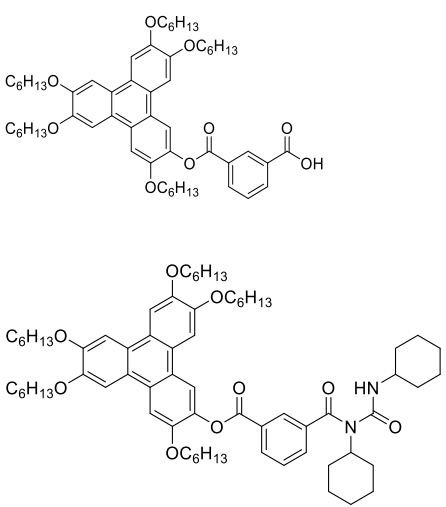
				
2	0 °C for 4 h then reflux	20 ml	5	<p>Rearrangement (intramolecular process)</p> 
3	-10 °C for 4 h then rt	4 ml	5	<p>Monomer + side product</p> 

Table: Esterification reaction condition of MHT with Benzene-1,4-dicarboxylic acid.

Based on the MALDI results, the main peak was identified as 745, which corresponds to the MHT product. Other peaks were also observed and identified for the monomer and side products (figure 2.11). It is therefore necessary to change this process, as it is undesirable.

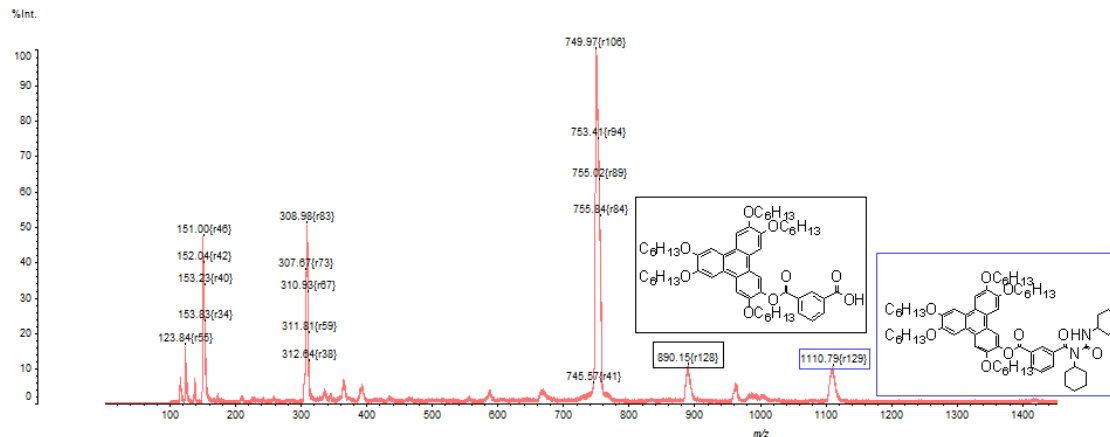
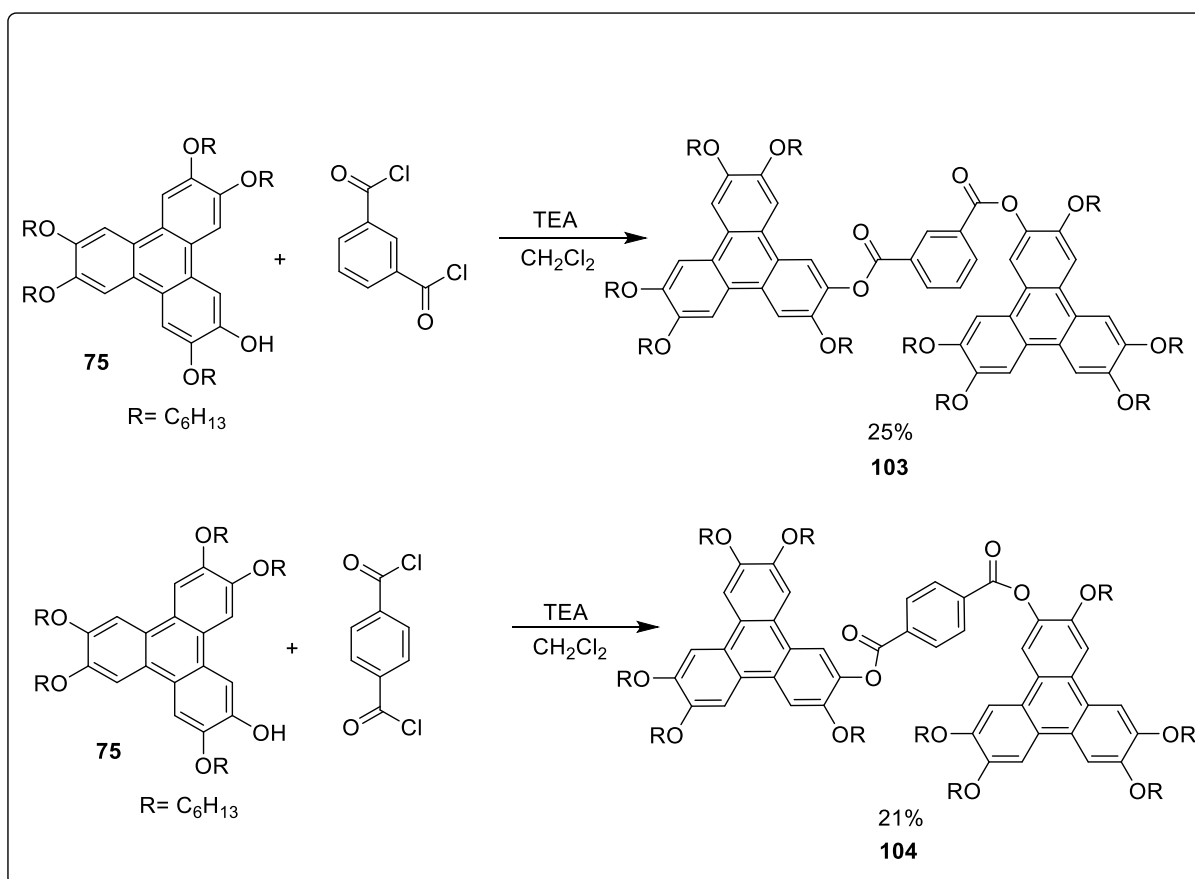


Figure 2.11: Crude MALDI-MS showing presence of monomer compounds and side product.

Dicarboxylic acid was consumed since there was no more of it as shown in TLC. There are also spots for MHT, monomer, and side products.

A modification of the previous methods to prepare dimers of the isomeric phthalic acid series **103-104** is to use acid chloride instead of carboxylic acid. This was carried out by reacting MHT (1 eq.) with benzene-1,4-dicarbonyl chloride (0.4 eq.) in dry DCM. Triethylamine is added at 0°C. The reaction proceeded successfully and forms a dimer.



Scheme 2.10: The synthesis of triphenylene di-esters with aryl dicarboxylate units.

We conducted the analyses in order to verify the formation of the target structure. The major product was clearly identified as the dimer product based on the ¹H NMR spectrum (Figure 2.12). The aliphatic regions for two isomers are almost the same, and there is no longer any singlet proton signal of hydroxyl groups. Triphenylene has six singlet protons in the aromatic regions for two isomers integrating two hydrogens each. Also, there is a multiplet of O-CH₂ peaks integrating for 20 hydrogens. For isophthalate (1,3-) protons, it appears as a triplet at 9.16 ppm with *J* = 1.8 Hz integrating one hydrogen, a doublet at 8.51 ppm with *J* = 7.8, 1.8 Hz integrating two hydrogens, and a triplet at 7.69 ppm with *J* = 1.8 Hz integrating one hydrogen. However, terephthalate (1,4-) appears as one singlet at 8.39 ppm integrating four hydrogens.

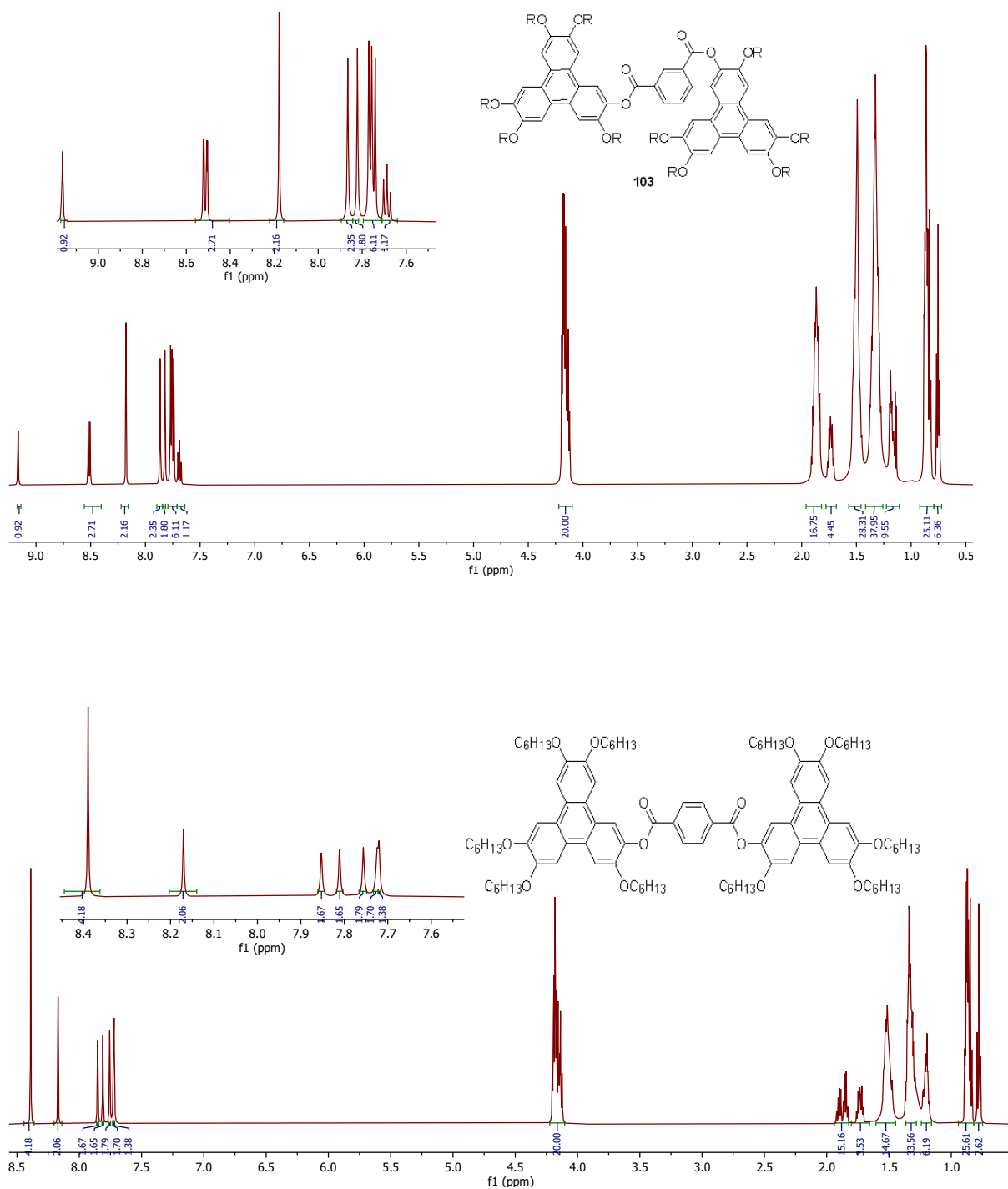


Figure 2.12: ^1H NMR spectrum of dimer compounds **103** and **104**

Liquid crystal properties for dimer with Isophthalate and terephthalate (103-104):

The thermal behaviour for Isophthalate (1,3-), **103** shows the formation of a columnar hexagonal phase on cooling (as indicated by its characteristic fan texture) which forms a glass almost immediately (150 ° C). In the case of terephthalate (1,4-) dimer **104**, it melts directly into the isotropic liquid at 175 ° C. Nematic and isotropic regions of glass are formed at the same time during cooling [89], so somewhat surprisingly this linear arrangement does not strongly support liquid crystal formation.

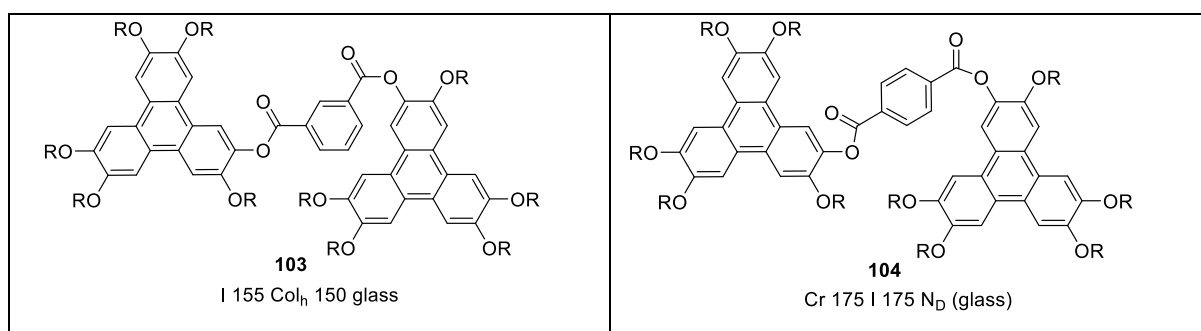


Figure 2.13: Liquid crystal properties and transition temperature of **103** and **104**

In our final exploration of triphenylene ester dimers, we decided to investigate a totally different arrangement of the two triphenylene cores. It was decided to target a dimer structure using a ferrocene bridge to link to monohydroxy-pentahexyloxytriphenylene and study its liquid crystal properties.

We have chosen ferrocene dicarboxylates to link triphenylene diesters because the joining units are parallel to each other, the ring can rotate freely, and the geometry has an enforced staggered arrangement. We were curious to see if such an arrangement would support liquid crystallinity. In the offset conformation (Figure 2.14, left) the Tp separation closely matches that in our thiophene linked system (nematic and columnar phases), yet the in-line arrangement is no longer easily achieved. Conversely, an eclipsed conformation (Figure 2.14, right) could allow the Tps to occupy the same column.

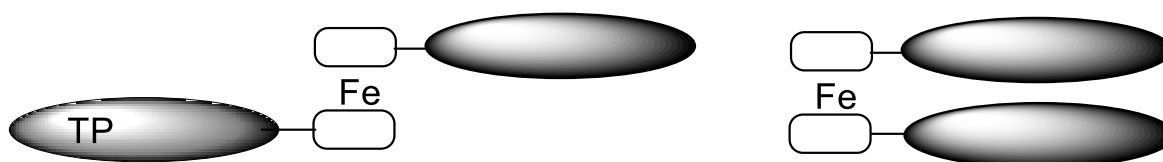


Figure 2.14: The geometry of the connecting group (ferrocene) within the dimer conformations.

Introduction to ferrocene:

The first ferrocene was discovered in 1951 (called dicyclopentadienyl iron) and was then described separately by the groups of Kealy and Pauson [97]. In 1952, Fischer and Wilkinson (using preliminary X-ray data and IR data) [98, 99], identified the structure as a "sandwich" compound.

In addition, aromatic electrophilic substitution reactions, such as Friedel-Crafts acylation, were found to be successful in confirming the presence of aromaticity in the compound [100]. The anti-prismatic or staggered form of the Cp rings has been found to be the most stable in the solid form, whereas the other metallocenes of the same group (osmocene and ruthocene) have prismatic or eclipsed forms. (Figure 2.15). The reason for this is because there are fewer distances between the cp rings in ferrocene and therefore more interannular repulsion. As a consequence of the staggered form, nonbonded interactions between heteroannular carbons can be reduced to a minimum [101]. Due to the low rotational energy barrier, the rings can rotate freely around the five-fold symmetry axis (so that both eclipsed and staggered patterns can occur) [102].

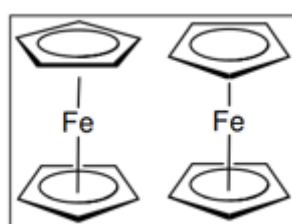


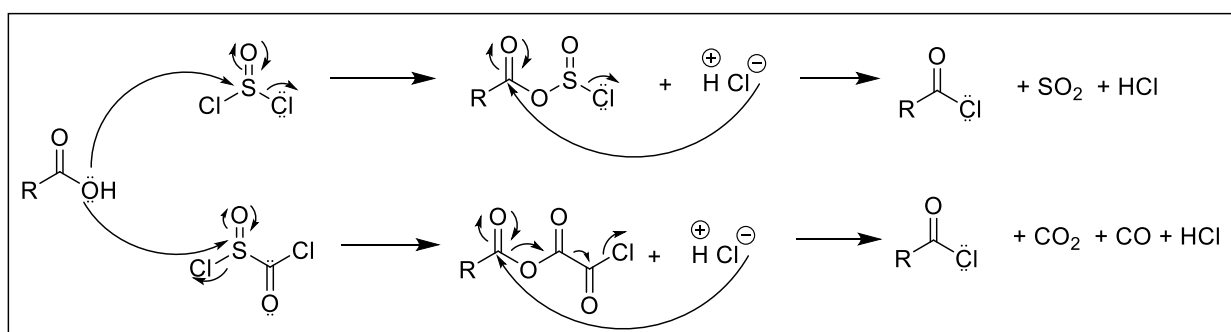
Figure 2.15 The staggered form of Ferrocene (left) and the eclipsed form (right).

Cp rings are parallel planar regular pentagons that are connected by sp^2 σ - bonds that are slightly bent. There is a possibility that the C_{2p} orbitals will form molecular orbitals extending around the ring (delocalization), which can then be involved in π - bonding with the metal. Cp is bonded to the iron atom by its d-orbitals and the π -orbitals on the rings. In the IR spectrum, the C-H bonds appear as a singlet stretch, indicating that they are all equivalent, as in benzene.

Consequently, there are no carbon-carbon double bonds, as there would be in cyclopentadienyl. This can also be seen in the lengths of the C-C bonds, which are all 1.40 Å [103]. In particular, it exhibits interesting redox chemistry; the iron atom can be oxidized from the +2 to +3 state in a reversible way using one electron [104].

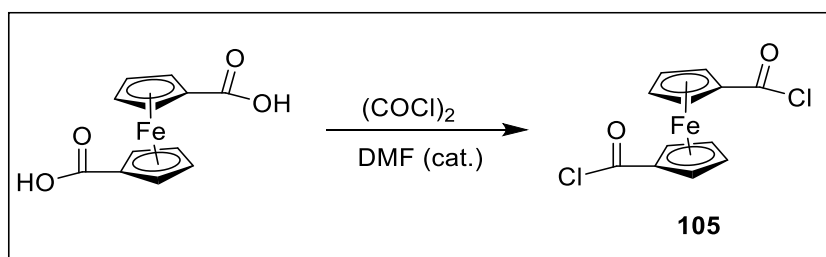
To synthesise triphenylene dyad with the linking of a ferrocene bridge, we convert ferrocene di carboxylic acid to acid chloride and then react with MHT.

The majority of representative methods used for esterification reactions involve the activation of acids into acyl halides, which then react with hydroxyl groups to produce corresponding esters. Acid chloride is typically generated by activating agents such as thionyl chloride, or oxalyl chloride. An overview of the general mechanism for activating acids using thionyl or oxalyl chloride is provided in Scheme 1.10 [105].



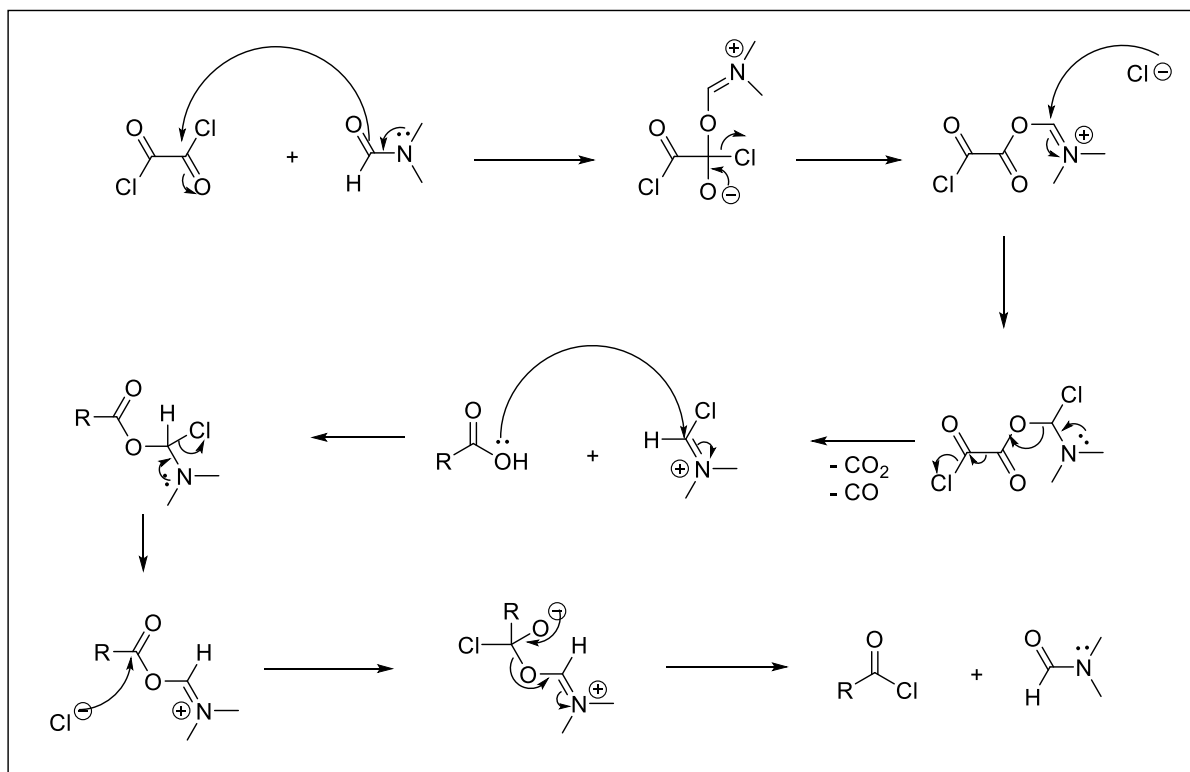
Scheme 2.11: Mechanism of acyl chloride formation using thionyl or oxalyl chlorides

We found that oxalyl chloride as an activating agent is better than thionyl chloride because our reactions gave pure red crystals without further purification (Scheme 2.12). The ^1H NMR spectrum confirmed the product, in which peaks are shifted from 4.70, 4.44 ppm to 5.05, 4.76 ppm.



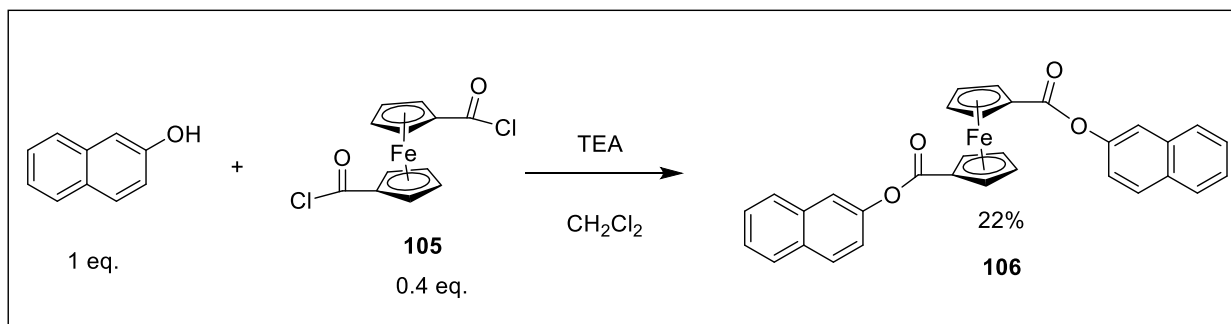
Scheme 2.12: Ferrocene dicarbonyl chloride synthesis.

Dimethylformamide (DMF) catalyses the process by reacting with oxalyl chloride to form the Vilsmeier reagent. After that, the iminium intermediate is combined with carboxylic acid to form a mixed imino-anhydride. This structure reacts with the released chloride to produce the acid chloride and the liberation of the regenerated DMF molecule (Scheme 2.13) [106].



Scheme 2.13: Mechanism of DMF catalysis in reaction of oxalyl chloride with carboxylic acids.

Initial experiments with MHT gave confusing results, so we decided to optimise the reaction using an excess of 2-naphthol because it is commercially available and a reasonable mimic for MHT. It was reacted with ferrocene dicarbonyl chloride by mixing it in dry DCM and adding triethylamine at 0 °C and it was synthesised successfully (Scheme 2.14).



Scheme 2.14: Synthesis of 2-Naphthol with Ferrocene dicarbonyl chloride.

At this point, TLC was used to monitor the entire reaction, which confirmed the new orange spot of the desired product. Column chromatography was used to purify it. The ^1H NMR spectrum showed the diagnostic peaks of the ferrocene ring appearing as two triplets at 5.18 ppm with $J = 1.9$ Hz, integrating four hydrogens, and at 4.70 ppm with $J = 1.9$ Hz, integrating four hydrogens. Others appear for the aromatic region of 2-Naphthyl fragment (Figure 2.16).

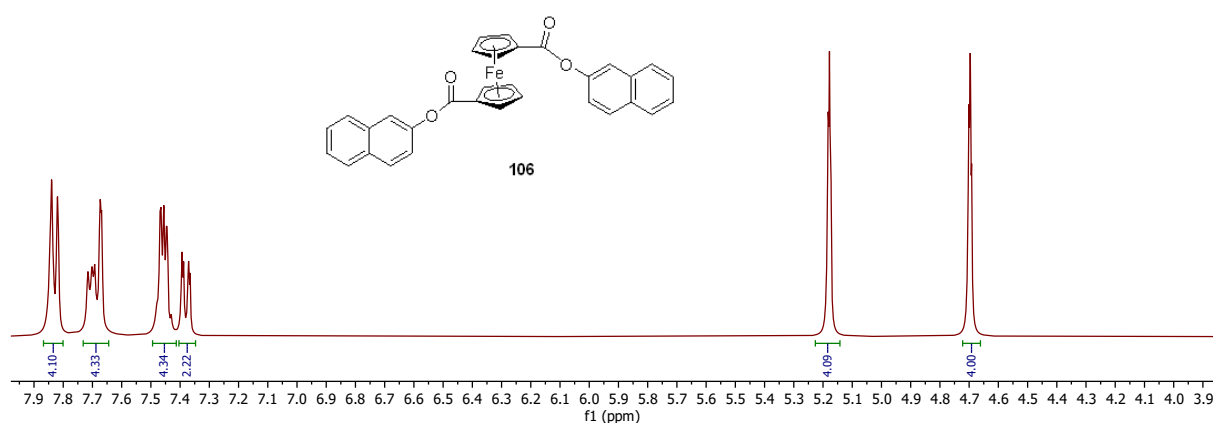
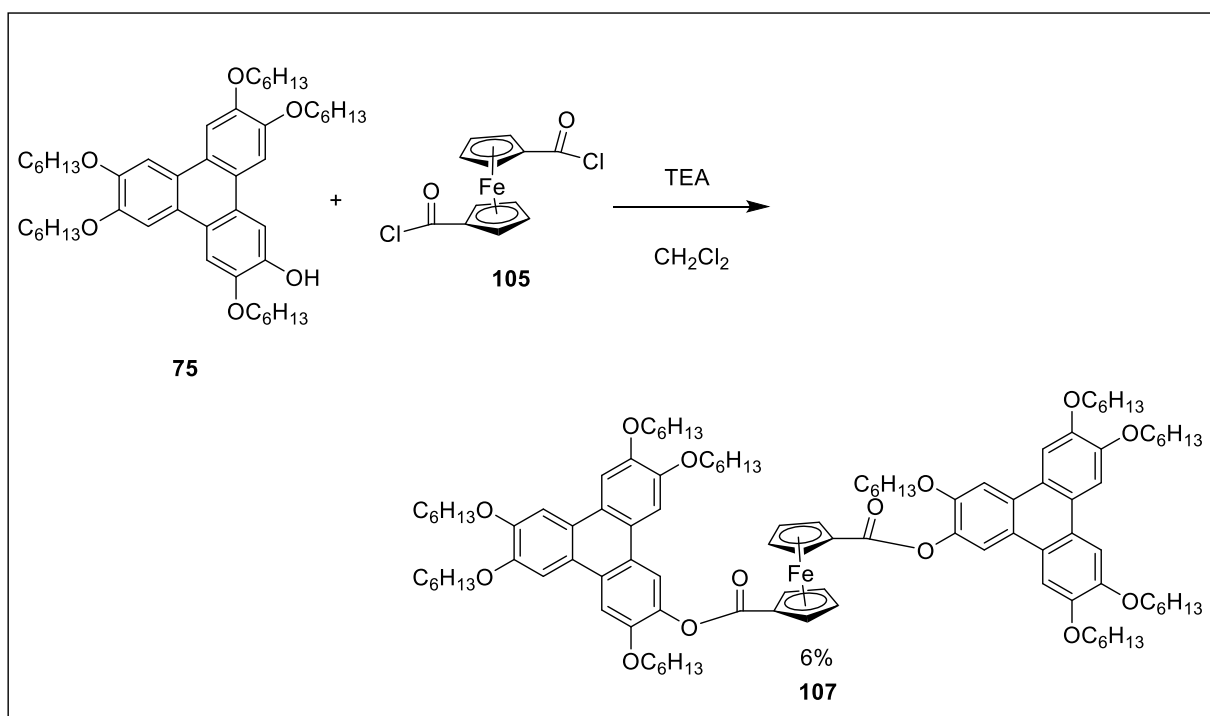


Figure 2.16. The ^1H NMR spectrum of dimer compounds **106**.

We applied the same procedure to the synthesis of MHT and it was successfully completed.

This was done by mixing MHT with Ferrocene dicarbonyl chloride in dry DCM at RT, then the mixture was cooled, and dry TEA was added slowly at 0 °C. TLC showed a new spot corresponding to the compound and it was orange. It was purified by column chromatography using (1:2) DCM / pet.ether (Scheme 2.15)..



Scheme 2.15: Triphenylene dimer **107** synthesis.

Figure 2.17 shows the diagnostic peaks of the ferrocene ring appearing as two triplets at 5.25 ppm with $J = 2.0$ Hz, integrating four hydrogens, and at 4.54 ppm with $J = 2.0$ Hz, integrating four hydrogens. Also, the aromatic region of triphenylene in the NMR spectrum appears as four singlets at 7.96, 7.33, 6.97, and 6.78 ppm integrating two hydrogens each and as overlapping signals between 7.45 and 7.46 ppm integrating four hydrogens.

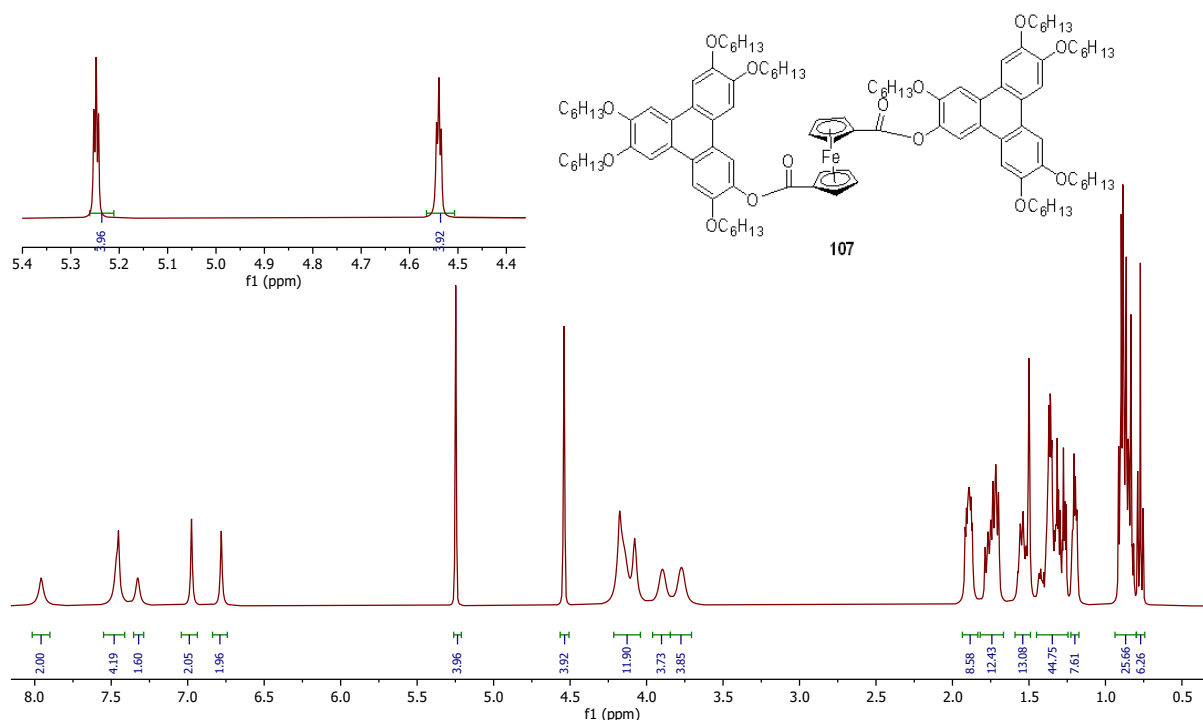


Figure 2.17: ^1H NMR spectrum of triphenylene dyad using a ferrocene link.

Liquid crystal properties of triphenylene dimer **107**:

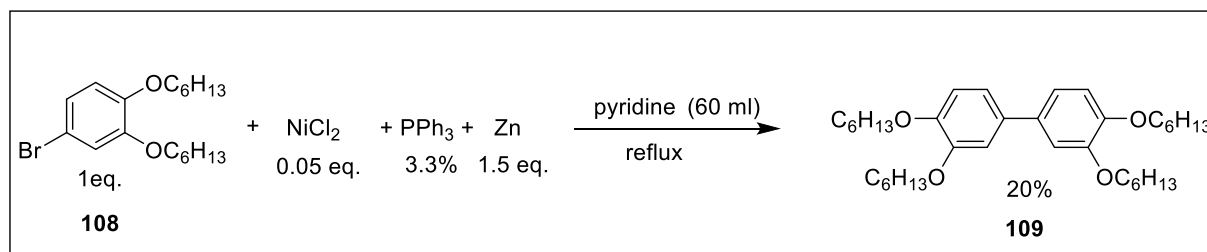
The diad structure **107** exists as a solid which has not demonstrated any transition temperature which suggests that it has completely melted into an isotropic phase at 70°C . Furthermore, when the sample is cooled, no liquid crystal behaviour is observed. The staggered arrangement of ferrocene connections most likely prevents close packing and reduces mesophase stability (and also the melting point).

An alternative synthesis of diesters:

As part of the study, we also investigated a new synthesis of novel macrocyclic dyads by using triphenylene synthesis as the first step (the biphenyl route). The aim of this study is to obtain functionalized triphenylene dimers with carboxylate aryl links by indirect synthesis using phenolic and methoxy triphenylenes as intermediates. To begin the synthesis of biphenyl, our group had already prepared the first material, bis(hexyloxy)phenylbromide **108**. This product is converted to tetrakis(hexyloxy) biphenyl **109** in an Ullman -type coupling reaction. It was

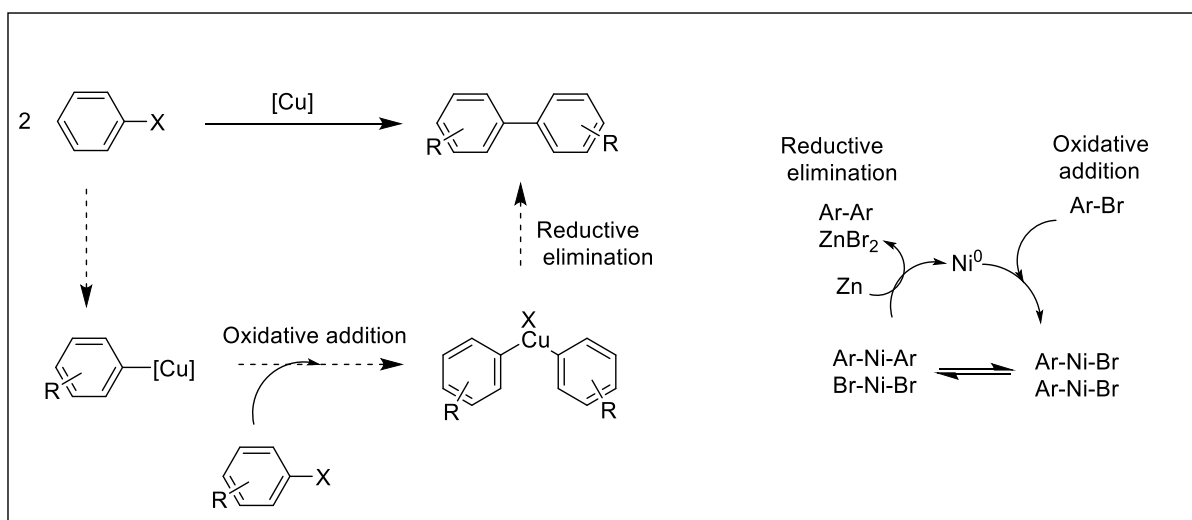
discovered by our group that the (Ullmann coupling) method yields a much greater amount of tetrakis(hexyloxy)biphenyl **109** than the Suzuki-Miyaura coupling method. It is made by combining two molecules of 4-bromo-1,2-bis(hexyloxy)benzene **108** and uses a nickel catalyst, NiCl_2 with PPh_3 , to carry out the coupling in the presence of zinc in dry pyridine at reflux [37]. The reaction was stirred and cooled overnight. Following the addition of 50 mL of DCM, the zinc powder was filtered off. After extraction, the extract was purified through column chromatography (4:1) Pet.ether: ethyl acetate. The tetrakis(hexyloxy)biphenyl was then collected as a white solid with a yield of 20% (Scheme 2.16).

However, due to the high reproducibility of the nickel catalyst method, one can obtain an adequate amount of biphenyl for the production of significant amounts of triphenylene by repeating the process several times.



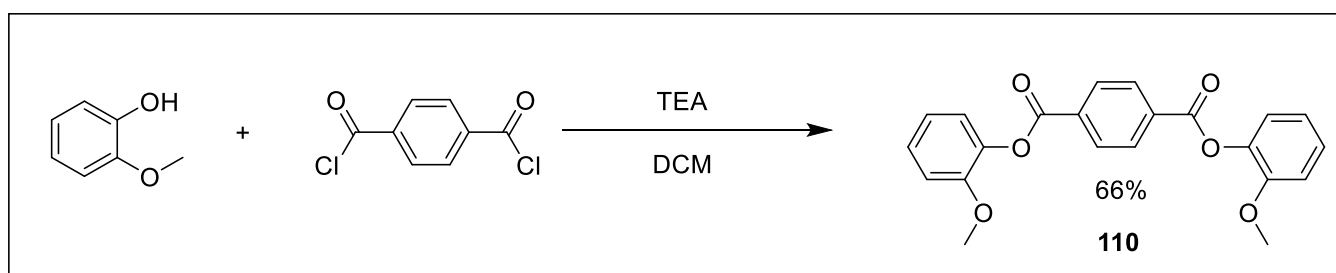
Scheme 2.16: synthesis of tetrakis(hexyloxy) biphenyl **109**

The Ullmann coupling is a classic method for synthesising biaryls through copper mediated coupling (scheme 2.15). A recent adaptation by Lin and co-workers uses nickel as a catalyst [107]. A common mechanism for this reaction involves the formation of an organocuprate intermediate from an aryl halide, which then reacts with a second molecule via oxidative addition, resulting in the final product from reductive elimination (Scheme 2.17) [108].



Scheme 2.17: Ullmann reaction mechanism by Cu and Ni.

For the second component, 2-methoxy phenol (1 eq) was reacted with benzene-1,4-dicarbonyl chloride (0.4 eq) in dry CH_2Cl_2 by slowly adding dry NEt_3 (2 ml) at 0°C . TLC confirmed the new spot for the product after two hours. It was concentrated in vacuo, recrystallised from $\text{DCM}:\text{MeOH}$, and the product, dimer **110**, was collected as pinkish crystals with a yield of 66% (Scheme 2.18).



Scheme 2.18: Diphenyl ester synthesis

Diphenyl ester **110** has a spectrum composed of one singlet for the central benzene protons, integrating 4H at 8.37 ppm, and others for the methoxybenzene protons. It appears as a ddd at 7.34 with $J = 8.3, 7.5, 1.6$ Hz, integrating two hydrogens, doublet of doublet at 7.23 with $J = 7.8, 1.7$ Hz, integrating two hydrogens, multiplets between 7.14 and 7.02 ppm, integrating four hydrogens; and $-\text{OCH}_3$ singlet peak at 3.87 ppm, integrating six hydrogens (figure 2.18).

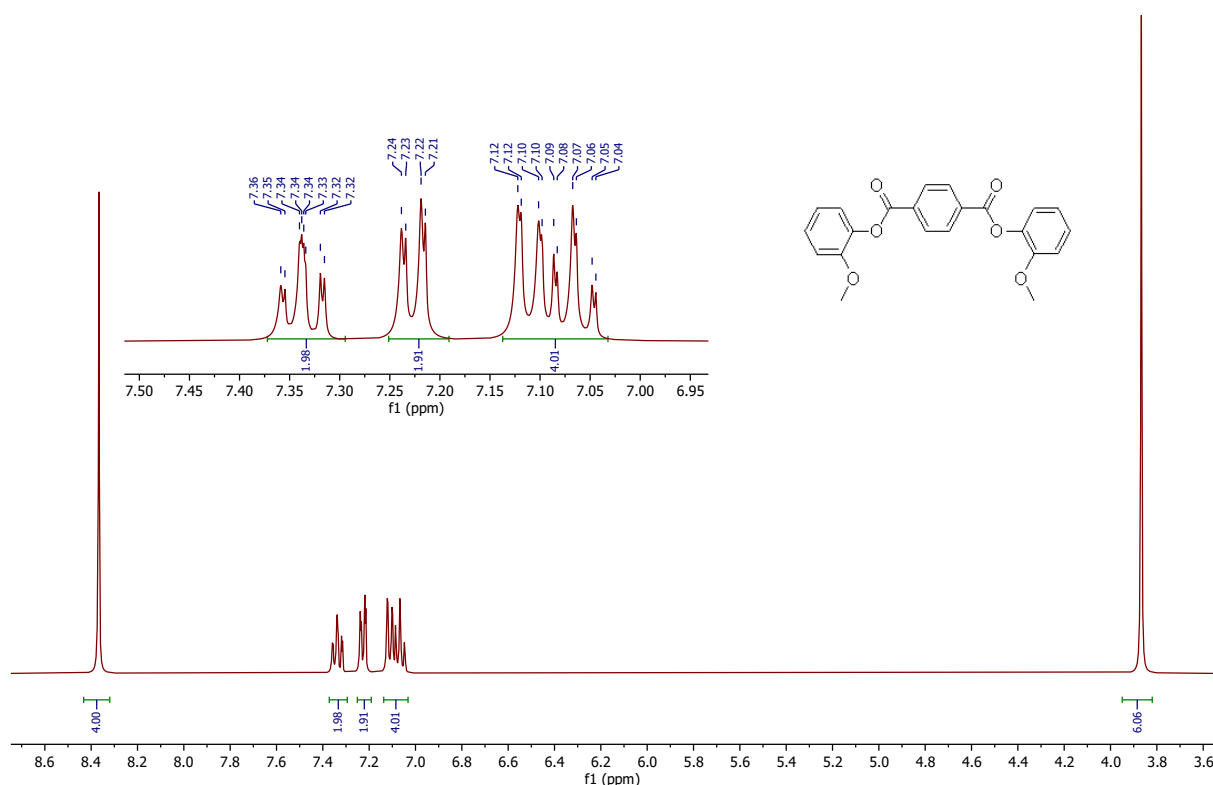
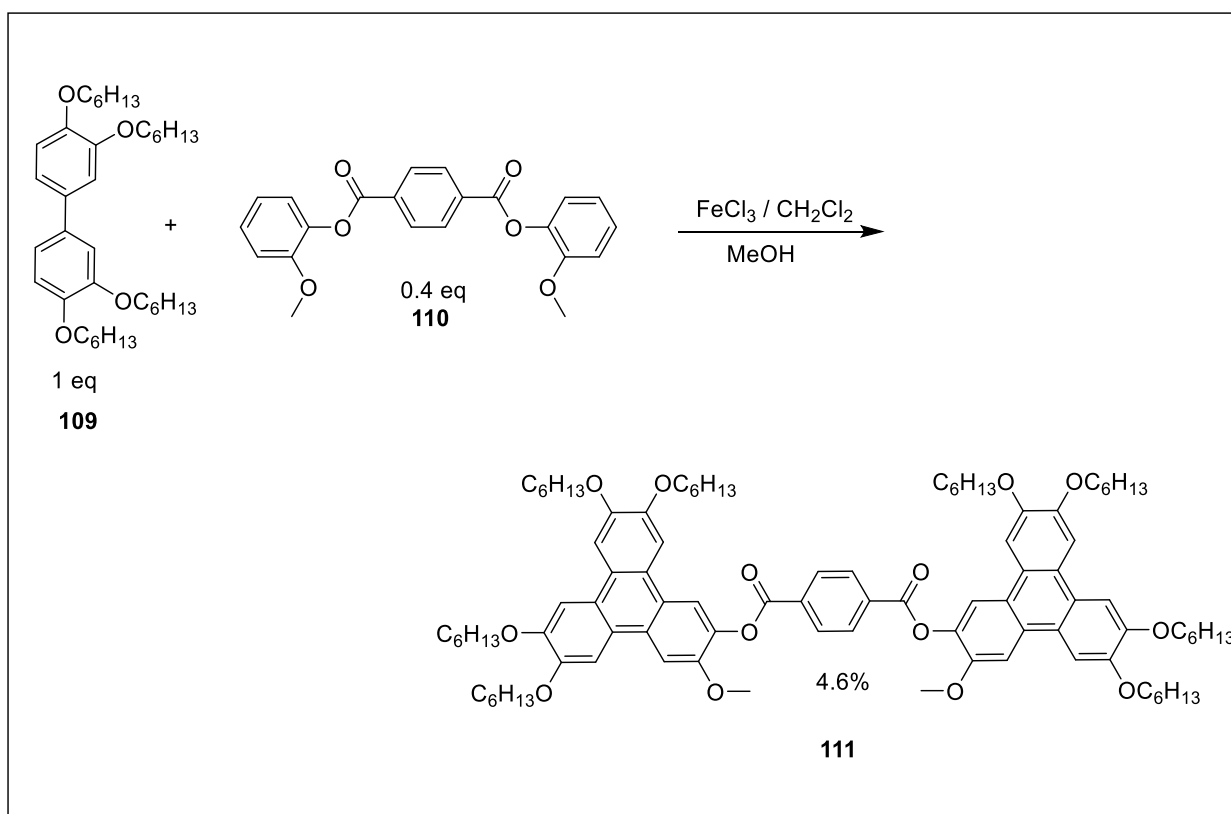


Figure 2.18: ^1H NMR spectrum of benzene dimer **110**

In the final step we investigated formation of triphenylene dimers by biphenyl route, which involves oxidative cyclization between tetraalkoxybiphenyl **109** and diester **110** with FeCl_3 in CH_2Cl_2 , followed by quench with MeOH (Scheme 2.19).

This synthesis pathway produced the product but only in 5% yield, which is quite low. One major side product was produced when biphenyl reacted with itself, but we also reasoned that acid catalysed hydrolysis might be a problem. Then, to avoid the side product, we used K_2CO_3 , but the yield remained the same.



Scheme 2.19: Alternative triphenylene dimer ester synthesis.

Figure 2.19 shows ^1H -NMR signals, and the analysis of these is concentrated on the aromatic region and around 4 ppm, as these are the areas of the signals that are most affected by pattern of substitution. The benzene ring signal appear as a singlet at 8.41 ppm, integrating four hydrogens, and the triphenylene protons appear as singlets at 8.17, 7.86, 7.83, 7.77, 7.74, and 7.73 ppm, integrating two hydrogens each.

The $-\text{OCH}_2$ group integrates 16 hydrogens and appears as a multiplet between 4.21 and 4.12. in addition, the methoxy group appears as singlet at 4.01 ppm integration six hydrogens.

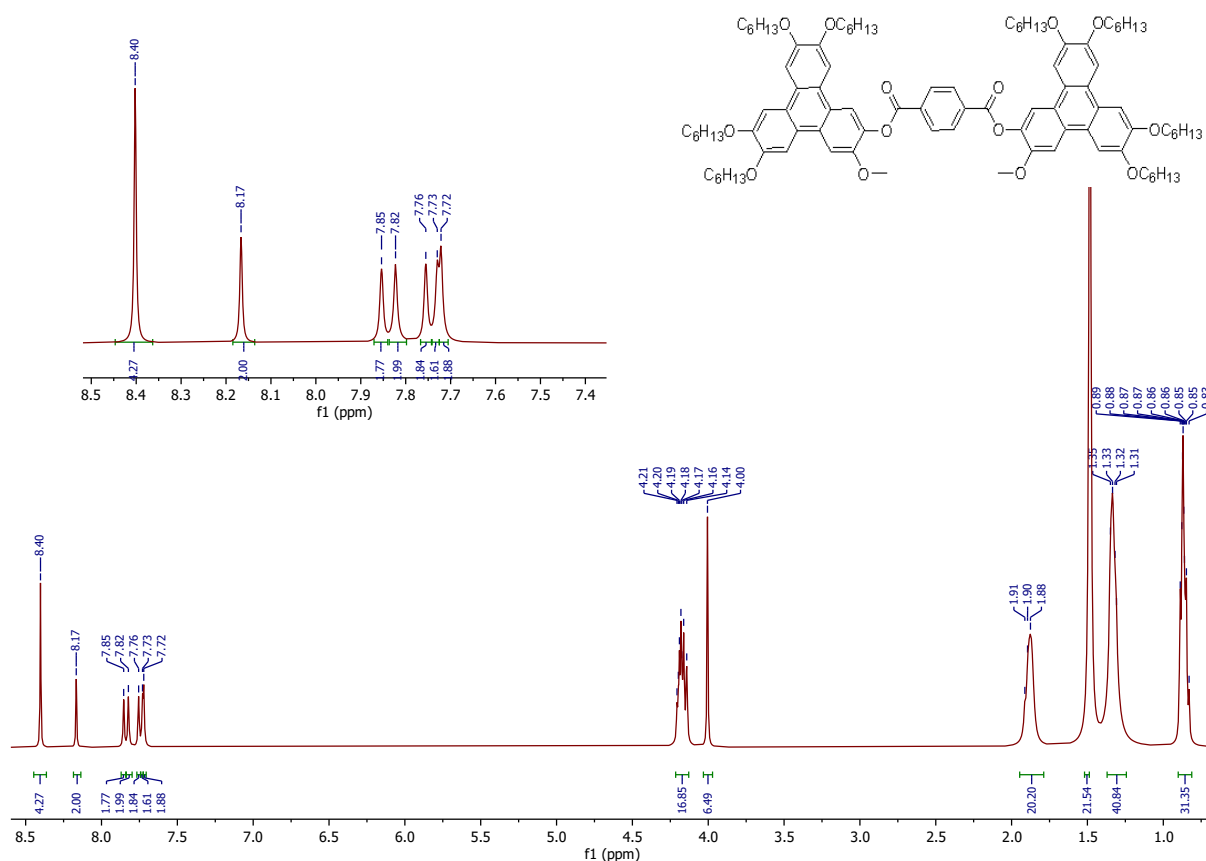


Figure 2.19: ^1H NMR spectrum of triphenylene dimer **111**.

Liquid crystal properties of triphenylene dimer **111**:

Dimer **111** is a new compound and liquid crystal properties, investigated by using POM, showed texture typical of hexagonal columnar mesophases were observed when the isotropic sample was either heated or cooled from 261 °C (Figure 2.20).

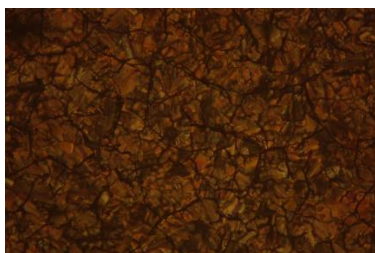
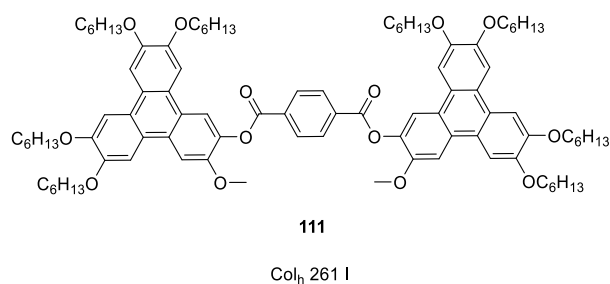


Figure 2.20: Texture and transition temperature for **111**.

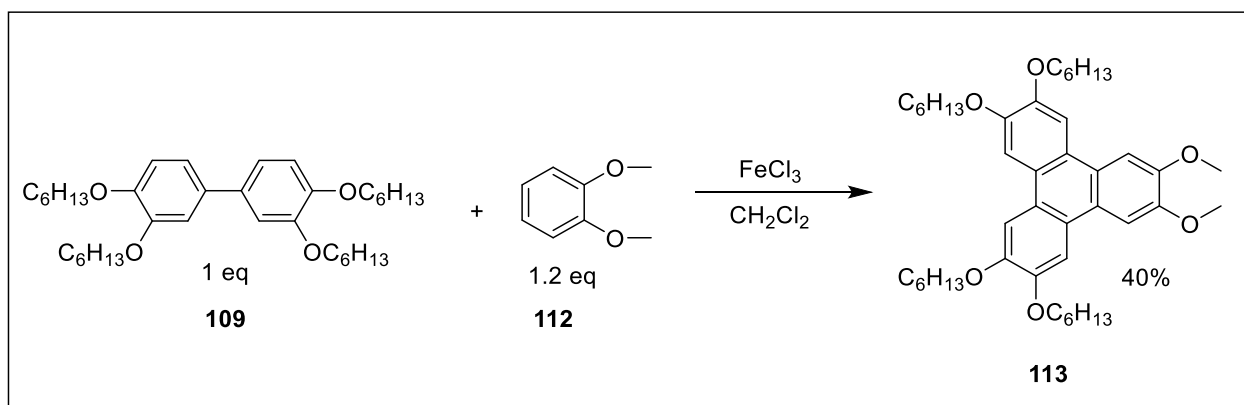
Triphenylene diester:

Our investigation concluded with an examination of triphenylene diesters, connecting 2,3- and 3,6-dihydroxy triphenylene with benzoates. This was accomplished by using the same conditions as before. The attempt to prepare a triphenylene diester seemed logical to complement the previous series and see if the onset of nematic behaviour would be observed.

Two similar procedures were used to carry out the reactions for 2,3-bis(hydroxy)triphenylene and 3,6-bis(hydroxy)triphenylene.

Synthesis of 2,3-dimethoxytriphenylene **113**:

The biphenyl route was used to synthesise 2,3-dimethoxy triphenylene (**113**), yielding 40 % by reacting tetrakis(hexyloxy)biphenyl biphenyl and 1,2-dimethoxybenzene with FeCl₃ (Scheme 2.20). [109].



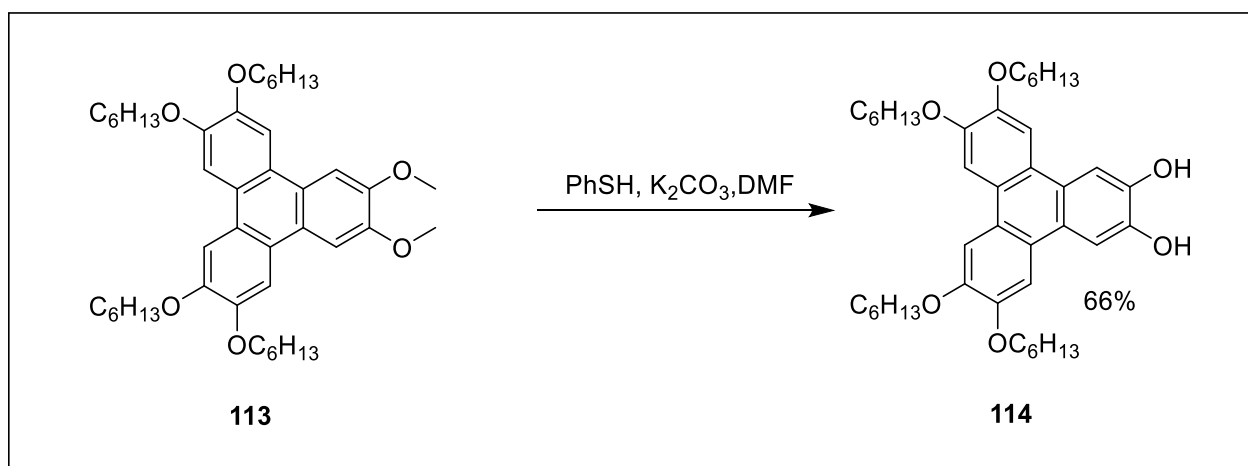
Scheme 2.20: 2,3-bis(methoxy) triphenylene (**111**) synthesis.

Synthesis of 2,3-bis(hydroxy)triphenylene **112**:

2,3-Dimethoxytriphenylene **113** is deprotected by cleaving its methoxy groups to phenolic groups. Several reactions have been described as being capable of performing such a hydrolysis, including using boron tribromide at room temperature [110] or refluxing the methoxy substrate in a mixture of hydrobromic acid and acetic acid, as described by Bechgaard *et al.* [111] However, both of these methods were considered too harsh to be used on 2,3-dimethoxytriphenylene **113** as the hexyloxy groups present on the molecule are also susceptible to hydrolysis. It has been demonstrated that lithium diphenylphosphide can be used to selectively remove methyl ethers, and this method has been successfully applied to triphenylenes [112]. We, however, utilized a newer, milder method employing thiophenol

[113]. The result was that 2,3-dimethoxytriphenylene **113** was reacted with PhSH/K₂CO₃ in refluxing dry DMF. Our group modified the demethylation pathway for 2,3-dimethoxytriphenylene or 3,6-dimethoxytriphenylene by using thiophenol, successfully using microwave irradiation [114] for around 5 hours on 1g scale of dimethoxy triphenylene. The reaction is monitored by NMR analysis of aliquots until the singlet peak of the methoxy protons is no longer present.

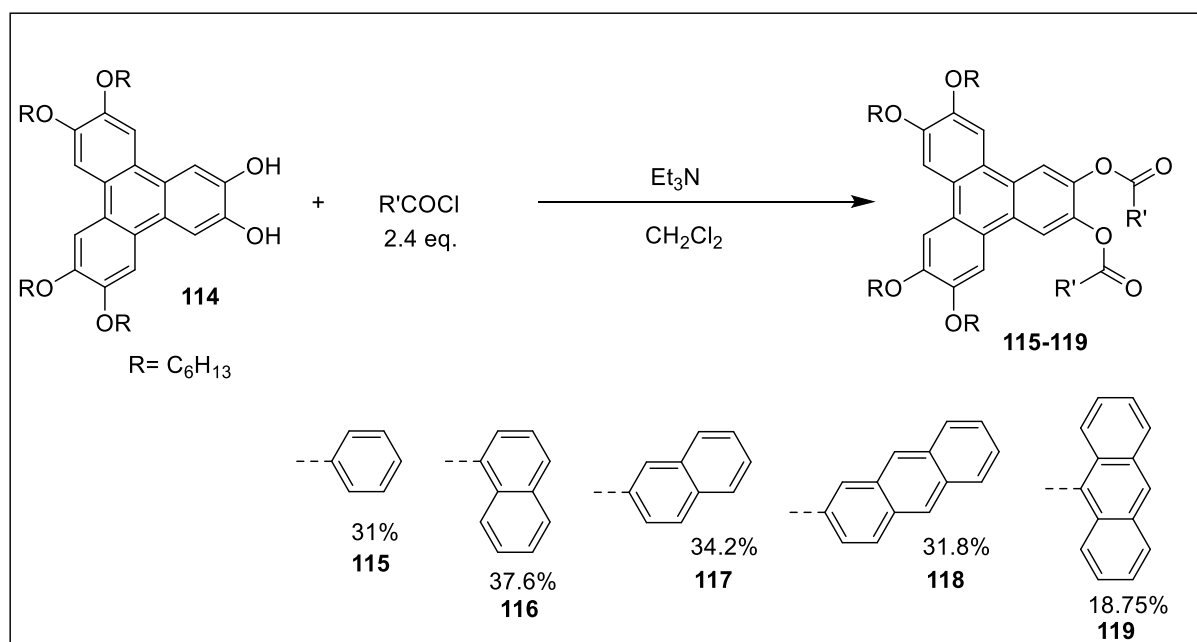
2,3-dihydroxytriphenylene **114** was produced by acidifying (HCl), cooling, and purifying the crude product through crystallisation from MeOH with a yield of 66 % (Scheme2.21).



Scheme 2.21: 2,3-dihydroxy triphenylene (**114**) synthesis.

Synthesis of 2,3-Diesters (**115-119**):

A selection of benzoyl, 1-naphthoyl, 2-naphthoyl, 2-anthracenoyl and 9-anthracenoyl derivatives was evaluated. Some acid chlorides are commercial chemicals that can be directly reacted with Dihydroxytriphenylene **114**. SOCl₂ was used to convert 2-anthracene carboxylic acid and 9-anthracene carboxylic acid into acid chloride, as previously described, which were then treated with 2,3-dihydroxytriphenylene **114**. The reaction of these compounds (acid chloride) with 2,3-dihydroxytriphenylene **114** follows the same steps described for triphenylene monoesters (Scheme 2.22).



Scheme 2.22: Synthesis of 2,3-Diesters of triphenylene **115-119**.

It was found that diester compounds (**115-119**) were formed based on 1H -NMR spectra. The aliphatic regions for all substituents are almost the same as for dihydroxytriphenylene **114**, and there are no longer any singlet proton signals for hydroxyl groups. There is also a multiplet of O-CH₂ peaks that integrate for eight hydrogens. Figure 2.21 illustrates the aromatic regions of the 1H -NMR spectrum for (**115-119**). Triphenylene-2,3-benzoate (**115**) shows three singlet protons for the triphenylene protons at 8.35, 7.80, and 7.77 ppm, integrating two hydrogens each. The other is for the benzoate protons, which appear as a doublet of doublet at 8.08 ppm with $J = 8.4$ Hz, integrating four hydrogens; multiplet between 7.54 and 7.47 ppm, integrating two hydrogens; multiplet between 7.37 and 7.32 ppm, integrating four hydrogens.

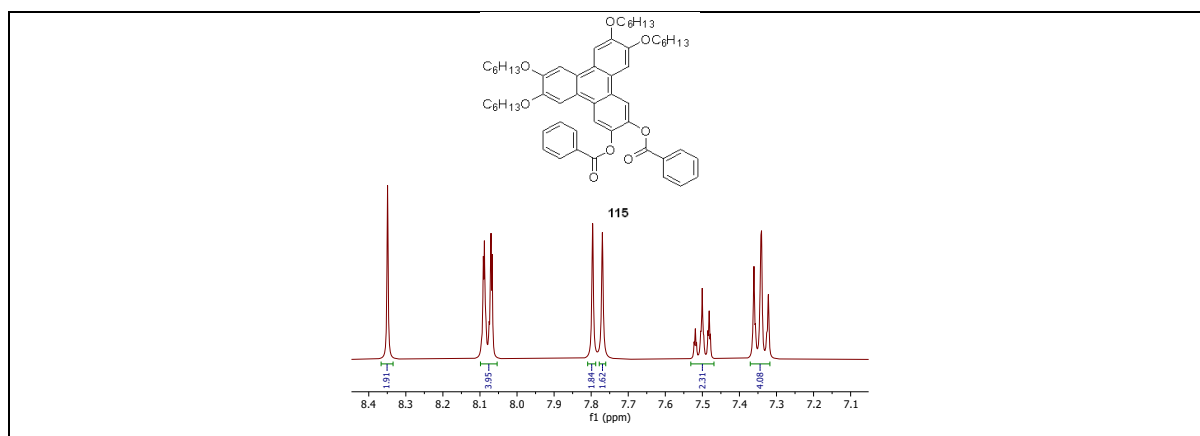
Triphenylene-di-2,3(1-naphthalenoate) (**116**) shows three singlet signals for the triphenylene protons at 8.42, 7.84, and 7.78 ppm, integrating two hydrogens each. The other is for 1-naphthalenoate protons, which appear as multiplet between 8.99 and 8.93, integrating two hydrogens; a doublet of doublet at 8.35 ppm with $J = 7.4, 1.3$ Hz, integrating two hydrogens; a doublet of triplet at 7.88 ppm with $J = 8.3, 1.1$ Hz, integrating two hydrogens; multiplet between 7.77 and 7.74 ppm, integrating two hydrogens; multiplet between 7.48 and 7.41 ppm, integrating four hydrogens, a doublet of doublet at 7.20 ppm with $J = 8.2, 7.3$ Hz, integrating two hydrogens.

Triphenylene-di-2,3(2-naphthalenoate) (**117**) shows three singlet protons for the triphenylene protons at 8.44, 7.82, and 7.77 ppm, integrating two hydrogens each. The other is for 2-

naphthalenoate protons, which appear as a singlet at 8.64 integrating two hydrogens; a doublet of doublet at 8.06 ppm with $J = 8.6, 1.8$ Hz, integrating two hydrogens; multiplet between 7.74 and 7.69 ppm, integrating four hydrogens; a doublet at 7.66 ppm with $J = 7.5$ Hz, integrating two hydrogens; a doublet of doublet of doublet at 7.47 ppm with $J = 8.2, 6.9, 1.3$ Hz, integrating two hydrogens; a doublet of doublet of doublet at 7.36 ppm with $J = 8.1, 6.9, 1.2$ Hz, integrating two hydrogens.

Triphenylene-di-2,3-di (2-anthracenoate) (**118**) shows three singlet protons for the triphenylene protons at 7.83, 7.81, and 7.79 ppm, integrating two hydrogens each. The other is for 2-Anthracenoate protons, which appear as a singlet at 8.82 integrating two hydrogens; a singlet at 8.51 integrating two hydrogens; a singlet at 8.17 integrating two hydrogens; a singlet at 8.09 integrating two hydrogens; a doublet of doublet at 7.99 ppm with $J = 8.9, 1.7$ Hz, integrating two hydrogens; a singlet at 7.86 integrating two hydrogens; a doublet at 7.61 ppm with $J = 8.5$ Hz, integrating two hydrogens; multiplet between 7.39 and 7.37 ppm, integrating two hydrogens; multiplet between 7.33 and 7.28 ppm, integrating two hydrogens.

Triphenylene-di-2,3-di (9-Anthracenoate) (**119**) shows three singlet protons for the triphenylene protons at 7.94, 7.92, and 7.89 ppm, integrating two hydrogens each. The other is for 9-Anthracenoate protons, which appear as a singlet at 8.79 integrating two hydrogens; a singlet at 8.47 integrating two hydrogens; a doublet at 8.11 ppm with $J = 9.0$ Hz, integrating four hydrogens; a singlet at 8.03 integrating two hydrogens; a doublet of doublet of doublet at 7.31 ppm with $J = 8.3, 6.6, 1.1$ Hz, integrating four hydrogens; a doublet of doublet of doublet at 6.95 ppm with $J = 8.9, 6.6, 1.3$ Hz, integrating four hydrogens.



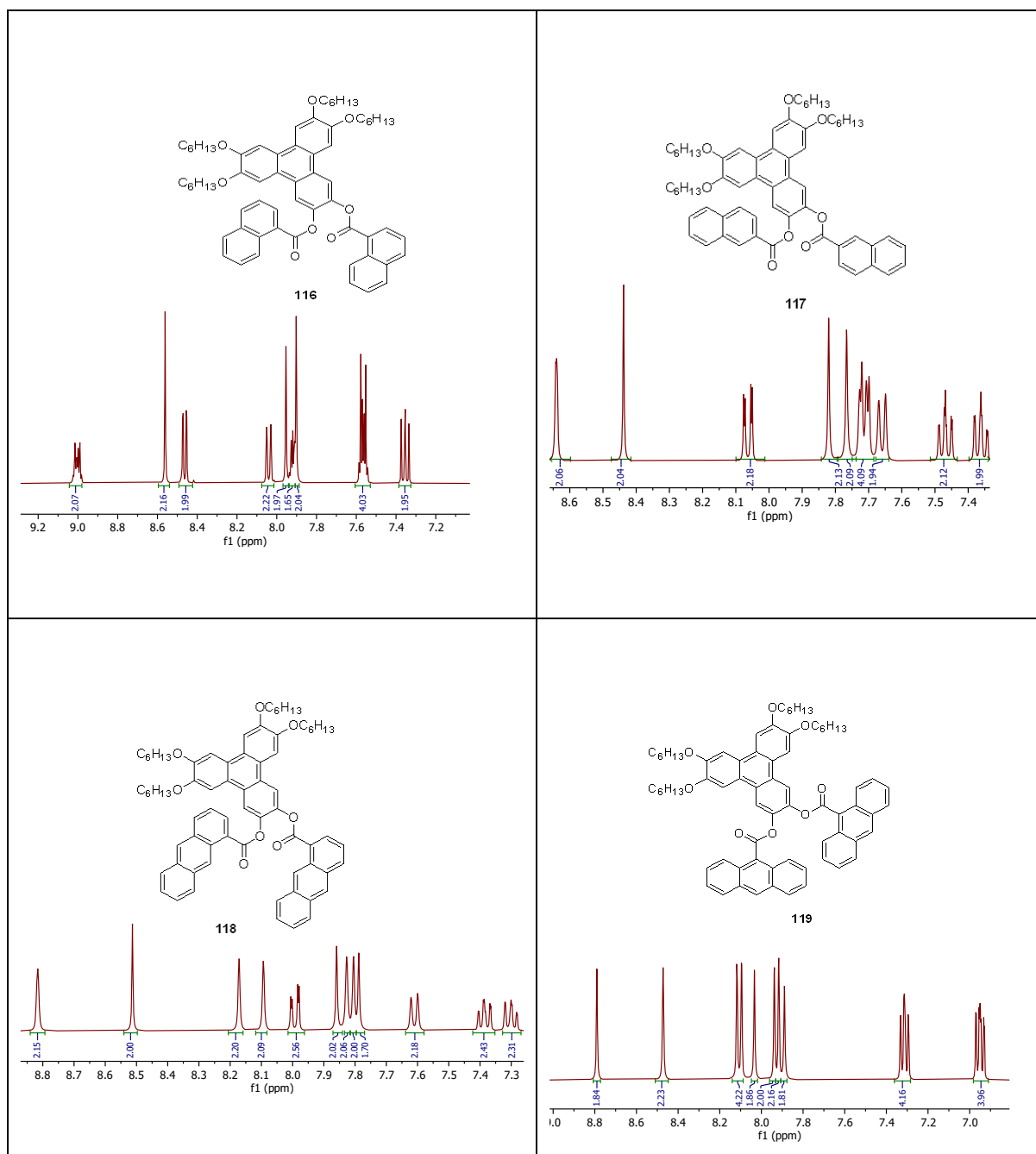


Figure 2.21: The aromatic peaks of NMR triphenylene esters **115-119**.

Liquid crystal properties for 2,3- Diesters (115-119):

The mesophase behaviour is summarised in Figure 2.22. Diester architectures based on 2,3-substituted triphenylene aromatic cores and benzoate derivatives resulted in improved thermal properties, such as higher melting points and higher clearing points. In addition, it did not directly lead to nematic behaviour, but rather prevented crystallization, resulting in a columnar phase that has the property of persisting at room temperature as a glass with intramolecular

stacking. In comparison to the corresponding monomeric liquid crystal at position-2 (**95-98**), broad Col_h phases and higher transition temperatures were observed.

Also, these diesters have a wider mesophase range than the parent hexaalkoxy or hexaalkanoyloxytriphenylene. When the ester group is bulky, as in **116-119**, crystallisation is suppressed and the mesophase is stabilised.

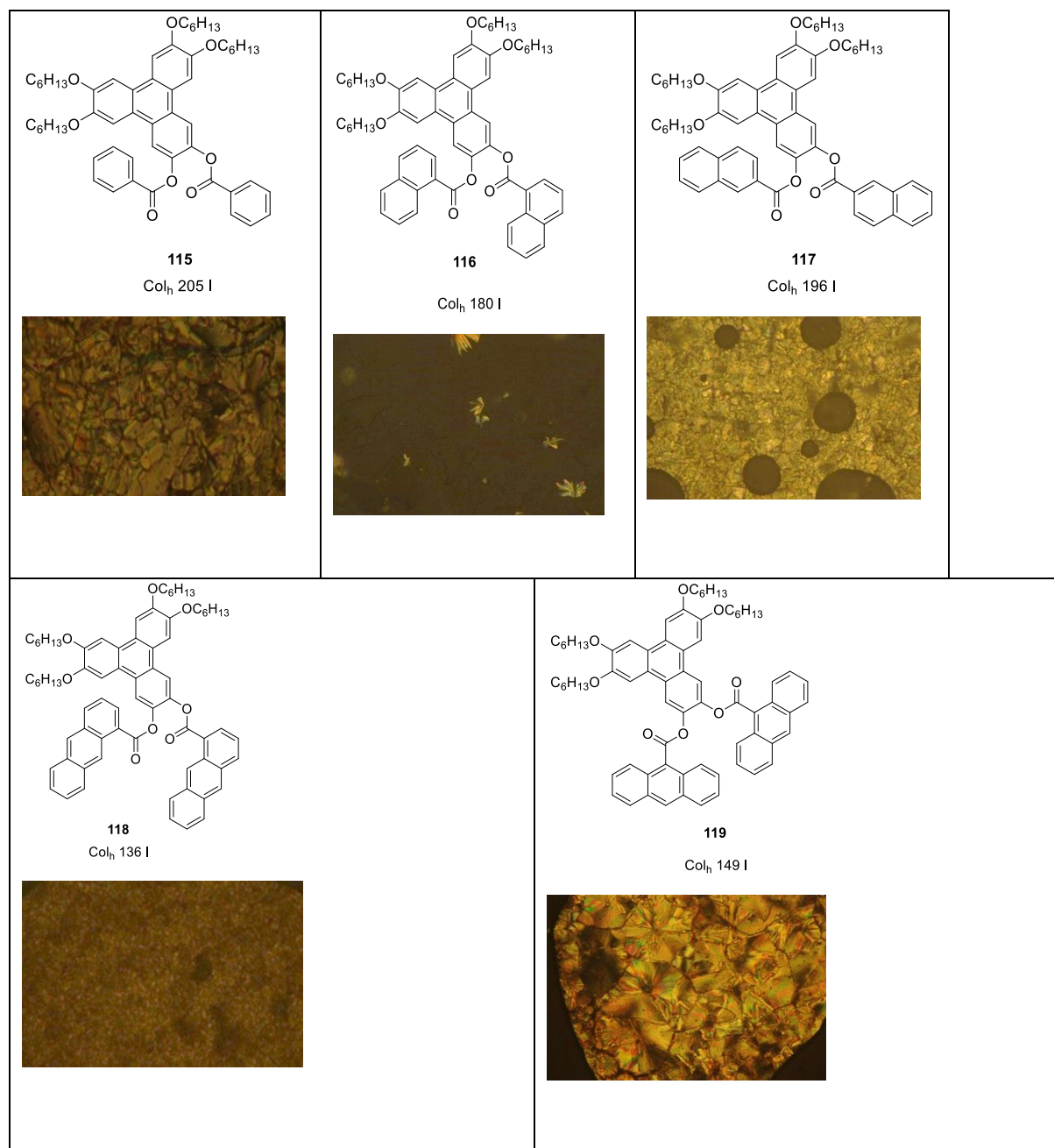
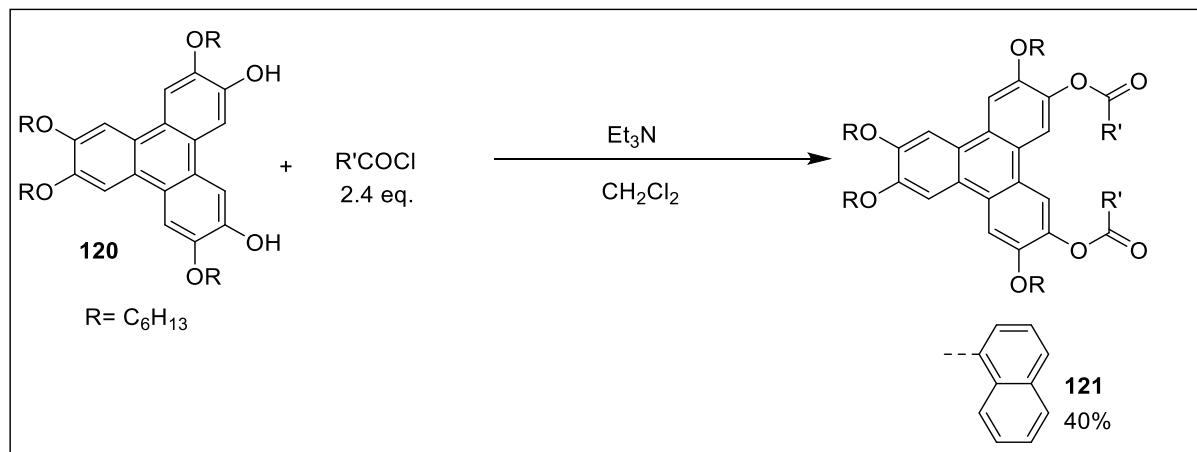


Figure 2.22: Columnar mesophase textures and transition temperatures of the triphenylene-2,3-diester **115–119**, bearing different substituents with simple benzoates and higher steric demand.

Synthesis of 3,6-Diester (**121**):

3,6-Dihydroxytriphenylene **120** was provided by our group [115]. A single derivative using 1-naphthoyl selection was examined. It is commercial acid chloride and can be treated immediately with 3,6-dihydroxytriphenylene **120**. These molecules (acid chloride) react with 3,6-dihydroxytriphenylene **120** in the same manner as triphenylene monoesters (Scheme 2.23).



Scheme 2.23: Synthesis of 3,6-Diester (**121**):

Triphenylene-di-3,6 (1-naphthalenoate) (**121**) shows three singlet protons for the triphenylene protons at 8.43, 7.85, and 7.80 ppm, integrating two hydrogens each. The other is for 1-naphthalenoate protons, which appear as multiplet between 9.00 and 8.91, integrating two hydrogens; a doublet of doublet at 8.36 ppm with $J = 7.4, 1.3$ Hz, integrating two hydrogens; a doublet at 7.90 ppm with $J = 8.2$ Hz, integrating two hydrogens; multiplet between 7.78 and 7.74 ppm, integrating two hydrogens; multiplet between 7.51 and 7.42 ppm, integrating four hydrogens; multiplet between 7.26 and 7.21 ppm, integrating two hydrogens. Mesophase analysis is ongoing.

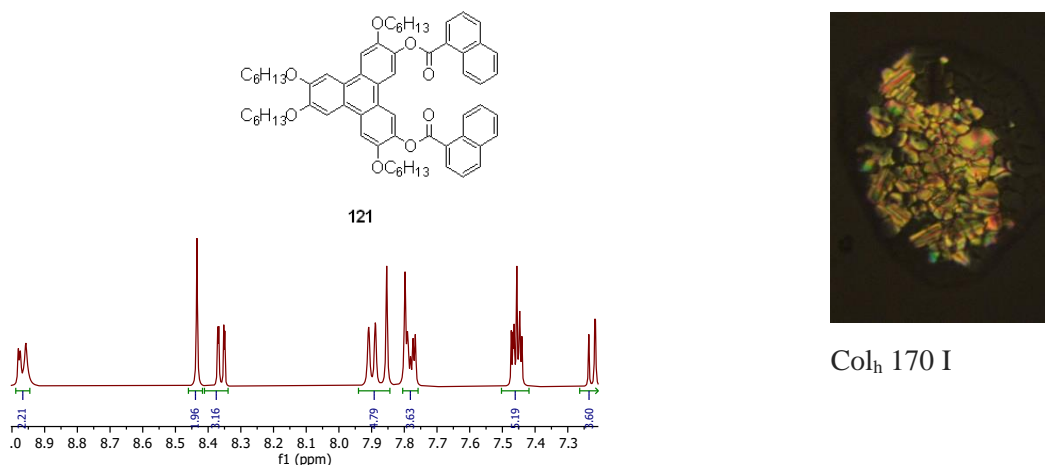


Figure 2.22: The aromatic peaks of NMR triphenylene esters **121**

Conclusion:

We designed and synthesised a group of discotic ester monomers, dimers, and diesters with various substitutions and explored the effects of structural modifications on the characteristics of the (macro)molecules in this work. Our findings are described below:

1. The monomers are synthesised in two step routes. The method was to link the triphenylene with the single aryl ester containing nitro or methoxy group at same position (para) or bromo group in different positions (meta and ortho). At room temperature, they are all liquid crystalline and form hexagonal columnar phases. Also, the stability of mesophase is not significantly affected by the simple ester used.

Then we increased perturbation in the triphenylene system by increasing the size of the aromatic ester. This was done by using naphthalene and anthracene substituted in different positions. It was found that all derivatives also only formed hexagonal columnar mesophases. Again, it can be inferred that these substituents have only a little impact on the mesophase's stability.

2. The dimers are synthesised in two steps (direct and indirect synthesis). The structural change in the linker groups of aryl carboxylate in different positions has affected the structure and packing of the mesomorphic dimers. It was found that, when changing from isophthalate (1,3-) to terephthalate (1,4-), the mesophase changed from Col_h to N_D (with simultaneous glass formation). The dimer with the 1,1'-ferrocene link introduces a unique offset arrangement and failed to show liquid crystal properties, likely because the staggered formation prevented packing and reduced stability and melting point.

A related dyad has been prepared by a new synthesis following the biphenyl route, and it showed a hexagonal columnar phase.

3. Finally, we synthesised and examined a series of triphenylenes bearing two aryl esters. The goal was to apply the same procedure as before to link 2,3-dihydroxy triphenylene and 3,6-dihydroxy triphenylene with benzoates. They were prepared by a one-step reaction route.

The columnar hexagonal mesophases were produced in all samples. Although the clearing temperatures are greater than those of monoesters, the ester utilised has no significant influence on their stability.

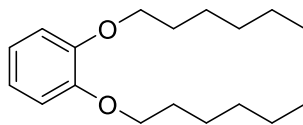
3. Experimental section:

General information:

We obtained reagents and solvents from commercial sources. There was no further purification unless stated otherwise. Thin-layer chromatography (TLC) was carried out on aluminium sheets coated with silica gel/UV254 (Macherey-Nagel), and UV light was used to visualise the results. Using a Büchi rotary evaporator, the solvents were evaporated at reduced pressure. The NMR spectra were recorded by a Bruker 500 and 400 (for ^1H NMR, 500 and 400 MHz was used, whereas for ^{13}C NMR, 126 and 101 MHz was used). We used the residual solvent peak as a reference. This was performed at room temperature. Both ^1H and ^{13}C NMR signals are expressed in ppm, whereas coupling constants J are expressed in Hertz. The IR spectrum was recorded with a Perkin-Elmer Spectrum 100 FT-IR spectrometer. Absorption bands are indicated in cm^{-1} . MALDI-TOF analyses were recorded using a Shimadzu Biotech Axima Spectrometer. Melting points were measured using a Reichert Thermovar microscope with a thermometer-based temperature control. In the stated solvents, UV-VIS spectra were recorded using a Perkin Elmer Lambda 35 UV/VIS instrument. Column chromatography was performed using silica gel (Material Harvest 40–63 micron). Optical microscopes (POMs) were used to identify the phases and phase transitions of liquid crystal compounds. We recorded the DSC analyses using a TA Instruments DSC 2500 device.

Synthetic procedures and characterization data:

Synthesis of 1,2-Dihexyloxybenzene (DHB) **55** [37]



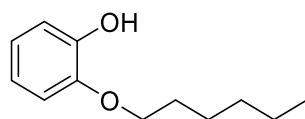
55

Pyrocatechol (40.78 g, 0.43 mol, 1 eq), an excess of 1-bromohexane (170.1 g, 1.042 mol, 2.4 eq), and potassium carbonate (144 g, 1.042 mol, 2.4 eq) were refluxed at 80 °C in ethanol (300 ml). After three days, the reaction was stopped, and TLC showed that the reaction was completed. The mixture was filtered to remove potassium salts and washed with DCM (3 x 50 ml). A rotary evaporator was used for evaporating the ethanol and DCM. A vacuum distillation was applied, and the title compound was collected in the third fraction at (185 °C/20 mm Hg). A colourless oil was collected (60 g, 59.4%).

¹H-NMR (500 MHz, CDCl₃) δ 6.91 (s, 4H), 4.02 (t, *J* = 7.0 Hz, 4H), 1.79-1.88 (m, 4H), 1.47-1.55 (m, 4H), 1.32-1.42 (m, 8H), 0.91-0.97 (m, 6H) ppm.

¹³C-NMR (126 MHz, CDCl₃) δ 149.4, 121.1, 114.2, 69.4, 31.74, 29.5, 25.9, 22.7, 14.1 ppm.

Synthesis of 2-hexyloxyphenol **74** [116]

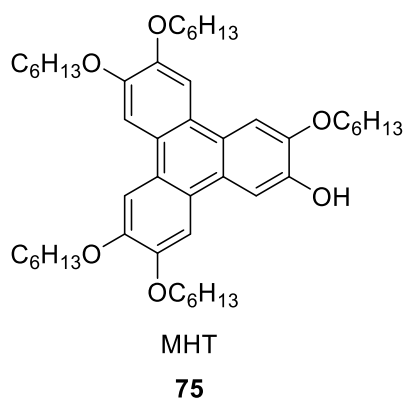


74

Pyrocatechol (40 g, 0.36 mol, 1 eq), 1-bromohexane (60 g, 0.36 mol, 1 eq) and potassium carbonate (50.2 g, 0.36 mol, 1 eq) were stirred in ethanol (200 ml) at 80 °C. After 3 days, the reaction was stopped after checking the ^1H -NMR spectrum of a small portion that showed that the bromohexane was consumed. The mixture was filtered, removing potassium carbonate, and washed with DCM (3 x 50 ml). A rotary evaporator was used for evaporating the ethanol and DCM. The crude product was dissolved in petroleum ether and passed through silica gel. After evaporation of the solvent, a colourless oil was collected (30 g, mono 69.8 %, di 27.8 %). The compound ratio of mono to di was (3.6:1), and we changed it to (1:4) by adding a specified amount of DHB. Also, it can be separated by distillation at (150-161 °C/20 mm Hg).

^1H NMR (500 MHz, Chloroform-*d*) δ 6.97 – 6.78 (m, 4H), 5.65 (s, 1H), 4.04 (t, J = 6.6 Hz, 2H), 1.82 (m, 2H), 1.44 – 1.26 (m, 6H), 0.87 (t, J = 7.0 Hz, 3H).

Synthesis of monohydroxy- pentahexyloxytriphenylene (MHT) **75** [91]

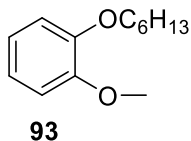


A 2:1 mixture of 1,2-Dihexyloxybenzene DHB **55** and monohexyloxyphenol **74** (3g, 0.0063 mol) was added slowly to the mixture of FeCl₃ (6.48g, 0.0399 mol), CH₃NO₂ (4 ml) in DCM (40 ml) over 30 mins and it was stirred at 0 °C. After 2 h, the reaction was quenched by adding methanol (30 ml) and the organic layer was extracted with DCM and H₂O, dried with magnesium sulphate, filtrated and then evaporated in vacuo. A column chromatography was applied, and the titled compound was collected in the second fraction (petroleum ether/EtOAc, 30:1/20:1). The pink solid was recrystallized in DCM: ethanol (1:1) (0.5 g, 34 %).

¹H NMR (500 MHz, Chloroform-*d*) δ 7.96 (s, 1H), 7.84 – 7.81 (m, 4H), 7.77 (s, 1H), 5.90 (s, 1H), 4.29 (t, *J* = 6.6, 1.4 Hz, 2H), 4.26 – 4.19 (m, 8H), 1.97 – 1.90 (m, 10H), 1.62 – 1.53 (m, 10H), 1.44 – 1.36 (m, 20H), 0.97 – 0.91 (m, 15H).

¹³C- NMR (126 MHz, CDCl₃) δ 149.0, 149.1, 148.9, 148.8, 145.9, 145.3, 124.0, 123.8, 123.7, 123.6, 123.3, 123.0, 107.7, 107.5, 107.4, 106.6, 104.4, 70.0, 69.9, 69.7, 69.2, 31.7, 31.6, 29.5, 29.4, 29.3, 25.9, 25.8, 22.7, 22.6, 14.1 ppm.

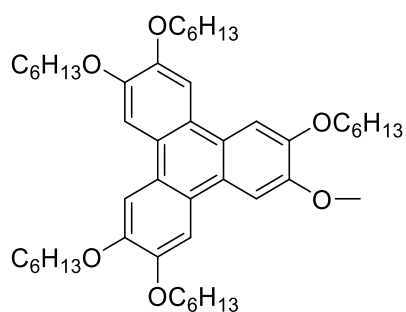
Synthesis of 1-Hexyloxy 2-methoxybenzene **93**



2-Methoxy phenol (40 g, 0.322 mol, 1 eq), 1-bromohexane (79.7 g, 0.483 mol, 1.5 eq) and potassium carbonate (44.5 g, 0.322 mol, 1 eq) were suspended in ethanol (300 mL) and refluxed for 48 h. The mixture was then cooled to room temperature, filtered and the solvents were removed in vacuo. The crude product was purified by distillation to give 1-hexyloxy-2-methoxybenzene **93** as a colourless oil. (18.55g, 27.6 %).

¹H NMR (400 MHz, Chloroform-*d*) δ 6.90 (s, 4H), 4.01 (t, $J = 6.9$ Hz, 2H), 3.87 (s, 3H), 1.91 – 1.78 (m, 2H), 1.49 – 1.42 (m, 2H), 1.36 – 1.29 (m, 4H), 0.96 – 0.87 (m, 3H).

Synthesis of Methoxy-pentahexyloxytriphenylene **94**

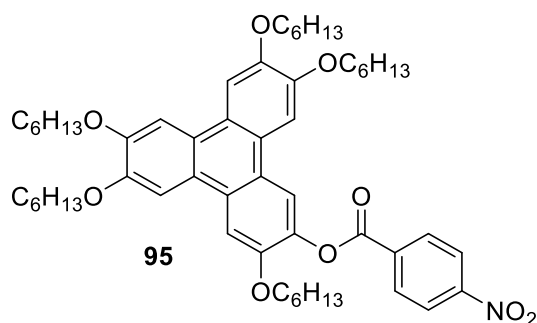


94

1-Hexyloxy 2-methoxybenzene (0.83 g, 3.99 mmol) and 1,2-Dihexyloxybenzene (1.11 g, 3.98 mmol) were added to a mixture of FeCl₃ (3.24 g, 19.97 mmol), nitromethane (2 ml), in dichloromethane (20 ml) and stirred at 0 °C for 2 h. It was quenched by methanol (30 mL). It was then worked up and purified by column chromatography, eluting with (ethyl acetate: petroleum ether/ 1: 8). The solvents were then removed in vacuo. The titled compound was collected as a pink solid (0.4 g, 37 %).

¹H NMR (400 MHz, Chloroform-*d*) δ 7.89 – 7.75 (m, 6H), 4.32 – 4.20 (m, 10H), 4.10 (s, 3H), 2.01 – 1.88 (m, 10H), 1.63 – 1.53 (m, 10H), 1.46 – 1.35 (m, 20H), 1.03 – 0.87 (m, 15H).

Synthesis of (4-Nitrobenzoate) ester **95**



MHT (150 mg, 0.0002 mol) and 4-nitro benzoyl chloride (0.044 g, 0.023 mol, 1.2 eq) were stirred in CH₂Cl₂ (25 ml) at 0 °C. Then 1 ml of NEt₃ was slowly added. After 2 h, the reaction was stopped, the solution was evaporated and recrystallized from methanol, and the titled compound was collected as a yellow solid (0.058, 32.2%).

¹H NMR (500 MHz, Chloroform-*d*) δ 8.48 (d, *J* = 8.8 Hz, 2H), 8.40 (d, *J* = 8.8 Hz, 2H), 8.22 (s, 1H), 7.93 (s, 1H), 7.88 (s, 1H), 7.84 (s, 1H), 7.83 (s, 1H), 7.79 (s, 1H), 4.29 – 4.15 (m, 10H), 2.00 – 1.88 (m, 8H), 1.79 – 1.72 (m, 2H), 1.63 – 1.52 (m, 10H), 1.47 – 1.34 (m, 16H), 1.26 – 1.19 (m, 4H), 1.08 – 0.88 (m, 12H), 0.80 (t, *J* = 7.0 Hz, 3H).

¹³C NMR (126 MHz, Chloroform-*d*) δ 163.30, 150.88, 149.91, 149.30, 149.09, 148.87, 139.57, 135.05, 131.39, 128.34, 124.77, 123.73, 123.34, 123.28, 123.22, 122.87, 116.56, 107.99, 107.24, 106.86, 106.45, 106.25, 69.92, 69.79, 69.50, 69.24, 68.91, 31.72, 31.66, 31.45, 29.47, 29.45, 29.42, 29.35, 29.18, 25.90, 25.87, 25.84, 25.66, 22.69, 22.66, 22.55, 14.08, 14.06, 13.92.

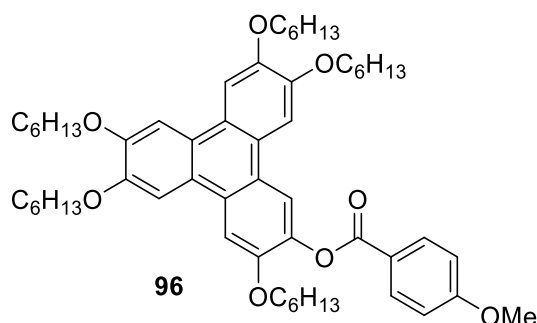
IR (thin film, cm⁻¹) 2924, 2856, 1740, 1614, 1514, 1435, 1387, 1345, 1258.

Transition temperatures Col 171 I

UV-vis (DCM, λ_{max}, nm (rel. int.)): 310 (0.0106), 279 (0.497), 271 (0.346), 225 (0.142)

MS (MALDI): *m/z* calculated for C₅₅H₇₅NO₉ (M⁺, 100%): 894.00 found 894.20

Synthesis of 4-Methoxybenzoate ester 96



MHT (150 mg, 0.0002 mol) and 4-methoxy benzoyl chloride (0.0408 g, 0.00024 mol, 1.2 eq) were stirred in CH₂Cl₂ (25 ml) at 0 °C. Then, NEt₃ (1 ml) was added slowly. After 2 h, the reaction was stopped, the solution was evaporated and recrystallized from methanol, and the titled compound was collected as a white solid (0.03g, 16.9 %).

¹H NMR (500 MHz, Chloroform-*d*) δ 8.25 (d, *J* = 8.9 Hz, 2H), 8.20 (s, 1H), 7.91 (s, 1H), 7.88 (s, 1H), 7.84 (s, 1H), 7.83 (s, 1H), 7.80 (s, 1H), 7.02 (d, *J* = 8.9 Hz, 2H), 4.33 – 4.15 (m, 10H), 3.93 (s, 3H), 2.04 – 1.88 (m, 8H), 1.86 – 1.69 (m, 2H), 1.62 – 1.50 (m, 10H), 1.47 – 1.32 (m, 16H), 1.25 – 1.18 (m, 4H), 0.95 – 0.88 (m, 12H), 0.82 (t, *J* = 6.5 Hz, 3H).

¹³C NMR (126 MHz, CDCl₃) δ 164.89, 163.85, 149.68, 149.23, 148.86, 148.79, 140.29, 132.43, 127.92, 124.61, 123.56, 123.28, 123.14, 123.08, 121.97, 116.95, 113.82, 107.96, 107.30, 106.94, 106.41, 77.31, 77.05, 76.80, 69.86, 69.82, 69.52, 69.15, 69.06, 55.52, 31.73, 31.67, 31.53, 29.47, 29.43, 29.35, 29.27, 25.89, 25.83, 25.66, 22.69, 22.66, 22.55, 14.08, 14.05, 13.96.

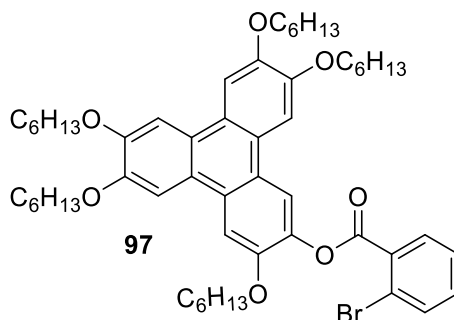
IR (thin film, cm⁻¹) 2928, 2854, 1721, 1605, 1511, 1468, 1434, 1392, 1316, 1253.

Transition temperatures Col 143 I

UV-vis (DCM, λ_{max}, nm (rel. int.)): 310 (0.0146), 279 (0.461), 271 (0.341)

MS (MALDI): m/z calculated for C₅₆H₇₈O₈ (M⁺, 100%): 878.57 found 879.23

Synthesis of 2-Bromobenzoate ester 97



MHT (150 mg, 0.0002 mol), 2-bromo benzoyl chloride (0.052g, 0.00024 mol, 1.2 eq) were stirred in CH₂Cl₂ (25 ml) at 0 °C. Then, NEt₃ (1 ml) was added slowly. After 2 h, the reaction was stopped, the solution was evaporated and recrystallized from methanol and the titled compound was collected as a pale brown solid (0.03g, 16.6%).

¹H NMR (400 MHz, Chloroform-*d*) δ 8.24 (dd, *J* = 8.0, 2.0 Hz, 1H), 8.21 (s, 1H), 7.91 (s, 1H), 7.88 (s, 1H), 7.84 (s, 1H), 7.83 (s, 1H), 7.81 (s, 1H), 7.78 (dd, *J* = 8.0, 2.0 Hz, 1H), 7.51-7.41 (m, 2H), 4.34 – 4.17 (m, 10H), 2.02 – 1.88 (m, 8H), 1.88 – 1.79 (m, 2H), 1.66 – 1.52 (m, 10H), 1.50 – 1.33 (m, 16H), 1.28 (qt, *J* = 6.5, 3.4 Hz, 4H), 1.00 – 0.89 (m, 12H), 0.88 – 0.81 (m, 3H).
¹³C NMR (101 MHz, CDCl₃) δ 164.09, 149.82, 149.42, 149.28, 148.99, 148.84, 139.71, 134.73, 133.20, 132.35, 131.11, 128.18, 127.23, 124.74, 123.52, 123.20, 123.02, 122.68, 116.82, 108.09, 107.34, 106.98, 106.64, 106.08, 77.34, 77.02, 76.70, 69.95, 69.83, 69.53, 69.28, 68.94, 31.70, 31.65, 31.60, 30.93, 29.45, 29.40, 29.33, 25.87, 25.82, 25.78, 22.67, 22.56, 14.06, 13.98.

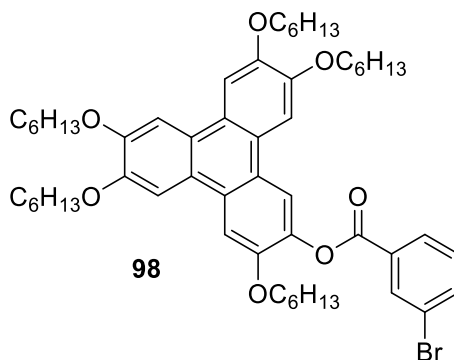
IR (thin film, cm⁻¹) 3534, 2972, 2855, 1746, 1616, 1512, 1433, 1392, 1258.

Transition temperatures Col 169 I

UV-vis (DCM, λ_{max}, nm (rel. int.)): 310 (0.112), 279 (0.486), 271 (0.361)

MS (MALDI): *m/z* calculated for C₅₅H₇₅BrO₇ (M⁺, 100%): 928.10 found 928.00

Synthesis of 3-Bromobenzoate ester **98**



MHT (150 mg, 0.0002 mol), 3-bromo benzoyl chloride (0.052 g, 0.00024 mol, 1.2 eq) were stirred in CH_2Cl_2 (25 ml) at 0 °C. Then, NEt_3 (1 ml) was added slowly. After 2 h, the reaction was stopped, the solution was evaporated and recrystallized from methanol and the titled compound was collected as a pale brown solid (0.07 g, 38.8%).

^1H NMR (500 MHz, Chloroform-*d*) δ 8.45 (t, J = 2.0 Hz, 1H), 8.22 (dt, J = 8.0, 2.0 Hz, 2H), 8.19 (s, 1H), 7.91 (s, 1H), 7.88 (s, 1H), 7.83 (s, 1H), 7.82 (s, 1H), 7.81-7.78 (m, 2H), 7.43 (t, J = 8.0 Hz, 1H), 4.32 – 4.16 (m, 10H), 2.06 – 1.90 (m, 8H), 1.86 – 1.72 (m, 2H), 1.71 – 1.50 (m, 10H), 1.48 – 1.36 (m, 16H), 1.28 – 1.18 (m, 4H), 1.02 - 0.88 (m, 12H), 0.82 (t, J = 7.0 Hz, 3H).

^{13}C NMR (126 MHz, Chloroform-*d*) δ 163.82, 149.81, 149.37, 148.97, 148.83, 139.86, 136.45, 133.25, 131.58, 130.16, 128.87, 128.18, 124.71, 123.46, 123.25, 123.20, 122.98, 122.68, 116.70, 107.99, 107.31, 106.93, 106.37, 69.90, 69.83, 69.52, 69.18, 69.03, 31.72, 31.66, 31.51, 29.46, 29.42, 29.34, 29.24, 25.89, 25.87, 25.83, 25.72, 22.69, 22.66, 22.56, 14.08, 14.06, 13.95.

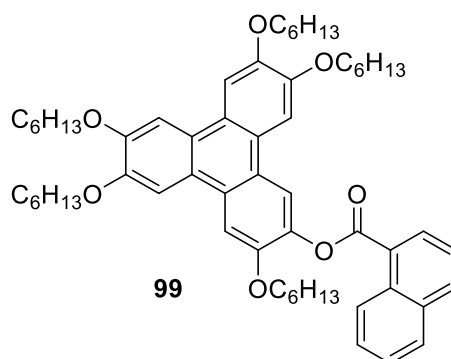
IR (thin film, cm^{-1}) 2956, 2920, 2855, 2364, 1736, 1620, 1517, 1434, 1393, 1281, 1245.

Transition temperatures Col 179 I

UV-vis (DCM, λ_{max} , nm (rel. int.)): 312 (0.128), 278 (0.559), 267 (0.393)

MS (MALDI): m/z calculated for $\text{C}_{55}\text{H}_{75}\text{BrO}_7$ (M^+ , 100%): 928.10 found 928.99

Synthesis of (1-Naphthoate) ester **99**



MHT (150 mg, 0.0002 mol), 1-naphthoyl chloride (0.115 g, 0.0006 mol, 3 eq) and were stirred in dry CH₂Cl₂ (20 ml) under N₂ at 0 °C. Then, dry NEt₃ (1 ml) was added slowly. After 2 h, the reaction was stopped, the solution was evaporated and recrystallized from methanol and the titled compound was collected as a pale green solid (0.116g, 64.4%).

¹H NMR (500 MHz, Chloroform-*d*) δ 9.11 (d, *J* = 8.7 Hz, 1H), 8.59 (dd, *J* = 8.0, 1.3 Hz, 1H), 8.26 (s, 1H), 8.14 (d, *J* = 8.0 Hz, 1H), 7.96 (d, *J* = 8.0 Hz, 1H), 7.94 (s, 1H), 7.90 (s, 1H), 7.84 (s, 1H), 7.83 (s, 1H), 7.82 (s, 1H), 7.69-7.57 (m, 3H), 4.32 – 4.16 (m, 10H), 2.04 – 1.88 (m, 8H), 1.84 – 1.74 (m, 2H), 1.66 – 1.50 (m, 10H), 1.47 – 1.33 (m, 16H), 1.25 – 1.11 (m, 4H), 1.01 – 0.83 (m, 12H), 0.73 (t, *J* = 7.2 Hz, 3H). **¹³C NMR** (126 MHz, CDCl₃) δ 165.92, 149.78, 149.67, 149.29, 148.93, 148.83, 140.12, 134.04, 133.95, 131.72, 131.23, 128.60, 128.09, 128.00, 126.39, 126.35, 126.05, 124.71, 124.59, 123.58, 123.29, 123.19, 123.09, 117.00, 108.08, 107.36, 106.97, 106.51, 106.13, 77.29, 77.03, 76.78, 69.94, 69.84, 69.53, 69.20, 68.95, 31.71, 31.65, 31.50, 29.47, 29.45, 29.42, 29.33, 25.89, 25.86, 25.81, 25.73, 22.69, 22.64, 22.45, 14.08, 14.04, 13.86.

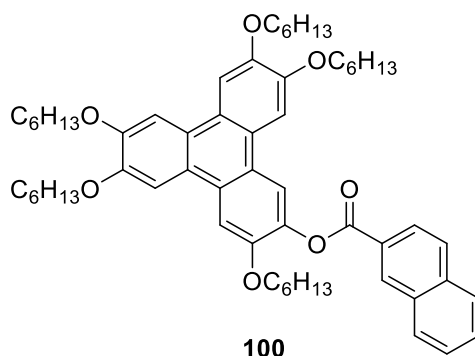
IR (thin film, cm⁻¹) 2926, 2855, 1727, 1616, 1511, 1467, 1433, 1391, 1285.

Transition temperatures Col 151 I

UV-vis (DCM, λ_{max}, nm (rel. int.)): 310 (0.214), 279 (0.651), 269 (0.479), 238 (0.272)

MS (MALDI): *m/z* calculated for C₅₉H₇₈O₇ (M⁺, 100%): 898.57 found 899.02

Synthesis of (2-Naphthoate) ester **100**



MHT (150 mg, 0.0002 mol), and 2-naphthoyl chloride (0.045 g, 0.00024 mol, 1.2 eq) were stirred in dry CH₂Cl₂ (20 ml) under N₂ at 0 °C. Then, dry NEt₃ (1 ml) was added slowly. After 2 h, the reaction was stopped, the solution was evaporated and recrystallized from methanol and the titled compound was collected as a white solid (0.05 g, 28%).

¹H NMR (500 MHz, Chloroform-*d*) δ 8.90 (s, 1H), 8.29 (dd, *J* = 8.5, 1.7 Hz, 1H), 8.26 (s, 1H), 8.04 (d, *J* = 8.5 Hz, 1H), 7.99 (d, *J* = 8.6 Hz, 1H), 7.95 (d, *J* = 8.5, 1H), 7.93 (s, 1H), 7.90 (s, 1H), 7.84 (s, 1H), 7.83 (s, 1H), 7.82 (s, 1H), 7.66 (ddd, *J* = 8.2, 6.9, 1.3 Hz, 1H), 7.60 (ddd, *J* = 8.2, 6.9, 1.3 Hz, 1H), 4.29 – 4.16 (m, 10H), 2.00 – 1.86 (m, 8H), 1.81 – 1.72 (m, 2H), 1.64 – 1.48 (m, 10H), 1.44 – 1.32 (m, 16H), 1.26 – 1.09 (m, 4H), 1.00 – 0.85 (m, 12H), 0.72 (t, *J* = 7.1 Hz, 3H). **¹³C NMR** (126 MHz, CDCl₃) δ 165.32, 149.76, 149.64, 149.29, 148.93, 148.84, 140.27, 135.87, 132.62, 132.02, 129.52, 128.55, 128.38, 128.07, 127.87, 126.82, 126.80, 125.71, 124.69, 123.57, 123.33, 123.19, 123.08, 116.91, 108.02, 107.36, 106.99, 106.47, 106.43, 77.28, 77.23, 77.03, 76.77, 69.91, 69.84, 69.54, 69.18, 69.08, 31.71, 31.63, 31.45, 29.46, 29.45, 29.42, 29.32, 29.24, 25.88, 25.86, 25.80, 25.66, 22.68, 22.63, 22.48, 14.07, 14.03, 13.84.

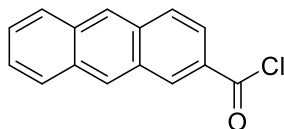
IR (thin film, cm⁻¹) 2930, 2853, 1731, 1614, 1515, 1434, 1391, 1285.

Transition temperatures Col 163 I

UV-vis (DCM, λ_{max}, nm (rel. int.)): 312 (0.110), 279 (0.468), 270 (0.343), 244 (0.284), 224 (0.253)

MS (MALDI): m/z calculated for C₅₉H₇₈O₇ (M⁺, 100%):898.57 found 899.26

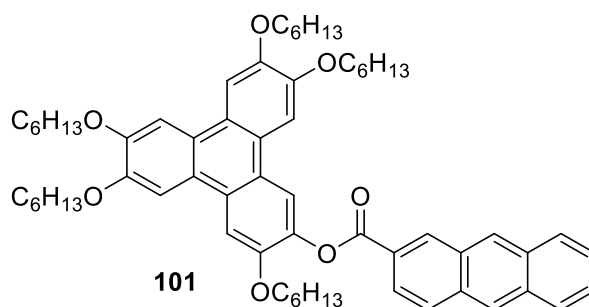
Synthesis of anthracene-2-carbonyl chloride 101a [117]



Anthracene-2-carboxylic acid (0.5 g, 0.0022 mol) and five drops of dry DMF were stirred in thionyl chloride (1.5 ml) under N₂ at RT for 30 minutes. The solvents were removed under vacuum and recrystallized from hexane, and the titled compound was collected as a yellow solid (0.1, 20%).

¹H NMR (400 MHz, Chloroform-*d*) δ 8.62 (s, 1H), 8.36 (d, $J = 8.8$ Hz, 2H), 8.14 (d, $J = 8.8$ Hz, 2H), 8.10 (s, 1H), 8.08 (s, 1H), 7.65 (t, $J = 8.3, 6.6$ Hz, 1H), 7.57 (t, $J = 7.5$ Hz, 1H).

Synthesis of (2-Anthracenoate) ester **101**



MHT (150 mg, 0.0002 mol) and anthracene-2-carbonyl chloride (0.07 g, 0.0003 mol, 1.5 eq) were stirred in dry CH_2Cl_2 (20 ml) under N_2 at 0 °C. Then, dry NEt_3 (1 ml) was added slowly. After 2 h, the reaction was stopped, the solution was evaporated and recrystallized from methanol, and the titled compound was collected as a green solid (0.03g, 16%).

^1H NMR (500 MHz, Chloroform-*d*) δ 9.11 (s, 1H), 8.65 (s, 1H), 8.52 (s, 1H), 8.29 (s, 1H), 8.22 (dd, J = 8.5, 1.7 Hz, 1H), 8.13 (d, J = 8.0 Hz, 1H), 8.07 (t, J = 7.7 Hz, 2H), 7.95 (s, 1H), 7.91 (s, 1H), 7.88 (s, 1H), 7.86 (2 x s, 2H), 7.60-7.51 (m, 2H), 4.34 – 4.17 (m, 10H), 2.06 – 1.91 (m, 8H), 1.87 – 1.73 (m, 2H), 1.71 – 1.55 (m, 10H), 1.50 – 1.31 (m, 16H), 1.25 – 1.12 (m, 4H), 1.02 – 0.85 (m, 12H), 0.72 (t, J = 7.1 Hz, 3H). **^{13}C NMR** (126 MHz, CDCl_3) δ 165.34, 149.30, 133.38, 133.31, 132.89, 132.10, 130.46, 128.96, 128.69, 128.55, 128.24, 126.75, 126.34, 125.99, 124.70, 124.39, 116.95, 106.48, 77.27, 77.02, 76.77, 69.91, 69.85, 69.55, 69.18, 69.12, 31.71, 31.63, 31.44, 29.45, 29.42, 29.31, 29.25, 25.88, 25.85, 25.80, 25.67, 22.68, 22.62, 22.48, 14.07, 14.02, 13.83.

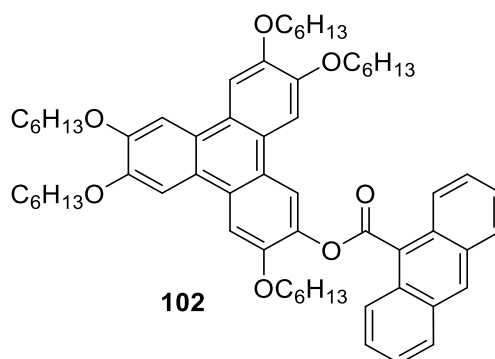
IR (thin film, cm^{-1}) 2923, 2851, 1728, 1616, 1511, 1433, 1384, 1311, 1258.

Transition temperatures Col 141 I

UV-vis (DCM, λ_{max} , nm (rel. int.)): 332 (0.049), 280 (0.560), 270 (0.456), 243 (0.191).

(MALDI): m/z calculated for $\text{C}_{63}\text{H}_{80}\text{O}_7$ (M^+ , 100%): 948.59 found 948.11

Synthesis of (9-Anthracenoate) ester **102**



MHT (150 mg, 0.0002 mol), anthracene-9-carboxylic acid (0.07 g, 0.0003 mol, 2.4 eq), and DMAP (0.004 g, 0.000038 mol, 0.19 eq) were stirred in dry CH_2Cl_2 (20 ml) under N_2 at 0 °C. Then, DCC (0.082 g, 0.049 mol, 2.4 eq) (1 ml) was slowly added. After 2 days, the reaction was stopped and evaporated. A column chromatography was applied (1:2) Pet.ether: DCM and the titled compound was collected. A white solid was recrystallized in methanol (0.044g, 23%).

^1H NMR (500 MHz, Chloroform-*d*) δ 8.70 (d, J = 8.7 Hz, 2H), 8.64 (s, 1H), 8.28 (s, 1H), 8.10 (d, J = 8.7 Hz, 2H), 8.04 (s, 1H), 7.95 (s, 1H), 7.86 (s, 1H), 7.85 (s, 1H), 7.85 (s, 1H), 7.68-7.53 (m, 4H), 4.43 (t, J = 6.6 Hz, 2H), 4.31 -4.17 (m, 8H), 2.09-2.04 (m, 2H), 2.01- 1.86 (m, 8H), 1.67-1.52 (m, 10H), 1.49-1.35 (m, 16H), 1.33-1.18 (m, 4H), 1.02 – 0.76 (m, 15H). **^{13}C NMR** (126 MHz, CDCl_3) δ 167.29, 149.94, 149.78, 149.30, 149.15, 148.89, 139.71, 131.08, 130.31, 129.28, 128.67, 128.39, 127.11, 126.71, 125.80, 125.58, 124.84, 123.49, 123.39, 123.32, 123.06, 116.90, 108.28, 107.42, 106.99, 106.04, 77.28, 77.02, 76.77, 70.06, 69.84, 69.52, 69.49, 69.21, 31.74, 31.71, 31.67, 31.65, 29.56, 29.49, 29.44, 29.42, 29.35, 25.90, 25.87, 25.84, 25.82, 22.70, 22.69, 22.65, 22.55, 14.08, 14.04, 13.97.

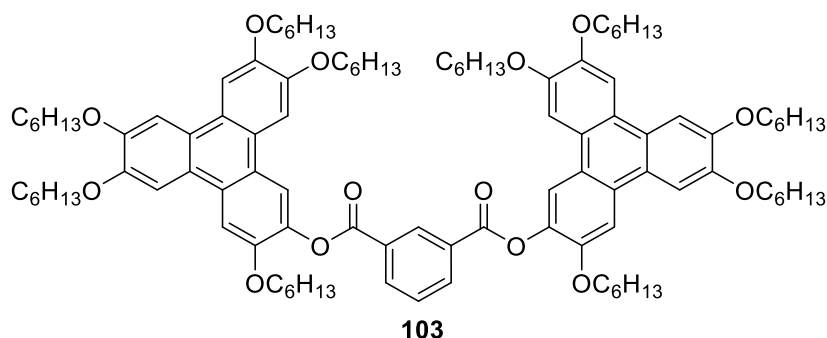
IR (thin film, cm^{-1}) 2922, 2855, 1739, 1615, 1513, 1467, 1432, 1389, 1353, 1257.

UV-vis (DCM, λ_{max} , nm (rel. int.)): 384 (0.131), 268 (0.022), 349 (0.020), 307 (0.071), 279 (0.29), 270 (0.211), 256 (0.555), 225 (0.184), 221 (0.22).

Transition temperatures Col 137 I

(MALDI): m/z calculated for $\text{C}_{63}\text{H}_{80}\text{O}_7$ (M^+ , 100%): 948.59 found 949.73

Synthesis of triphenylene dimer 103:



MHT (0.15g, 0.0002 mol, 1 eq), and benzene-1,3-dicarbonyl chloride (0.013 g, 0.00008 mol, 0.4 eq) were stirred in dry CH_2Cl_2 (10 ml) at 0 °C. Then, dry NEt_3 (1 ml) was added slowly. After 2 h, TLC confirmed the new spot for the product. The reaction was stopped, the solution was evaporated and recrystallized from methanol and the title compound was collected as a white solid (0.08 g, 25%).

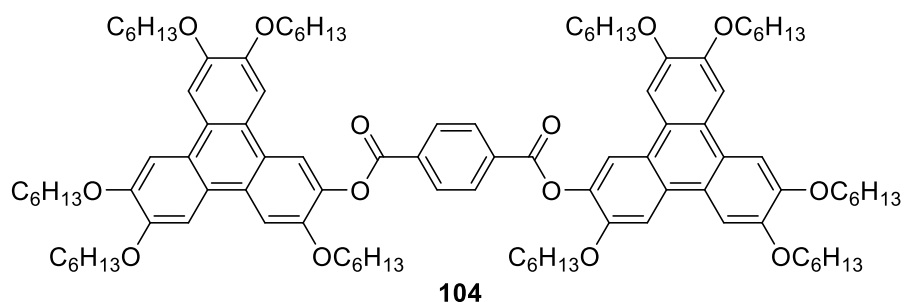
^1H NMR (500 MHz, Chloroform-*d*) δ 9.16 (t, $J = 1.8$ Hz, 1H), 8.51 (dd, $J = 7.8, 1.8$ Hz, 2H), 8.18 (s, 2H), 7.87 (s, 2H), 7.82 (s, 2H), 7.77 (s, 2H), 7.76 (s, 2H), 7.74 (s, 2H), 7.69 (t, $J = 7.8$ Hz, 1H), 4.38 – 4.03 (m, 20H), 1.94 – 1.82 (m, 16H), 1.78 – 1.65 (m, 4H), 1.50 (m, 12H), 1.41 – 1.24 (m, 40H), 1.23 – 1.11 (m, 8H), 0.91 – 0.80 (m, 24H), 0.79 – 0.72 (m, 6H).

^{13}C -NMR (126 MHz, Chloroform-*d*); δ 164.2, 149.8, 148.9, 139.9, 128.2, 124.7, 123.5, 123.3, 123.2, 116.8, 108.0, 107.0, 106.4, 69.9, 69.8, 69.2, 69.0, 31.7, 31.5, 29.6, 29.0, 25.8, 22.7, 22.6, 22.3, 14.1.

IR (thin film, cm^{-1}) 2954, 2858, 2928, 1741, 1616, 1511, 1432, 1260, 1225

MS (MALDI): m/z calculated for $\text{C}_{104}\text{H}_{146}\text{O}_{14}$ (M^+ , 100%): 1620.07 found 1620.38

Synthesis of triphenylene dimer **104**:



MHT (0.15g, 0.0002 mol, 1 eq), and benzene-1,4-dicarbonyl chloride (0.013 g, 0.00008 mol, 0.4 eq) were stirred in dry CH₂Cl₂ (10 ml) at 0 °C. Then, dry NEt₃ (1 ml) was added slowly. After 2 h, TLC confirmed the new spot for the product. The reaction was stopped, the solution was evaporated and recrystallized from methanol and the title compound was collected as a white solid (0.07 g, 21%).

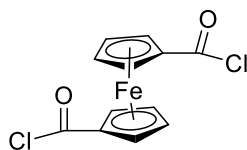
¹H NMR (500 MHz, Chloroform-*d*) δ 8.39 (s, 4H), 8.17 (s, 2H), 7.86 (s, 2H), 7.82 (s, 2H), 7.77 (s, 2H), 7.74 (s, 2H), 7.73 (s, 2H), 4.27 – 4.07 (m, 20H), 1.93 – 1.83 (m, 16H), 1.78 – 1.70 (m, 4H), 1.55 – 1.47 (m, 12H), 1.40 – 1.29 (m, 40H), 1.23 – 1.13 (m, 8H), 0.94 – 0.81 (m, 24H), 0.81 – 0.74 (m, 6H).

¹³C- NMR (126 MHz, Chloroformd); δ 164.5, 149.8, 149.5, 148.9, 140.0, 133.8, 130.3, 128.4, 124.9, 123.4, 123.1, 116.9, 108.2, 106.5, 69.4, 69.2, 31.9, 29.6, 25.8, 22.8, 14.1.

IR (thin film, cm⁻¹) 2918, 2850, 1731, 1515, 1435, 1261.

MS (MALDI): m/z calculated for C₁₀₄ H₁₄₆ O₁₄ (M⁺, 100%): 1620.07 found 1619.68.

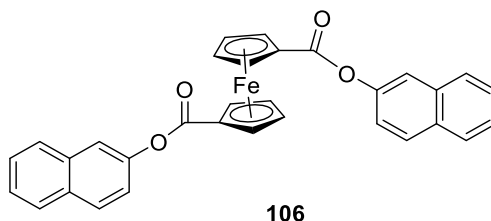
Synthesis of ferrocene dicarbonyl chloride 105 [118].



A mixture of 1,1'-ferrocenedicarboxylic acid (0.6 g, 0.0025 mol, 1 eq), dry methylene chloride (35 mL), oxalyl chloride (3.15g, 0.025 mol, 10 eq), and DMF (one drop) was stirred in the dark for 2 h at room temperature under nitrogen. The solution was concentrated in vacuo and the product of ferrocene dicarbonyl chloride was collected as red crystals (0.59 g, 84%).

¹H NMR (400 MHz, Chloroform-*d*) δ 5.05 (t, J = 2.0 Hz, 4H), 4.76 (t, J = 2.0 Hz, 4H).

Synthesis of dimer **106**



2-naphtol (0.6g, 0.004 mol, 1 eq), and ferrocene dicarbonyl chloride (0.5g, 0.0016 mol, 0.4 eq) were stirred in dry CH_2Cl_2 (30 ml) at 0 °C. Then, dry NEt_3 (1 ml) was added slowly. After 2 h, TLC confirmed the new spot of the product, which was an orange spot. A column chromatography was applied and the titled compound **106** was collected (1:2) Pet.ether: DCM. An orange solid was collected (0.5 g, 22 %).

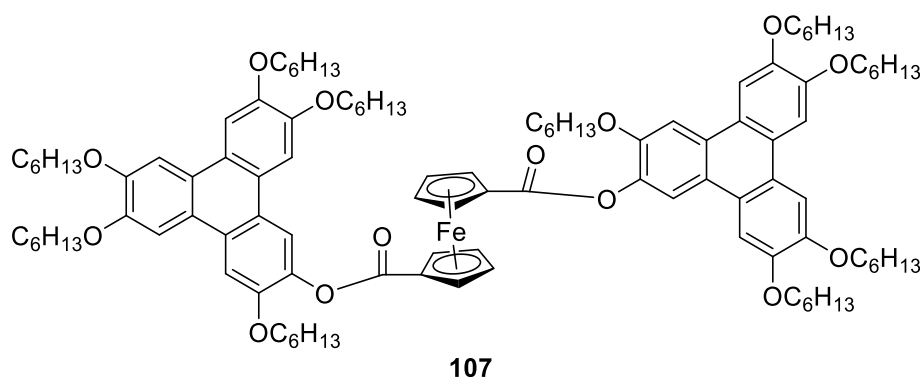
^1H NMR (400 MHz, Chloroform-*d*) δ 7.83 (d, J = 8.1 Hz, 4H), 7.72 – 7.65 (m, 4H), 7.48 – 7.43 (m, 4H), 7.38 (dd, J = 8.9, 2.3 Hz, 2H), 5.18 (t, J = 1.9 Hz, 4H), 4.70 (t, J = 1.9 Hz, 4H).

^{13}C NMR (101 MHz, CDCl_3) δ 169.24, 148.38, 133.77, 131.43, 129.34, 127.71, 127.67, 126.43, 125.59, 121.36, 118.76, 77.33, 77.02, 76.70, 73.38, 72.36, 72.32.

IR (thin film, cm^{-1}) 3059, 1723, 1597, 1511, 1452, 1382, 1272, 1243, 1214.

MS (MALDI): m/z calculated for $\text{C}_{34}\text{H}_{28}\text{O}_4\text{Fe}$ (M^+ , 100%): 526.39 found 528.00.

Synthesis of triphenylene dimer **107**:



MHT (0.13 g, 0.00017 mol, 1 eq), and ferrocene dicarbonyl chloride (0.021 g, 0.00007 mol, 0.4 eq) were stirred in dry CH_2Cl_2 (5 ml) at 0 °C. Then, dry NEt_3 (1 ml) was added slowly. After 2 h, TLC confirmed the new spot of the product, which was an orange spot. A column chromatography was applied and the titled compound **107** was collected (1:2) Pet.ether: DCM. An orange solid was collected (0.019g, 6%).

Rf 0.75 (1:2) Pet.ether: DCM

^1H NMR (400 MHz, Chloroform- d) δ 7.96 (s, 2H), 7.59 – 7.41 (m, 4H), 7.33 (s, 2H), 6.97 (s, 2H), 6.78 (s, 2H), 5.25 (t, J = 2.0 Hz, 4H), 4.54 (t, J = 2.0 Hz, 4H), 4.25 – 4.05 (m, 12H), 3.90 (s, 4H), 3.77 (s, 4H), 1.98 – 1.85 (m, 8H), 1.74 (dt, J = 20.5, 7.4 Hz, 12H), 1.60 – 1.49 (m, 20H), 1.48 – 1.17 (m, 40H), 0.98 – 0.81 (m, 25H), 0.79 – 0.74 (m, 6H).

^{13}C NMR (126 MHz, CDCl_3) δ 168.49, 148.96, 148.82, 148.25, 147.99, 147.90, 139.40, 127.47, 124.01, 123.37, 122.80, 122.52, 121.78, 119.32, 107.00, 106.07, 105.97, 77.29, 77.04, 76.78, 73.46, 71.99, 71.64, 69.85, 69.22, 69.16, 68.69, 68.39, 31.88, 31.85, 31.82, 31.63, 29.74, 29.61, 29.43, 29.41, 29.37, 26.07, 26.00, 25.87, 25.84, 25.77, 22.77, 22.74, 22.72, 22.59, 14.11, 14.09, 14.01.

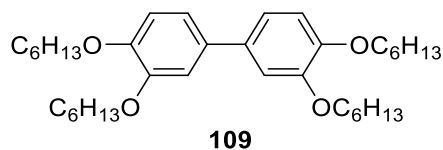
IR (thin film, cm^{-1}) 2928, 2852, 1721, 1615, 1513, 1433, 1379, 1258.

Mp 70 °C

UV-vis (DCM, λ_{max} , nm (rel. int.)): 314 (0.098), 256 (0.382), 236 (0.156)

MS (MALDI): m/z calculated for $\text{C}_{108}\text{H}_{150}\text{O}_{14}\text{Fe}$ (M^+ , 100%): 1727.11 found 1727.91

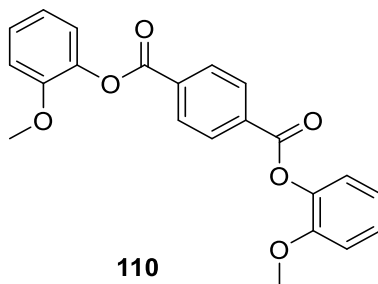
Synthesis of Tetra(hexyloxy)biphenyl **109** [119]



In a modification of the procedure described by Lin *et al.*, 3,4-bis(hexyloxy)phenylbromide **96** (20 g, 0.055 mol, 1 eq) provided by our group, NiCl₂ (0.36 g, 0.0027 mol, 0.05 eq), PPh₃ (4.3 g, 0.016 mol) and Zn powder (5.4 g, 0.08 mol, 1.5 eq) were refluxed under nitrogen in dry pyridine (60 mL) for 4h. The reaction was allowed to cool overnight. After adding 50 mL of DCM, the zinc powder was filtered off. We then washed the solution with water (3 x 50 mL) and extracted the aqueous washings with DCM (3 x 50 mL). After combining, the extracts were dried with magnesium sulphate. The solvent was reduced in vacuo to a minimum, methanol (50 mL) was added, and the product was filtered off. The titled compound was then collected using column chromatography (4:1) Pet.ether: ethyl acetate. Tetra(hexyloxy)biphenyl **97** was collected as a white solid. (6.32 g, 20%).

Mp 66 °C, lit [120]; ¹H NMR (400 MHz, Chloroform-*d*) δ 7.07(s,2H), 7.04 (d, J = 2.2 Hz, 2H), 6.93 (d, J = 0.8 Hz, 2H), 4.01-4.07 (m, 8H), 1.79-1.87 (m, 8H), 1.47-1.52 (m, 8H), 1.30-1.40 (m, 16H), 0.86-0.93 (m, 12H).

Synthesis of bis (2-methoxy phenyl) benzene 1,4 dicarboxylate **110**

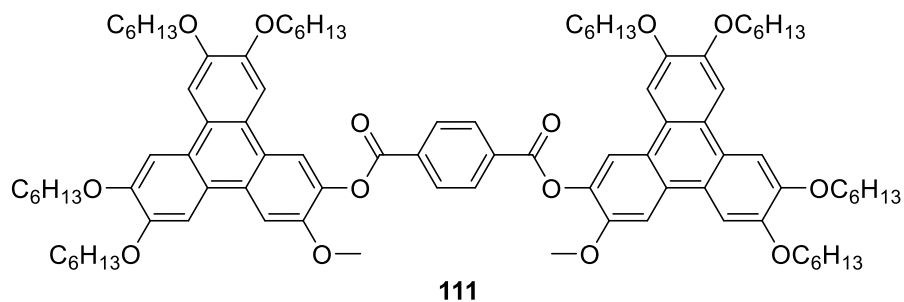


2-Methoxy phenol (0.2 g, 0.0016 mol, 1 eq), and benzene-1,4-dicarbonyl chloride (0.13 g, 0.0006 mol, 0.4 eq) were stirred in dry CH_2Cl_2 (20 ml) at 0 °C. Then, dry NEt_3 (2 ml) was added slowly. After 2 h, TLC confirmed the new spot of the product. The solution was concentrated in vacuo, recrystallised from (DCM:MeOH) and the product of dimer benzene **110** was collected as pink crystals (0.4g, 66 %).

^1H NMR (400 MHz, Methylene Chloride- d_2) δ 8.37 (s, 4H), 7.34 (ddd, $J = 8.3, 7.5, 1.6$ Hz, 2H), 7.23 (dd, $J = 7.8, 1.7$ Hz, 2H), 7.14 – 7.02 (m, 4H), 3.87 (s, 6H).

^{13}C NMR (101 MHz, CD_2Cl_2) δ 163.83, 151.31, 139.85, 133.74, 130.22, 127.17, 122.77, 120.72, 112.59, 55.86, 53.95, 53.68, 53.41, 53.14, 52.87.

Synthesis of triphenylene dimer **111**



Tetrakis(hexyloxy) biphenyl **109** (0.12 g, 0.00021 mol, 1 eq), and benzene dimer **110** (0.03 g, 0.000086 mol, 0.4 eq) were added to a mixture of FeCl_3 (0.2 g, 0.0013 mmol, 6 eq) in dichloromethane (20 mL) and stirred at 0 °C for 5 h. It was quenched by methanol (30 mL). It is then worked up and purified by column chromatography, eluting with (ethyl acetate: petroleum ether/1: 15). The solvents are then removed in a vacuum. A purple solid was collected (0.015g, 4.6%).

R_f 0.2 (1:2) Pet.ether: DCM

¹H NMR (500 MHz, Chloroform-*d*) δ 8.41 (s, 4H), 8.17 (s, 2H), 7.86 (s, 2H), 7.83 (s, 2H), 7.77 (s, 2H), 7.74 (s, 2H), 7.73 (s, 2H), 4.21 – 4.12 (m, 16H), 4.01 (s, 6H), 1.96 – 1.83 (m, 20H), 1.48 (s, 20H), 1.37 – 1.28 (m, 40H), 0.93 – 0.71 (m, 30H).

¹³C NMR no aromatic peaks due to aggregation.

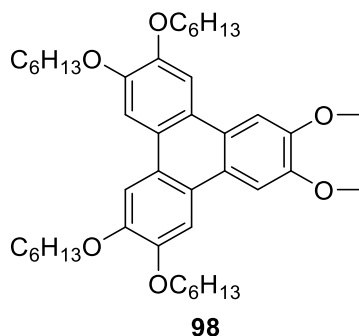
IR (thin film, cm^{-1}) 2921, 2852, 1614, 1585, 1537, 1503, 1467, 1449, 1413, 1390, 1353, 1310, 1240, 1214.

Transition temperatures Col 261 I

UV-vis (DCM, λ_{max} , nm (rel. int.)): 315 (0.039), 279 (0.060), 267 (0.058), 230 (0.053).

MS (MALDI): m/z calculated for $\text{C}_{72}\text{H}_{76}\text{O}_8$ (M^+ , 100%): 1478.91 found 1480.37

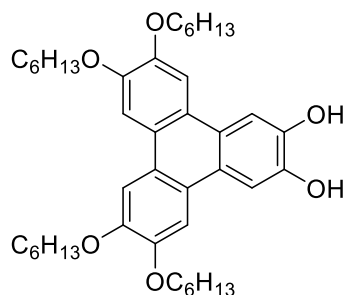
The synthesis of 2,3-bis(methoxy)triphenylene **113 by using biphenyl [121]:**



In 50 mL of DCM, tetra(hexyloxy)biphenyl **109** (3.86 g, 0.0069 mol, 1 eq), 1,2-dimethoxybenzene (1.15 g, 0.0083 mol, 1.2 eq), and FeCl₃ (6.8 g, 0.28 mol, 6 eq) were stirred for 1 hour. Following this, 70 mL of cold methanol was poured over the solid and filtered. It was then redissolved in 25 mL of DCM and filtered again. The filtrate was then concentrated and purified using column chromatography. The 2,3-bis(methoxy) triphenylene **113** was obtained by precipitating a white solid from DCM and cold methanol (1.8 g, 40 %).

¹H NMR (400 MHz, Chloroform-*d*) 7.85 (s, 4H), 7.81 (s, 2H), 4.24 (t, *J* = 4.9 Hz, 8H), 4.12 (s, 6H), 1.91-1.96 (m, 8H), 1.19-1.60 (m, 8H), 1.36-1.43 (m, 16H), 0.92- 0.95 (m, 12H).

Deprotection of 2,3-bis(methoxy)triphenylene **114**[113]:

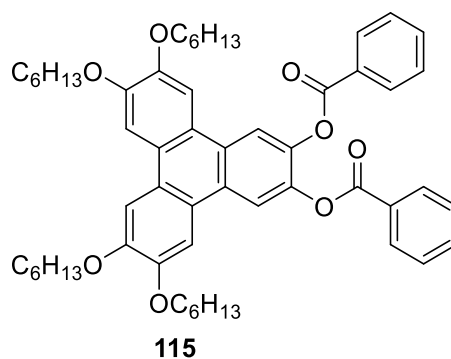


114

Our group modified the procedure described by Cammidge *et al.* 2,3-Bis(methoxy) triphenylene **113** (1 g, 0.00145 mol, 1 eq) and potassium carbonate (1.3 g, 0.009 mol, 6.5 eq) were stirred under nitrogen atmosphere. Then, dry DMF (6 mL) and thiophenol (0.8 g, 0.007 mol, 5 eq) were added, and the mixture was refluxed for 5 hours. The NMR aliquot was then checked, and there were no peaks for methoxy groups. The solution was then poured onto concentrated HCl (10 mL) and ice (50 mL), extracted with a little DCM and dried with MgSO₄. The solvents were removed under vacuum, and a white solid of 2,3-bis(hydroxy) triphenylene **114** (0.6 g, 66%) was recrystallised from DCM and methanol. No mp, slow decomposition.

¹H NMR (400 MHz, Chloroform-*d*) 7.86 (s, 2H), 7.70 (s, 2H), 7.76 (s, 2H), 6.11 (s, 2H), 4.15 – 4.26 (m, 4H), 3.95 – 4.08 (m, 4H), 1.72 – 1.81 (m, 4H), 1.58 – 1.69(m, 4H), 1.39 – 1.45 (m, 4H), 1.21 – 1.34 (m, 12H), 1.10 – 1.19 (m, 8H), 0.77 – 0.83 (m, 12H).

Synthesis 2,3-di benzoate ester **115**



2,3-Dihydroxy triphenylene (100 mg, 0.00015 mol, 1eq), and 2- benzoyl chloride (0.05 g, 0.00036 mol, 2.4 eq) were stirred in dry CH₂Cl₂ (10 ml) at 0 °C. Then, dry NEt₃ (2 ml) was added slowly. After 2 h, aliquot NMR confirmed the product, and the solvent were evaporated and the residue recrystallized from methanol. The compound titled **115** was collected as a white solid (0.034 g, 31%).

¹H NMR (400 MHz, Chloroform-*d*) δ 8.35 (s, 2H), 8.08 (dd, *J* = 8.4, 1.3 Hz, 4H), 7.80 (s, 2H), 7.77 (s, 2H), 7.54 – 7.47 (m, 2H), 7.37 – 7.32 (m, 4H), 4.16 (dt, *J* = 17.0, 6.6 Hz, 8H), 1.95 – 1.76 (m, 10H), 1.56 – 1.46 (m, 10H), 1.38 – 1.26 (m, 20H), 0.95 – 0.81 (m, 15H).

¹³C NMR (101 MHz, CDCl₃) δ 149.80, 149.20, 141.10, 133.70, 130.25, 128.94, 128.54, 127.92, 124.33, 122.87, 117.39, 106.97, 77.33, 77.01, 76.70, 69.66, 69.33, 31.69, 31.65, 29.39, 29.32, 25.85, 25.80, 22.66, 22.63, 14.06, 14.03.

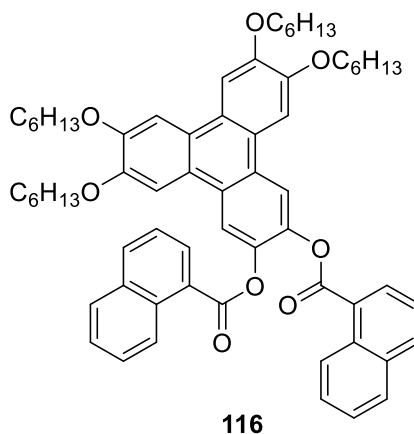
IR (thin film, cm⁻¹) 2929, 2857, 1732, 1617, 1514, 1433, 1390, 1244.

Transition temperatures Col 205 I

UV-vis (DCM, λ_{max}, nm (rel. int.)): 310 (0.076), 278 (0.249), 239 (0.112).

MS (MALDI): m/z calculated for C₅₆H₆₈O₈ (M⁺, 100%): 868.49 found 864.54.

Synthesis of 2,3-di (1-Naphthoate) esters **116**



2,3-Dihydroxy triphenylene (100 mg, 0.00015 mol), and 1-naphthoyl chloride (0.069 g, 0.00036 mol, 2.4 eq) were stirred in dry CH_2Cl_2 (10 ml) at 0 °C. Then, dry NEt_3 (2 ml) was added slowly. After 2 h, aliquot NMR confirmed the product, and the solvent were evaporated and recrystallized from methanol. The compound titled **116** was collected as a yellow solid was collected (0.055 g, 37.6%).

^1H NMR (400 MHz, Chloroform-*d*) δ 8.99 – 8.93 (m, 2H), 8.42 (s, 2H), 8.35 (dd, $J = 7.4, 1.3$ Hz, 2H), 7.88 (dt, $J = 8.3, 1.1$ Hz, 2H), 7.84 (s, 2H), 7.78 (s, 2H), 7.77 – 7.74 (m, 2H), 7.48 – 7.41 (m, 4H), 7.20 (dd, $J = 8.2, 7.3$ Hz, 2H), 4.18 (dt, $J = 15.3, 6.6$ Hz, 8H), 1.96 – 1.80 (m, 10H), 1.58 – 1.43 (m, 10H), 1.39 – 1.26 (m, 20H), 0.85 (dt, $J = 18.5, 7.2$ Hz, 15H).

^{13}C NMR (101 MHz, CD_2Cl_2) δ 165.15, 149.92, 149.23, 141.40, 134.39, 133.80, 131.46, 131.38, 128.59, 128.11, 127.86, 126.36, 125.42, 125.00, 124.37, 124.18, 122.54, 117.61, 106.80, 106.59, 69.47, 69.25, 53.96, 53.69, 53.42, 53.15, 52.88, 45.74, 31.69, 31.63, 30.58, 29.43, 29.37, 25.85, 25.78, 22.67, 22.62, 13.82, 13.78, 8.39.

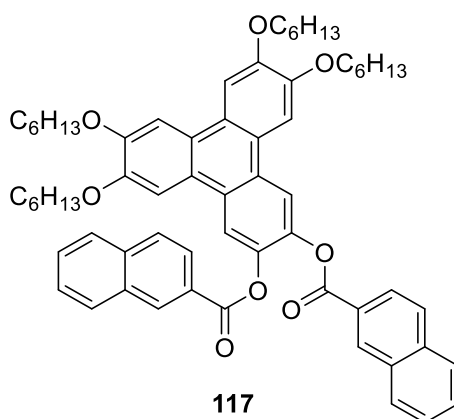
IR (thin film, cm^{-1}) 2929, 2852, 1727, 1615, 1510, 1432, 1392, 1258, 1245, 1235 .

Transition temperatures Col 180 I

UV-vis (DCM, λ_{max} , nm (rel. int.)): 309 (0.094), 277 (0.191), 237 (0.141).

MS (MALDI): m/z calculated for $\text{C}_{64}\text{H}_{72}\text{O}_8$ (M^+ , 100%): 968.52 found 964.61

Synthesis of 2,3-di (2-Naphthoate) esters **117**



2,3-Dihydroxy triphenylene (100 mg, 0.00015 mol), and 2-naphthoyl chloride (0.069 g, 0.00036 mol, 2.4 eq) were stirred in dry CH₂Cl₂ (10 ml) at 0 °C. Then, dry NEt₃ (2 ml) was added slowly. After 2 h, aliquot NMR confirmed the product, and the solvent were evaporated and recrystallized from methanol, and the compound titled **117** was collected as a yellow solid (0.05 g, 34.2 %).

¹H NMR (400 MHz, Chloroform-*d*) δ 8.64 (s, 2H), 8.44 (s, 2H), 8.06 (dd, *J* = 8.6, 1.8 Hz, 2H), 7.82 (s, 2H), 7.77 (s, 2H), 7.74 – 7.69 (m, 4H), 7.66 (d, *J* = 7.5 Hz, 2H), 7.47 (ddd, *J* = 8.2, 6.9, 1.3 Hz, 2H), 7.36 (ddd, *J* = 8.1, 6.9, 1.2 Hz, 2H), 4.22 – 4.11 (m, 8H), 2.00 – 1.80 (m, 10H), 1.59 – 1.44 (m, 10H), 1.42 – 1.22 (m, 20H), 0.99 – 0.60 (m, 15H).

¹³C NMR (101 MHz, CDCl₃) δ 164.94, 149.80, 149.22, 141.23, 135.78, 132.37, 132.15, 129.39, 128.62, 128.40, 127.93, 127.69, 126.70, 126.11, 125.35, 124.35, 122.92, 117.42, 107.06, 106.97, 77.33, 77.02, 76.70, 69.67, 69.33, 31.70, 31.65, 29.41, 29.33, 25.86, 25.81, 22.67, 22.63, 14.06, 14.03.

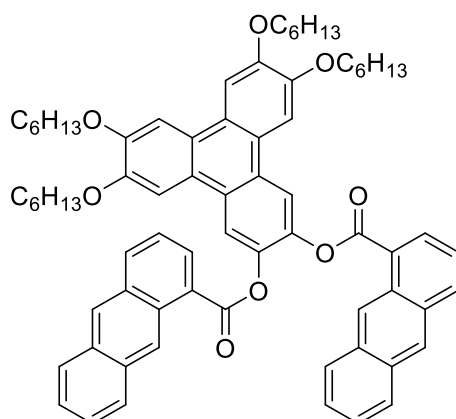
IR (thin film, cm⁻¹) 2920, 2852, 1731, 1616, 1514, 1465, 1433, 1391, 1258, 1226.

Transition temperatures Col 196 I

UV-vis (DCM, λ_{max}, nm (rel. int.)): 315 (0.173), 278 (0.605), 239 (0.591).

MS (MALDI): *m/z* calculated for C₆₄H₇₂O₈ (M⁺, 100%): 968.52 found 965.28.

Synthesis of 2,3-di (2-Anthracenoate) esters **118**



118

2,3-Dihydroxy triphenylene (100 mg, 0.00015 mol), and 2-anthracenoyl chloride (0.087 g, 0.00036 mol, 2.4 eq) were stirred in dry CH₂Cl₂ (10 ml) at 0 °C. Then, dry NEt₃ (2 ml) was added slowly. After 2 h, aliquot NMR confirmed the product, and the solvent were evaporated and recrystallized from methanol, and the compound titled **118** was collected as a yellow solid (0.051 g, 31.8 %).

¹H NMR (400 MHz, Chloroform-*d*) δ 8.82 (s, 2H), 8.51 (s, 2H), 8.17 (s, 2H), 8.09 (s, 2H), 7.99 (dd, *J* = 8.9, 1.7 Hz, 2H), 7.86 (s, 2H), 7.83 (s, 2H), 7.81 (s, 2H), 7.79 (s, 2H), 7.61 (d, *J* = 8.5 Hz, 2H), 7.39-7.37 (m, 2H), 7.33 – 7.28 (m, 2H), 4.26 – 4.15 (m, 8H), 1.95 – 1.82 (m, 10H), 1.59 – 1.44 (m, 10H), 1.40 – 1.26 (m, 20H), 0.98 – 0.76 (m, 15H).

¹³C NMR (101 MHz, CDCl₃) δ 164.99, 149.75, 149.19, 141.29, 133.65, 133.18, 132.57, 131.82, 130.01, 128.83, 128.70, 128.33, 128.01, 127.86, 126.69, 126.07, 125.78, 125.59, 124.31, 123.92, 122.93, 117.40, 107.03, 77.33, 77.02, 76.70, 69.66, 69.31, 31.72, 31.66, 29.43, 29.35, 25.87, 25.83, 22.68, 22.64, 14.07, 14.03.

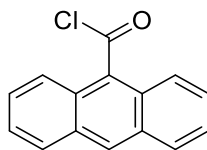
IR (thin film, cm⁻¹) 2922, 2852, 1783, 1729, 1615, 1504, 1467, 1429, 1382, 1308, 1261.

Transition temperatures Col 136 I

UV-vis (DCM, λ_{max}, nm (rel. int.)): 408 (0.016), 387 (0.017), 365 (0.021), 344 (0.036), 309 (0.102), 280 (0.498), 240 (0.182)

MS (MALDI): *m/z* calculated for C₇₂H₇₆O₈ (M⁺, 100%): 1068.55 found 1068.47.

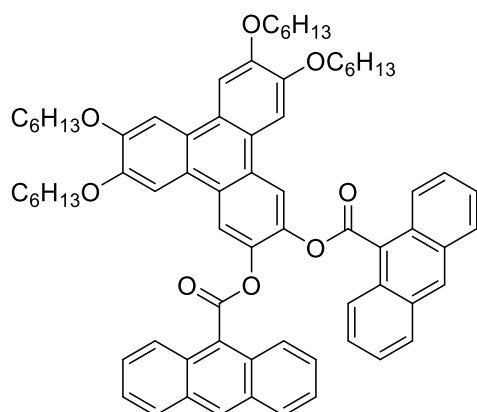
Synthesis of anthracene-9-carbonyl chloride 119a [122]:



Anthracene-9-carboxylic acid (0.2 g, 0.0009 mol) was stirred in thionyl chloride (3 ml) under N₂. One drop of DMF was added. The solution was stirred and refluxed for 5 h. The solvent was removed under reduced pressure and the compound was collected. A yellow powder was collected (0.19, 90%).

¹H NMR (400 MHz, CDCl₃) δ (ppm) 8.59(s, 1H), 8.13 – 8.11(d, J = 8.99 Hz, 2H), 8.06 – 8.04(d, J = 8.90 Hz, 2H), 7.63(t, J = 7.34 Hz, 2H), 7.54(t, J = 7.59 Hz, 2H).

Synthesis of 2,3-di (9-Anthracenoate) esters **119**



119

2,3-Dihydroxy triphenylene (100 mg, 0.00015 mol), and 9- anthracenoyl chloride (0.087 g, 0.00036 mol, 2.4 eq) were stirred in dry CH_2Cl_2 (10 ml) at 0 °C. Then, dry NEt_3 (2 ml) was added slowly. After 2 h, aliquot NMR confirmed the product, and the solvent were evaporated and recrystallized from methanol, and the compound titled **119** was collected. A green solid was collected (0.03 g, 18.75 %).

^1H NMR (400 MHz, Methylene Chloride- d_2) δ 8.79 (s, 2H), 8.47 (s, 2H), 8.11 (d, J = 9.0 Hz, 4H), 8.03 (s, 2H), 7.94 (s, 2H), 7.92 (s, 2H), 7.89 (s, 2H), 7.31 (ddd, J = 8.3, 6.6, 1.1 Hz, 4H), 6.95 (ddd, J = 8.9, 6.6, 1.3 Hz, 4H), 4.52 – 4.13 (m, 8H), 2.01 – 1.88 (m, 10H), 1.65 – 1.55 (m, 10H), 1.44 – 1.36 (m, 20H), 1.02 – 0.86 (m, 15H).

^{13}C NMR (101 MHz, CDCl_3) δ 167.38, 150.10, 149.24, 141.06, 130.68, 130.37, 128.81, 128.27, 128.10, 126.91, 125.79, 125.32, 124.87, 124.63, 122.85, 117.40, 107.75, 106.98, 85.51, 85.12, 82.94, 77.34, 77.02, 76.71, 69.73, 69.64, 40.84, 33.83, 31.94, 31.72, 31.70, 29.67, 29.42, 29.37, 28.43, 25.89, 25.87, 23.82, 22.69, 22.66, 20.78, 20.55, 17.49, 17.30, 14.64, 14.13, 14.08, 14.06, 7.92.

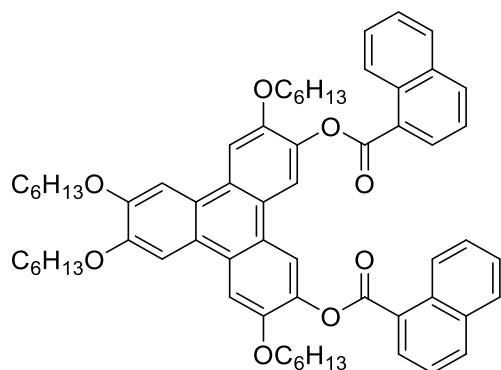
IR (thin film, cm^{-1}) 2919, 2852, 1741, 1612, 1509, 1504, 1428, 1385, 1346, 1261.

Transition temperatures Col 149 I

UV-vis (DCM, λ_{max} , nm (rel. int.)): 388 (0.016), 369 (0.019), 352 (0.017), 312 (0.066), 279 (0.292), 272 (0.210), 256 (0.555), 225 (0.184)

MS (MALDI): m/z calculated for $\text{C}_{72}\text{H}_{76}\text{O}_8$ (M^+ , 100%): 1068.55 found 1065.52

Synthesis of 3,6-di (1-Naphthoate) esters **121**



121

3,6-Dihydroxy triphenylene (100 mg, 0.00015 mol), and 1-naphthoyl chloride (0.069 g, 0.00036 mol, 2.4 eq) were stirred in dry CH_2Cl_2 (10 ml) at 0 °C. Then, dry NEt_3 (2 ml) was added slowly. After 2 h, aliquot NMR confirmed the product, and the solvent were evaporated and recrystallized from methanol, and the compound titled **121** was collected. A yellow solid was collected (0.056 g, 40 %).

^1H NMR (400 MHz, Chloroform- d) δ 9.00 – 8.91 (m, 2H), 8.43 (s, 2H), 8.36 (dd, $J = 7.4, 1.3$ Hz, 2H), 7.90 (d, $J = 8.2$ Hz, 2H), 7.85 (s, 2H), 7.80 (s, 2H), 7.78 – 7.74 (m, 2H), 7.51 – 7.42 (m, 4H), 7.23 (dd, $J = 7.9, 7.3$ Hz, 2H), 4.18 (dt, $J = 15.7, 6.6$ Hz, 8H), 2.00 – 1.82 (m, 10H), 1.48 (m, 10H), 1.39 – 1.28 (m, 20H), 0.85 (dt, $J = 18.4, 7.1$ Hz, 15H).

^{13}C NMR (101 MHz, CD_2Cl_2) δ 169.94, 150.72, 149.64, 141.58, 134.40, 134.02, 131.53, 131.44, 128.75, 128.13, 127.92, 126.36, 125.46, 125.30, 124.65, 124.34, 122.05, 117.83, 107.16, 106.53, 69.58, 69.12, 54.13, 53.86, 53.59, 53.31, 53.04, 52.79, 47.06, 31.79, 31.65, 29.55, 25.95, 25.89, 25.80, 22.72, 22.70, 13.85, 13.71, 9.13.

IR (thin film, cm^{-1}) 2929, 2852, 1727, 1615, 1510, 1432, 1392, 1258, 1245, 1235.

Transition temperatures Col 170 I

MS (MALDI): m/z calculated for $\text{C}_{64}\text{H}_{72}\text{O}_8$ (M^+ , 100%): 968.52 found 968.55.

References:

- [1] F. Reinitzer, *Monatsch Chem.*, 1888, **9**, 421–441.
- [2] D. Demus, J. W. Goodby, G. W. Gray, H. W. Spiess and V. Vill, in *Handb. Liq. Cryst*, vol. 3, 2008, John Wiley & Sons, pp. 1–16.
- [3] S. Chandrasekhar, B. K. Sadashiva and K. A. Suresh, *Pramana*, 1977, **9**, 471–480.
- [4] D.-K. Yang and S.-T. Wu, *Fundamentals of liquid crystal devices*, John Wiley & Sons Inc., 2014.
- [5] G. W. Gray, *Thermotropic liquid crystals*, John Wiley & Sons Inc, 1987.
- [6] S. Kumar, *Liq. Cryst.* 2004, **31**, 1037-1059.
- [7] F. S. Poletto, S. R. Montoro and M. L. Tebaldi, in *Design and Applications of Nanostructured Polymer Blends and Nanocomposite Systems*, Elsevier, 2016, pp. 39–54.
- [8] J. Luo, B. Zhao, H. S. O. Chan, C. Chi, *J. Mater. Chem.* 2010, **20**, 1932-1941.
- [9] S. Kumar, *Chem. Soc. Rev.*, 2006, **35**, 83–109.
- [10] S. Laschat, A. Baro, N. Steinke, F. Giesselmann, C. Hägele, G. Scalia, R. Judele, E. Kapatsina, S. Sauer, A. Schreivogel and M. Tosoni, *Angew. Chem. Int. Ed.*, 2007, **46**, 4832-4887.
- [11] S. Chandrasekhar, G. S. Ranganath, *Rep. Prog. Phys.*, 1990, **53**, 57-84.
- [12] S. Kumar, *Chemistry of Discotic Liquid Crystals*, CRC Press, 2016.
- [13] H. K. Bisoyi and S. Kumar, *Chem. Soc. Rev.*, 2010, **39**, 264–285.
- [14] H. Furuya and A. Abe, *Poly. Bulle.*, 1988, **20**, 467–470.
- [15] R. A. Soref, *J. Appl. Phys*, 1974, **45**, 5466–5468.
- [16] H. Sakashita, A. Nishitani, Y. Sumiya, H. Terauchi, K. Ohta and I. Yamamoto, *Mol. Cryst. Liq. Cryst. Incorporating Nonlinear Opt.*, 1988, **163**, 211–219.
- [17] N. Steinke, W. Frey, A. Baro, S. Laschat, C. Drees, M. Nimtz, C. Hägele and F. Giesselmann, *Chemistry - A European Journal*, 2006, **12**, 1026–1035.
- [18] K. Hatsusaka, K. Ohta, I. Yamamoto and H. Shirai, *J. Mater. Chem.*, 2001, **11**, 423–433.

- [19] M. Ichihara, A. Suzuki, K. Hatsusaka and K. Ohta, *Liq. Cryst.*, 2007, **34**, 555–567.
- [20] I. W. Hamley, *Introduction to Soft Matter*, Wiley-Blackwell, 2000.
- [21] G. R. Luckhurst and G. W. Gray, *The Molecular Physics of Liquid Crystals*, 1979.
- [22] P. J. Collings and Internet Archive, *Introduction to liquid crystals chemistry and physics*, London; Bristol, PA: Taylor & Francis, 1997.
- [23] S. Kumar and J. Brock, *Liquid Crystals: Experimental Study of Physical Properties and Phase Transitions*, Cambridge University Press, 2001.
- [24] R. Turner, PhD thesis, University of East Anglia, 2015.
- [25] D. Pérez and E. Guitián, *Chem. Soc. Rev.*, 2004, **33**, 274–283.
- [26] R. J. Bushby and C. Hardy, *J. Chem. Soc., Perkin Trans. 1*, 1986, 721–723.
- [27] R. C. Borner and R. F. W. Jackson, *J. Chem. Soc., Chem. Commun.*, 1994, 845.
- [28] A. N. Cammidge, H. Gopee, *J. Mater. Chem*, 2001, **11**, 2773–2783.
- [29] H. Hart, C. Lai, G. Chukuemeka Nwokogu and S. Shamouilian, *Tetrahedron*, 1987, **43**, 5203–5224.
- [30] N. Boden, R. J. Bushby and A. N. Cammidge, *J. Chem. Soc., Chem. Commun.*, 1994, 465.
- [31] N. Boden, R. J. Bushby, A. N. Cammidge and G. Headdock, *Synthesis*, 1995, 31–32.
- [32] G. W. Gribble, R. B. Perni and K. D. Onan, *J. Org. Chem.*, 1985, **50**, 2934–2939.
- [33] F. M. Raymo, M. F. Parisi and F. H. Kohnke, *Tetrahedron Lett.*, 1993, **34**, 5331–5332.
- [34] A. U. Rahman and O. L. Tombesi, *Chem. Ber.*, 1966, **99**, 1805–1809.
- [35] Y.-H. Lai, Y.-L. Yong and S.-Y. Wong, *J. Org. Chem.*, 1997, **62**, 4500–4503.
- [36] D. Peña, A. Cobas, D. Pérez, E. Guitián and L. Castedo, *Org. lett.*, 2000, **2**, 1629–1632.
- [37] N. Boden, R. C. Borner, R. J. Bushby, A. N. Cammidge and M. V. Jesudason, *Liq. Cryst.*, 1993, **15**, 851–858.
- [38] H. Shirai, N. Amano, Y. Hashimoto, E. Fukui, Y. Ishii and M. Ogawa, *J. Org. Chem.*, 1991, **56**, 2253–2256.
- [39] J. T. Rademacher, K. Kanakarajan and A. W. Czarnik, *Synthesis*, 1994, 378–380.

- [40] P. Canonne and A. Regnault, *Tetrahedron Lett.*, 1969, **10**, 243–246.
- [41] A. N. Cammidge, C. Chausson, H. Gopee, J. Li, D. L. Hughes, *Chem. Commun.*, 2009, 7375-7377.
- [42] X. Fang, H. Guo, J. Lin and F. Yang, *Tetrahedron Lett.*, 2016, **57**, 4939–4943.
- [43] K.-Q. Zhao, J.-Q. Du, X.-H. Long, M. Jing, B.-Q. Wang, P. Hu, H. Monobe, B. Henrich and B. Donnio, *Dyes Pigm.*, 2017, **143**, 252–260.
- [44] M. Schadt, W. Helfrich, *Appl. Phys. Lett.* 1971, **18**, 127-128.
- [45] P. Kirsch, M. Bremer, *Angew. Chem*, 2000, **39**, 4216-4235.
- [46] K. Kawata, *Chem. Rec.* 2002, **2**, 59-80.
- [47] M. Hird, *Liq. Cryst.*, 2011, **38**, 1467–1493.
- [48] G. G. Nair, D. S. S. Rao, S. K. Prasad, S. Chandrasekhar, S. Kumar, *Mol. Cryst. Liq. Cryst.* 2003, **397**, 245-252.
- [49] Y. Shirota, H. Kageyama, *Chem. Rev.* 2007, **107**, 953-1010.
- [50] D. O'Brien, A. Bleyer, D. G. Lidzey, D. D. C. Bradley, T. Tsutsui, *J. Appl. Phys.* 1997, **82**, 2662.
- [51] T. Hassheider, S. A. Benning, H.-S. Kitzerow, M.-F. Achard, H. Bock, *Angew. Chem. Int. Ed.* 2001, **40**, 2060-2063.
- [52] N. Boden, R. J. Bushby and A. N. Cammidge, *J. Chem. Soc. Chem. Commun.*, 1994, 465.
- [53] P. Peumans, A. Yakimov, S. R. Forrest, *J. Appl. Phys.*, 2003, **93**, 3693-3723.
- [54] L. Cisse, P. Destruel, S. Archambeau, I. Seguy, P. Jolinat, H. Bock, E. Grelet, *Chem. Phys. Lett.*, 2009, **476**, 89-91.
- [55] X. Chen, L. Chen and Y. Chen, *RSC Adv.*, 2014, **4**, 3627–3632.
- [56] M. Funahashi, F. Zhang and N. Tamaoki, *Adv. Mater.*, 2007, **19**, 353–358.
- [57] V. I. Kopp, B. Fan, H. K. Vithana and A. Z. Genack, *Opt. Lett.*, 1998, **23**, 1707–1709.
- [58] T. Manabe, K. Sonoyama, Y. Takanishi, K. Ishikawa and H. Takezoe, *J. Mater. Chem.*, 2008, **18**, 3040.

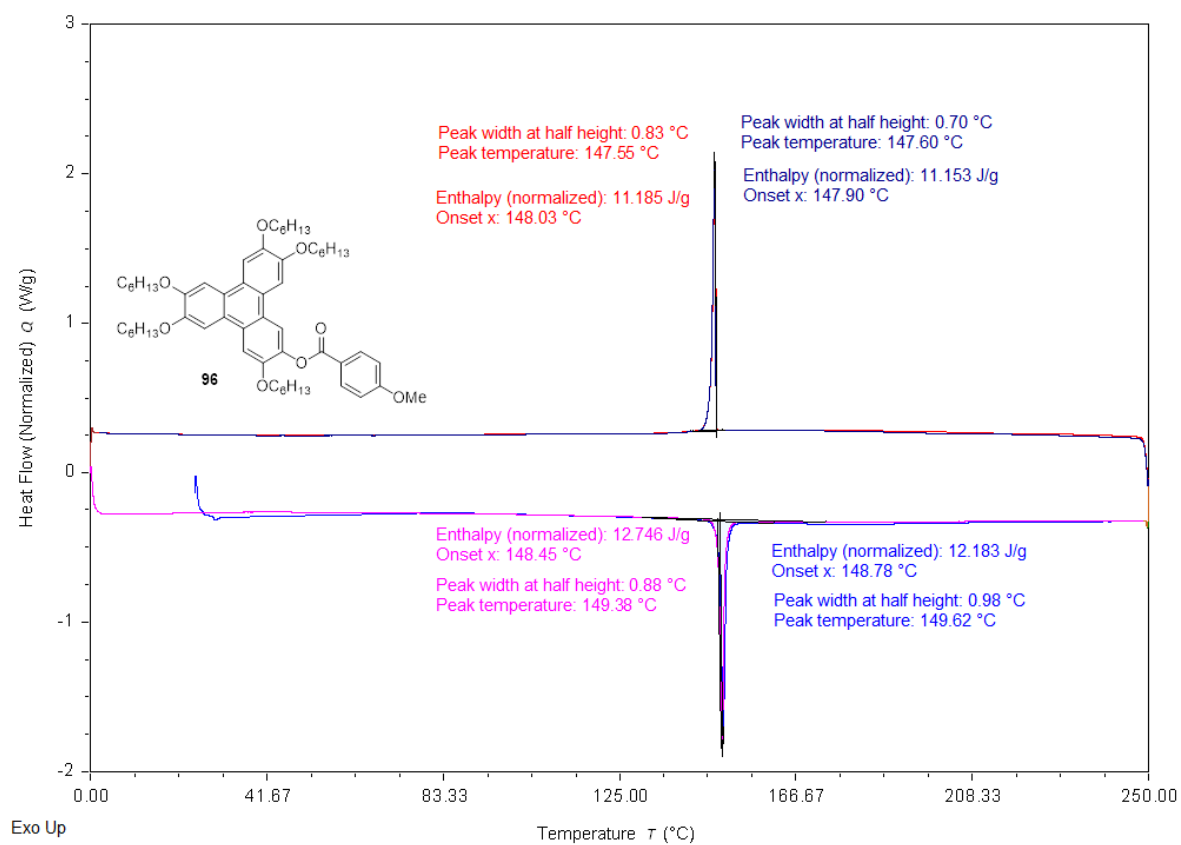
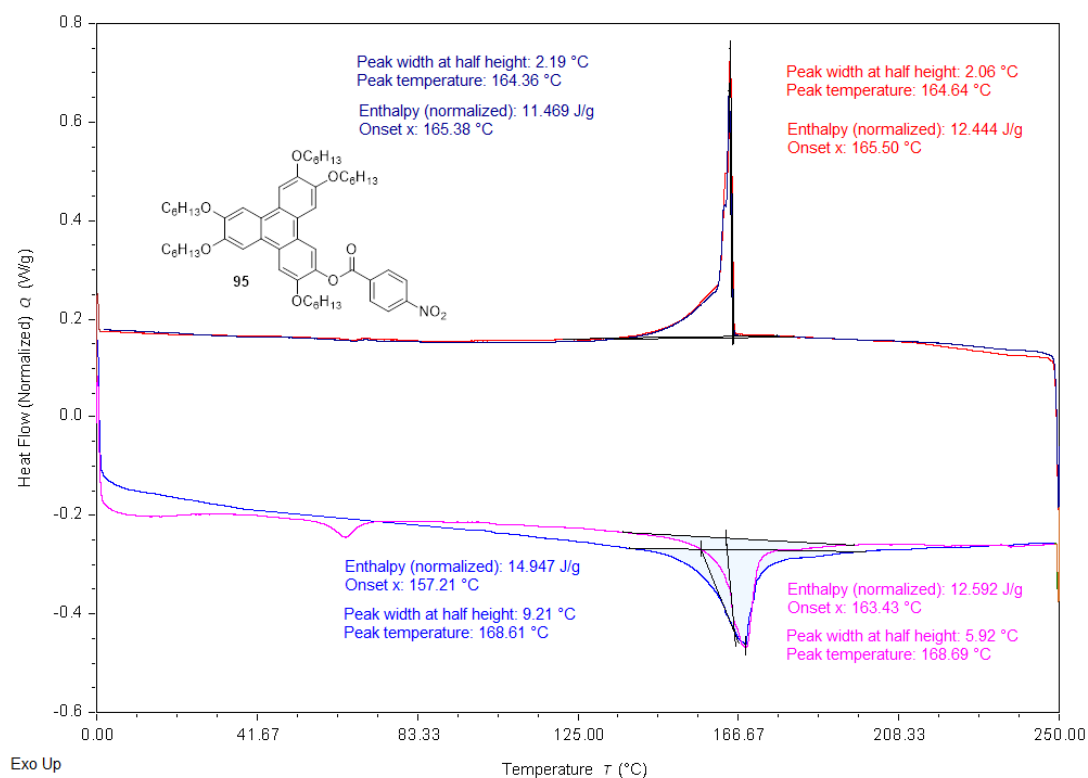
- [59] D. Demus, J. W. Goodby, G. W. Gray, H. W. Spiess and V. Vill, *Handbook of Liquid Crystals, High Molecular Weight Liquid Crystals*, Wiley-VCH, 1998.
- [60] F. Hoffmann, M. Cornelius, J. Morell, M. Fröba, *Angew. Chem. Int. Ed.* 2006, **45**, 3216–3251.
- [61] J. Clements, N. Boden, T. D. Gibson, R. C. Chandler, J. N. Hulbert, E. A. Ruck-Keene, *Sens. Actuators B*, 1998, **47**, 37–42.
- [62] K.-Y. Law, *Chem. Rev.* 1993, **93**, 449–486.
- [63] I. M. Matheson (née Davidson), O. C. Musgrave and C. J. Webster, *Chem. Commun.* (London), 1965, 278–279.
- [64] K. Bechgaard and V. D. Parker, *J. Am. Chem. Soc.*, 1972, **94**, 4749–4750.
- [65] H. Bengs, O. Karthaus, H. Ringsdorf, C. Baehr, M. Ebert and J. H. Wendorff, *Liq. Cryst.*, 1991, **10**, 161–168.
- [66] S. Kumar and M. Manickam, *Chem. Commun.*, 1997, 1615–1666.
- [67] S. Kumar and S. K. Varshney, *Synthesis*, 2001, 0305–0311.
- [68] X. Kong, Z. He, H. Gopee, X. Jing and A. N. Cammidge, *Tetrahedron Lett.*, 2011, **52**, 77–79.
- [69] J. L. Schulte, S. Laschat, R. Schulte-Ladbeck, V. von Arnim, A. Schneider and H. Finkelmann, *J. Organomet. Chem.*, 1998, **552**, 171–176.
- [70] P. Rempala, J. Kroulík and B. T. King, *J. Am. Chem. Soc.*, 2004, **126**, 15002–15003.
- [71] L. Zhai, R. Shukla, S. H. Wadumethrige and R. Rathore, *J. Org. Chem.*, 2010, **75**, 4748–4760.
- [72] W. Kreuder and H. Ringsdorf, *Makromol. Chem., Rapid Commun.*, 1983, **4**, 807–815.
- [73] N. H. Tinh, H. Gasparoux and C. Destrade, *Mol. Cryst. Liq. Cryst.*, 1981, **68**, 101–111.
- [74] B. Y. Tang, A. J. Jing, C. Y. Li, Z. Shen, H. Wang, F. W. Harris and S. Z. Cheng, *Cryst. Growth Des.*, 2003, **3**, 375–382.
- [75] S. Kohmoto, E. Mori and K. Kishikawa, *J. Am. Chem. Soc.*, 2007, **129**, 13364–13365.
- [76] J. J. Ge, S.-C., Hong, B. Y. Tang, C. Y. Li, D. Zhang, F. Bai, B. Mansdorf, F. W. Harris, D. Yang, Y.-R., Shen and S. Z. D. Cheng, *Adv. Funct. Mater.*, 2003, **13**, 718–725.

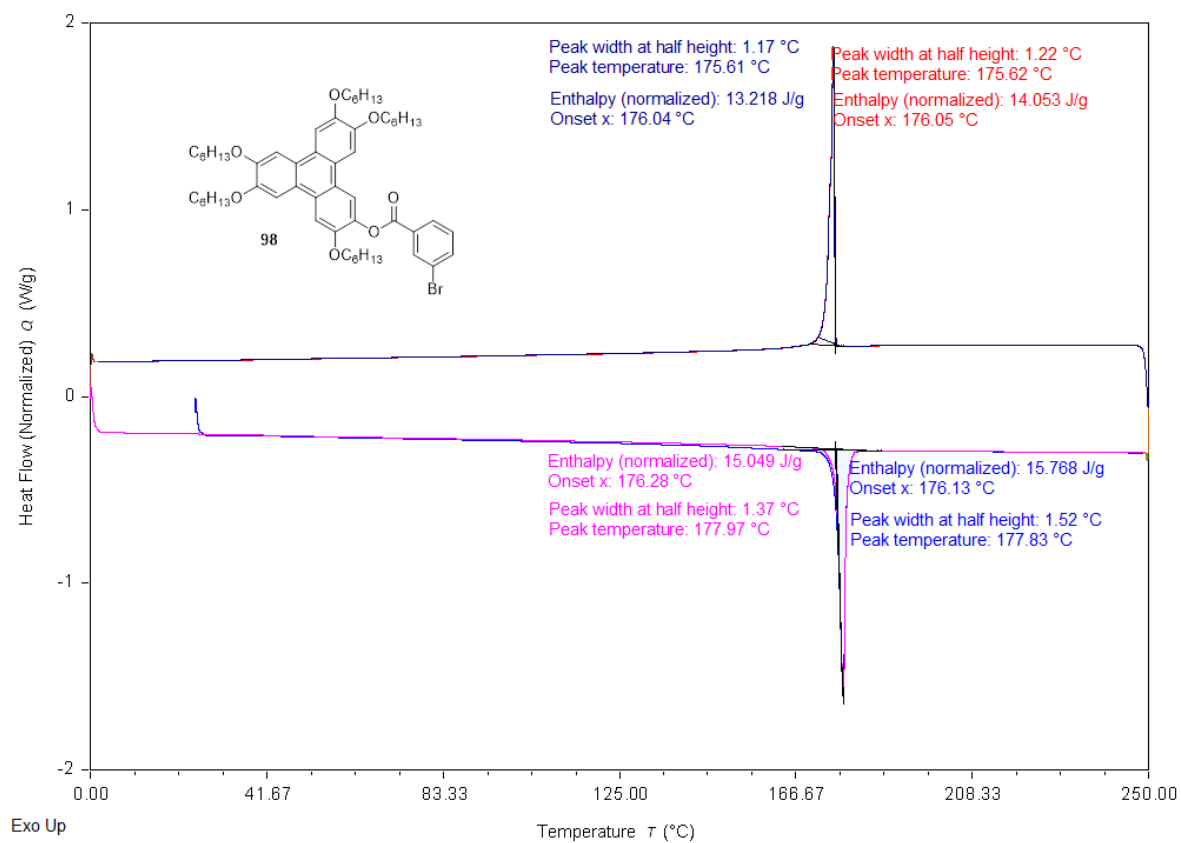
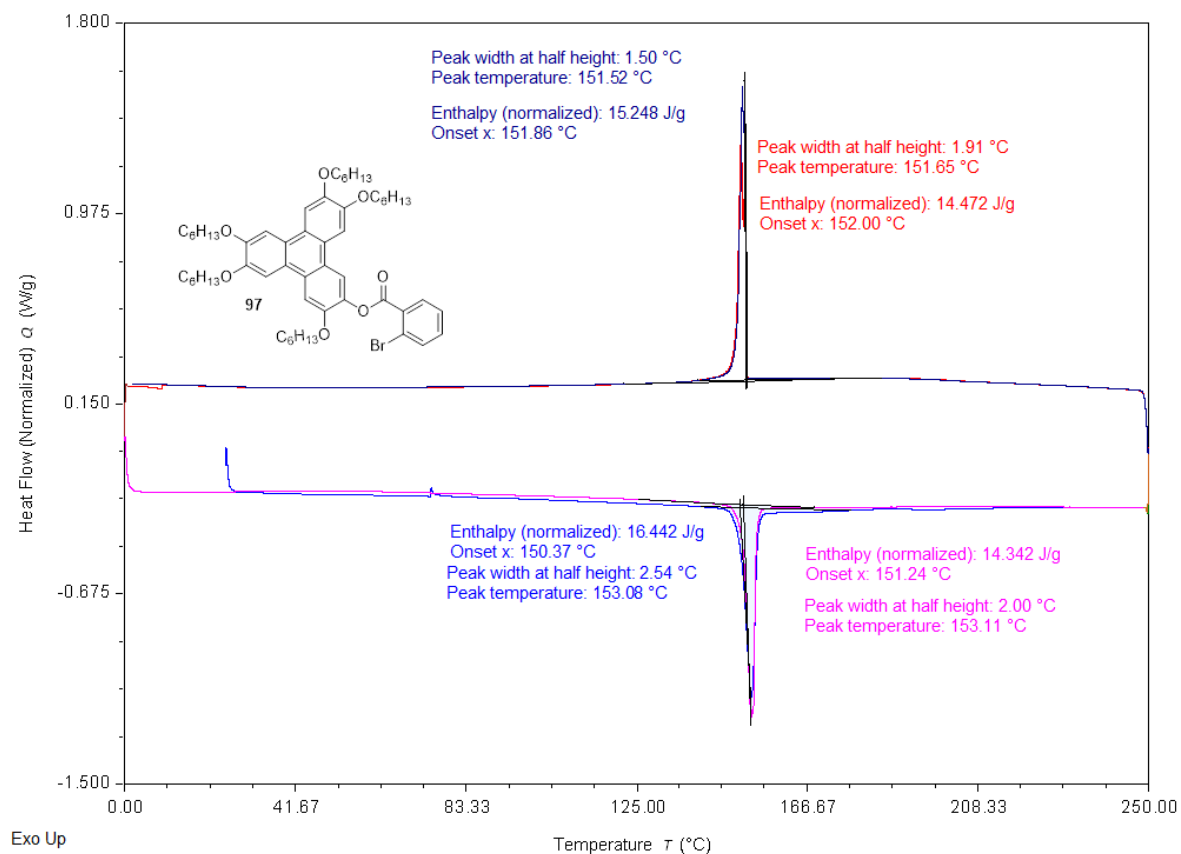
- [77] A. Kotlewski, W. F. Jager, E. Mendes and S. J. Picken, *Liq. Cryst.*, 2010, **37**, 579–586.
- [78] S. Silong, L. Rahman, W. W. Yunus, M. Z. Rahman, M. Ahmad and J. Haron, *Mat. Res. Soc. Proc.*, 2002, **709**, 105.
- [79] D. Tanaka, H. Ishiguro, Y. Shimizu and K. Uchida, *J. Mat. Chem.*, 2012, **22**, 25065.
- [80] C. V. Yelamaggad, V. Prasad, M. Manickam and S. Kumar, *Mol. Cryst. Liq. Cryst. Sci. Technol., Sect. A. Mol. Cryst. Liq. Cryst.*, 1998, **325**, 33–41.
- [81] P. Hindmarsh, M. J. Watson, M. Hird and J. W. Goodby, *J. Mater. Chem.*, 1995, **5**, 2111.
- [82] T. J. Phillips, J. C. Jones and D. G. McDonnell, *Liq. Cryst.*, 1993, **15**, 203–215.
- [83] P. Hindmarsh, M. Hird, P. Styring and J. W. Goodby, *J. Mater. Chem.*, 1993, **3**, 1117–1128.
- [84] S. Kumar and B. Lakshmi, *Tetrahedron Lett.*, 2005, **46**, 2603–2605.
- [85] C. Xing, J. W. Y. Lam, K. Zhao and B. Z. Tang, *J. Polym. Sci., Part A: Polym. Chem.*, 2008, **46**, 2960–2974.
- [86] S. K. Varshney, H. Monobe, Y. Shimizu, H. Takezoe and V. Prasad, *Liq. Cryst.*, 2010, **37**, 607–615.
- [87] W. Zhang, S. Zhang, Z. Zhang, H. Yang, A. Zhang, X. Hao, J. Wang, C. Zhang and J. Pu, *J. Phys. Chem. B*, 2017, **121**, 7519–7525.
- [88] C. Wei, X. Zhao, A. Zhang, M. Wang, X. Zhang, M. Zhang, J. Wang, Y. Fang, H. Wu and C. Zhang, *New J. Chem.*, 2022, **46**, 13037–13046.
- [89] B. N. Alanazi, A. M. Alruwaili, R. D. Beskeni, A. N. Cammidge and S. S. Samman, *Liq. Cryst.*, 2021, **49**, 1174–1183.
- [90] J. Ban, S. Chen and H. Zhang, *RSC Adv.*, 2014, **4**, 54158–54167.
- [91] X. Kong, Z. He, H. Gopee, X. Jing and A. N. Cammidge, *Tetrahedron Lett.*, 2011, **52**, 77–79.
- [92] M. Werth, S. Vallerien and H. Spiess, *Liq. Cryst.*, 1991, **10**, 759–770.
- [93] D. R. Klein, *Organic Chemistry: John Wiley & Sons*, 2020.
- [94] P. Y. Bruice, *Organic Chemistry*, Pearson, 2016.
- [95] B. Neises and W. Steglich, *Angew. Chem. Int. Ed.*, 1978, **17**, 522–524.
- [96] E. Boden and G. E. Keck, *J. Org. Chem.*, 1985, **50**, 2395–2395.
- [97] T. J. Kealy and P. L. Pauson, *Nat.*, 1951, **168**, 1039–1040.
- [98] E. O. Fischer and W. Pfab, *Z. Naturforsch. B, J. Chem. Sci.*, 1952, **7**, 377–379.

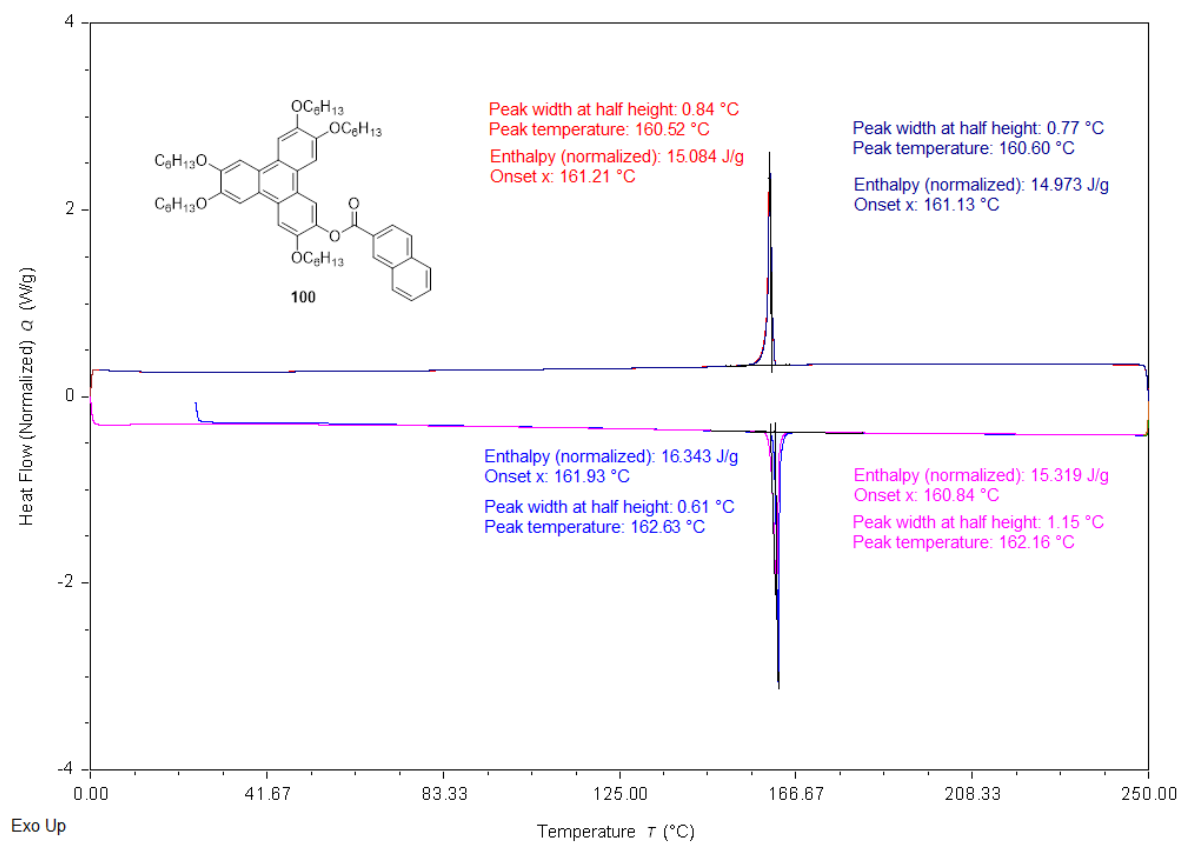
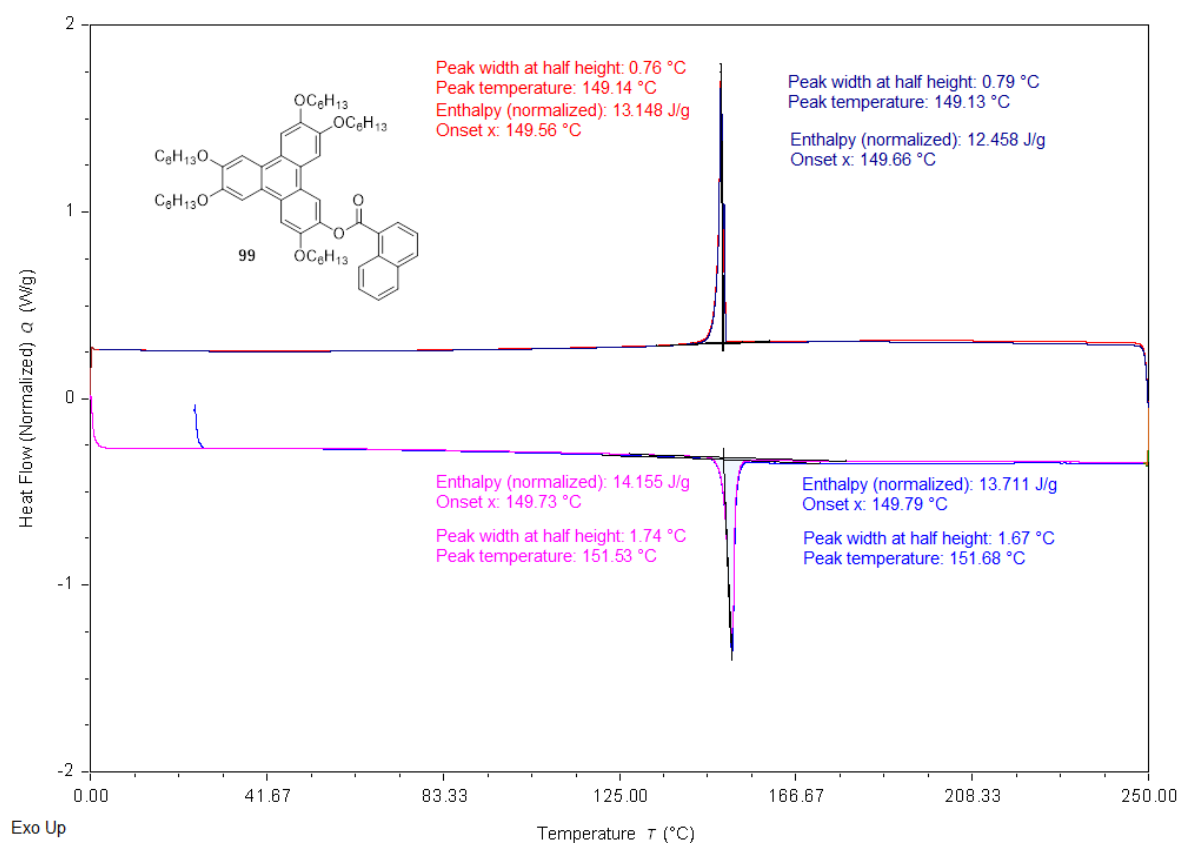
- [99] G. Wilkinson, M. Rosenblum, M. C. Whiting and R. B. Woodward, *J. Am. Chem. Soc.*, 1952, **74**, 2125–2126.
- [100] R. B. Woodward, M. Rosenblum and M. C. Whiting, *J. Am. Chem. Soc.*, 1952, **74**, 3458–3459.
- [101] M. Rosenblum, *Chemistry of the Iron Group Metallocenes: Ferrocene, Ruthenocene, Osmocene*, Interscience Publishers, 1965.
- [102] N. Hagihara, M. Kumada and R. Okawara, *Handbook of Organometallic Compounds*, W. A. Benjamin, 1968.
- [103] G. Coates, *Organometallic compounds*; Methuen and Co., 1960.
- [104] J. A. Page and G. Wilkinson, *J. Am. Chem. Soc.*, 1952, **74**, 6149–6150.
- [105] C. Montalbetti and V. Falque, *Tetrahedron*, 2005, **61**, 10827–10852.
- [106] J. Clayden, N. Greeves and S. G. Warren, *Organic chemistry*, Oxford University Press, Oxford, 2012.
- [107] W.-W. Chen, Q. Zhao, M.-H. Xu and G.-Q. Lin, *Organic Lett.*, 2010, **12**, 1072–1075.
- [108] T. Cohen and I. Cristea, *J. Am. Chem. Soc.*, 1976, **98**, 748–753.
- [109] Little, R. G., *J. Heterocycl. Chem.*, 1981, **18**, 129–133.
- [110] D. R. Beattie, P. Hindmarsh, J. W. Goodby, S. D. Haslam and R. M. Richardson, *J. Mater. Chem.*, 1992, **2**, 1261.
- [111] F. C. Krebs, N. C. Schiødt, W. Batsberg and K. Bechgaard, *Synthesis*, 1997, 1285–1290.
- [112] I. Fujimori, T. Mita, K. Maki, M. Shiro, A. Sato, S. Furusho, M. Kanai and M. Shibasaki, *Tetrahedron*, 2007, **63**, 5820–5831.
- [113] J. Li, Z. He, H. Gopee and A. N. Cammidge, *Org. Lett.*, 2010, **12**, 472–475.
- [114] A. de la Hoz, Á. Díaz-Ortiz and A. Moreno, *Chem. Soc. Rev.*, 2005, **34**, 164–178.
- [115] S. Alhunayhin, PhD probation review, University of East Anglia, 2020.
- [116] N. Boden, R. J. Bushby and A. N. Cammidge, *J. Am. Chem. Soc.*, 1995, **117**, 924–927.
- [117] F. Giroud and S. D. Minter, *Electrochemistry Communications*, 2013, **34**, 157–160.
- [118] F. W. Knobloch, W. H. Rauscher, *J. Polym. Sci.*, 1961, **54**, 651
- [119] W. Chen, Q. Zhao, M. Xu and G. Lin, *Org. Lett.*, 2010, **12**, 1072–1075.
- [120] N. Boden, R. Bushby, A. Cammidge and P. Martin, *J. Mater. Chem.*, 1995, **5**, 1857.
- [121] N. Boden, R. Bushby and A. Cammidge, *J. Chem. Soc., Chem. Commun.*, 1994, 465.
- [122] J. Hardy, MSc thesis, Victoria University of Wellington, 2020.

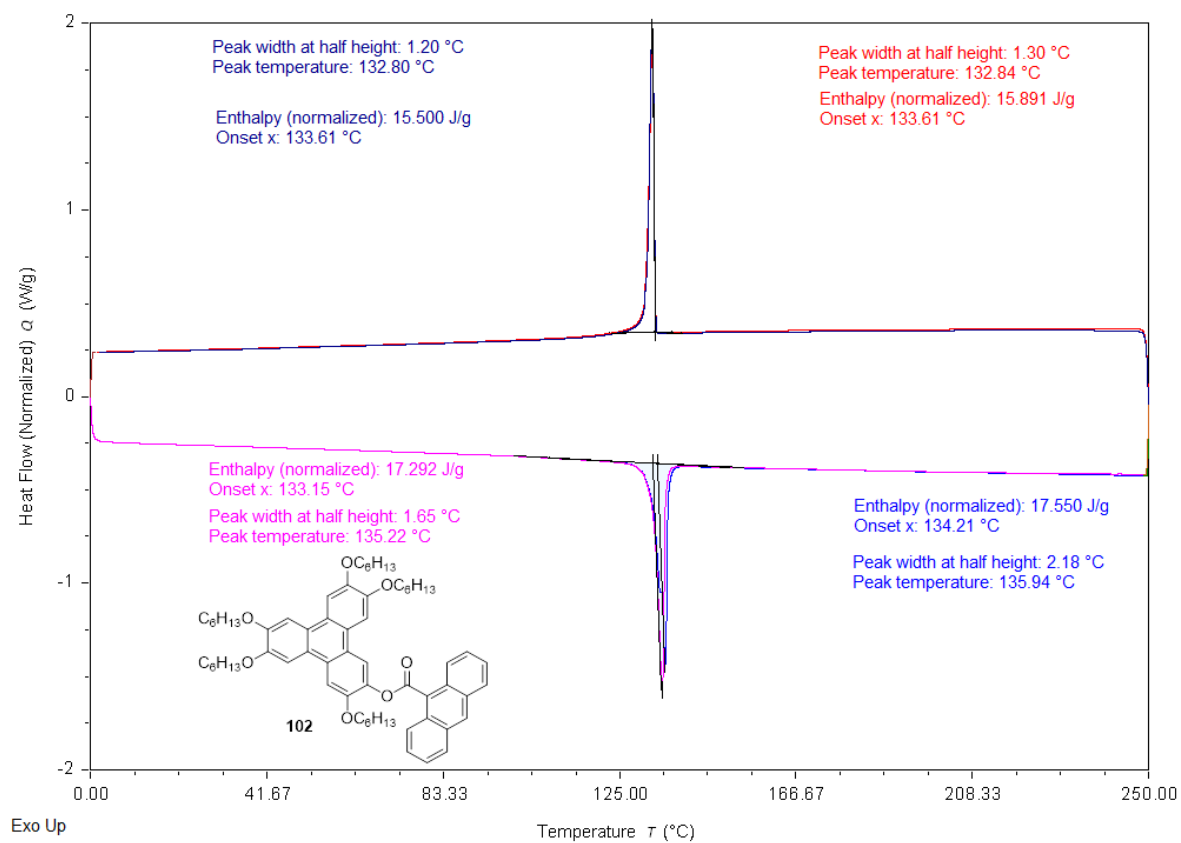
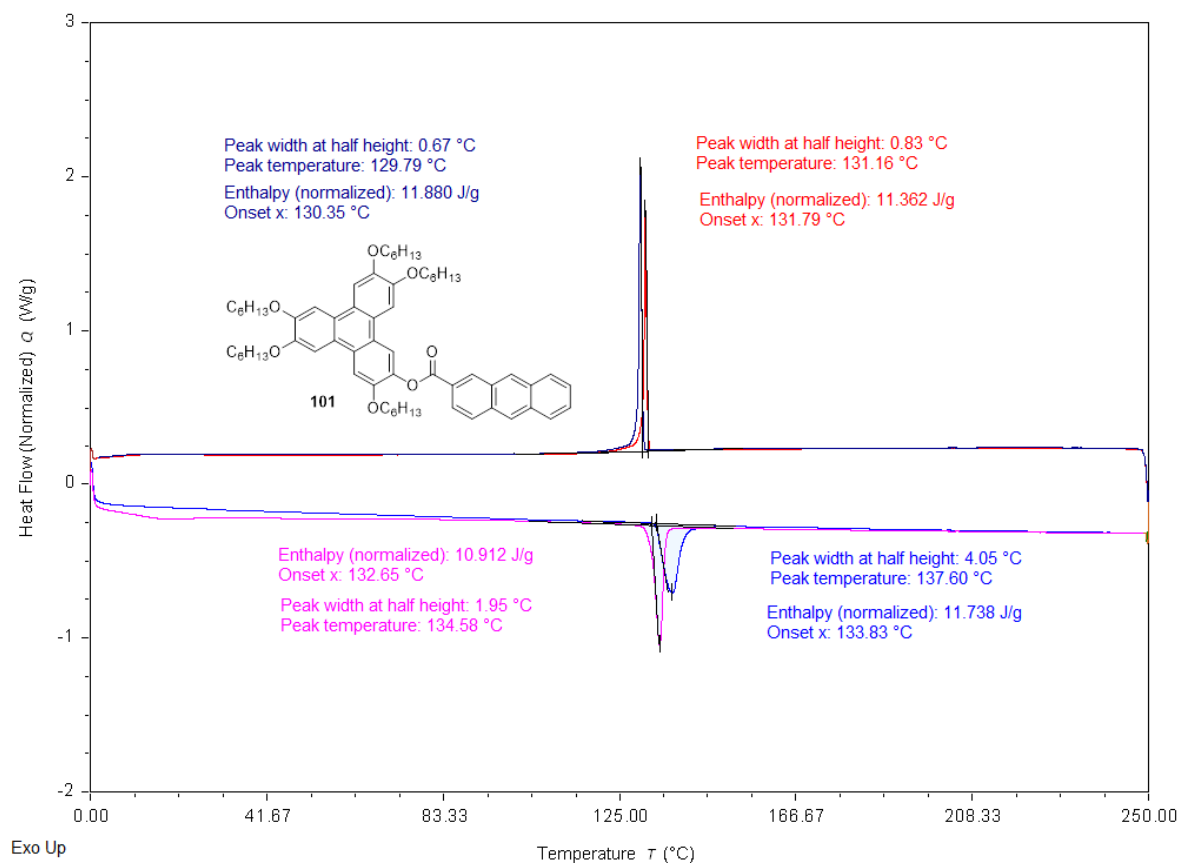
Appendices:

DSC results:









9(1)

